Kora – A Study of a Miocene, Submarine Arc-Stratovolcano, North Taranaki Basin, New Zealand

A Thesis
submitted in partial fulfilment
of the requirements for the Degree of

Master of Science with Honours

at

Massey University

By

Joshua Donald Busby Adams

MASSEY
UNIVERSITY

1998

Abstract

Kora is a relict submarine arc-stratovolcano buried offshore in north Taranaki Basin, New Zealand. Kora was active on the seafloor in middle to upper bathyal water depths from the late Early Miocene to Late Miocene times. Post-eruptive burial of the volcanic edifice by Mohakatino Formation and Giant Foresets Formation sediments has preserved the edifice and its flanking volcaniclastic deposits.

Arco Petroleum New Zealand Inc. drilled the Kora feature in 1987 and 1988. Core recovered from the Kora-1A, Kora-2, and Kora-3 wells contain lithologies derived entirely from fragmented volcanic rocks, with no evidence for massive lavas or pillow lavas. Typical lithologies are interbedded tuffs, hyaloclastite tuffs, volcanic conglomerates, and tuff breccias. The framework clasts in the tuff breccias and conglomerates are porphyritic andesite lithic clasts and andesite eruptives. The lithics were derived from subvolcanic intrusions that formed prior to the main period of edifice construction between 16 Ma. and 12 Ma. The round porphyritic conglomerate framework clasts were shaped in *transit* through the volcanic conduit during volcanic eruptions. Conglomerates lack a planar clast fabric and have a polymodal matrix. They were deposited as density modified grain flows. The tuff breccias are the suspended tails of these deposits. The interbedded tuffs and sparse pebble trains are interpreted to be suspension deposits derived from primary subaqueous eruptions.

The fragmental volcaniclastic rocks erupted from Kora were formed entirely at the water-magma interface from fuel-coolant interactions, and cooling-contraction granulation. In contrast, modern volcaniclastic rocks on the southern Kermadec submarine arc-volcanoes, Rumble IV and Rumble V, commonly form from collapsing proximal pillow lava outcrops and small eruptive vents. Like Kora, epiclastic redeposition of volcaniclastic debris on Rumble IV and Rumble V include avalanche slides, debris flows, and grain flows, with little evidence for large-scale channel deposits.

Seismic facies comprising the Kora edifice were determined from seismic reflection profiles. The individual apron facies reflectors are identified. These comprise a downlapping terminal wedge that marks the downslope limit of volcaniclastic debris, or the surface along which they travelled. Long continuous, subparallel, individual apron facies reflectors typify northwestern aspects of Kora; these reflectors can be traced laterally from the crest of the edifice to the long thin terminal wedge at the toe of the edifice. The southeastern aspect consists of individual apron facies reflectors that are hummocky, discontinuous and intertwined, with short thick terminal wedges. The edifice has been subject to a sector collapse on NW slopes, where a slump scar occurs. The eastern slopes dip more steeply than the western slopes. The edifice has a conical morphology and is some 10 – 12 km in diameter.

The major element geochemical analyses from Kora have been compared to geochemical anlayses from the Coromandel, Waitakere, Rumble IV, Wairakau, Egmont, Titiraupenga, Alexandra, Kiwitahi, and Tongariro volcanic centres using discriminant function analysis. Results have identified four assemblages of volcanic centres with comparable major element geochemistry. Kora, which fits in to the Waitakere, Wairakau and Alexandra volcanic assemblage is a southward extension of the Northland volcanic "trend".

Acknowledgements

My sincerest thanks to all those people who have generously given me their time and support over the past two years. In particular, thanks to my supervisors Julie Palmer and Bob Stewart, for your patience, and for the continuous supply of constructive feedback and guidance. Special thanks to Steve Bergman at Arco Exploration and Production Technology, for providing the raw geochemical data for Kora, and for sharing your knowledge of Kora so willingly. Special thanks also to Vaughan Stagpoole at IGNS for assisting with the seismic analysis, and to Ian Wright at NIWA for providing very useful comments in the initial stages of the research. The Sydney Campbell Trust, Massey Graduate Research Fund and the Geological Society of New Zealand have also assisted by graciously providing grants that reduced the cost of the research, for these I'm most appreciative.

To the QMAP team at the Institute of Geological and Nuclear Sciences: Working with you people over the summer holidays convinced me to persevere with science as a career option. Your undying enthusiasm towards geology despite a difficult working environment was inspirational. Thanks also to the Massey University Soil Science Department for offering advice on a number of issues and for providing the laboratory facilities. To my friends: thanks for the good-times - I have many unforgettable memories and a few blurry ones as well! Your colourful personalities always provided a welcome respite from the frequently dull Palmerston North weather.

Finally, but with no less meaning, to my parents and family: Thanks for providing food and shelter when the size of my student loan became excessive. Your patience and understanding throughout the past 6 months has been tremendous and won't be forgotten.

Joshua Adams
August 1998

Table of Contents

List of Figures

Chapter 1

Chapter 2

Chapter 3

Chapter 4

Chapter 5

List of Tables

Chapter 2

Chapter 4

List of Plates

Chapter 2

1.0 INTRODUCTION

1.1 BACKGROUND

Kora is a Miocene submarine arc-volcano buried beneath the western margin of the Northern Graben in New Zealand's offshore Taranaki Basin (Fig. 1.1). The Kora Structure was first studied in 1988 after processing of seismic reflection data and subsequent drilling by Arco Petroleum N.Z Inc. unveiled a potential hydrocarbon reservoir. The exploration programme around the Kora Structure was abandoned by Arco after assessment of the structure revealed sub-economic quantities of marine sourced oil (Reed, 1992). A large amount of well and seismic reflection data associated with the Kora prospect are now held on open file with the New Zealand Ministry of Commerce in Wellington under prospect license PPL 38447. These data have been used in this study to model the volcaniclastic processes associated with the development of the Kora edifice, and to define a "parent arc" for the Kora volcano.

Major element geochemical analyses from eruptive rocks at Kora have been compared with published major element analyses from 9 North Island Miocene to Recent volcanic centres using discriminant function analysis to determine the likely parent arc for the Kora Volcanic Centre. The size and extent of the Kora volcaniclastic depositional units flanking the volcanic edifice has been defined through interpretation of seismic reflection profiles, while the transport mechanisms have been inferred from analyses of the textural fabric observed in the cores. These data have been combined with previously published data, including radiometric dating, XRD analyses, and geophysical well logs (Arco Petroleum N.Z Inc., 1988a; 1988b; 1988c; and Bergman *et al.,* 1992) to develop a model of the Kora Structure. This model has been "tested" by comparing it with published observations of volcaniclastic processes associated with modern submarine arc volcanoes in the Tonga-Kermadec arc (Gamble *et al.,* 1993; Wright, 1993a,1993b,1996) and in the Izu-Ogasawara arc (Dietz, 1954; Fiske *et al.,* 1998).

There has been limited research in the field of submarine arc volcanism and the associated volcaniclastic processes and deposits. This is largely because of the practical limitations that restrict the study of modern analogues in deep submarine environments. The large amount of well and seismic data associated with Kora, and

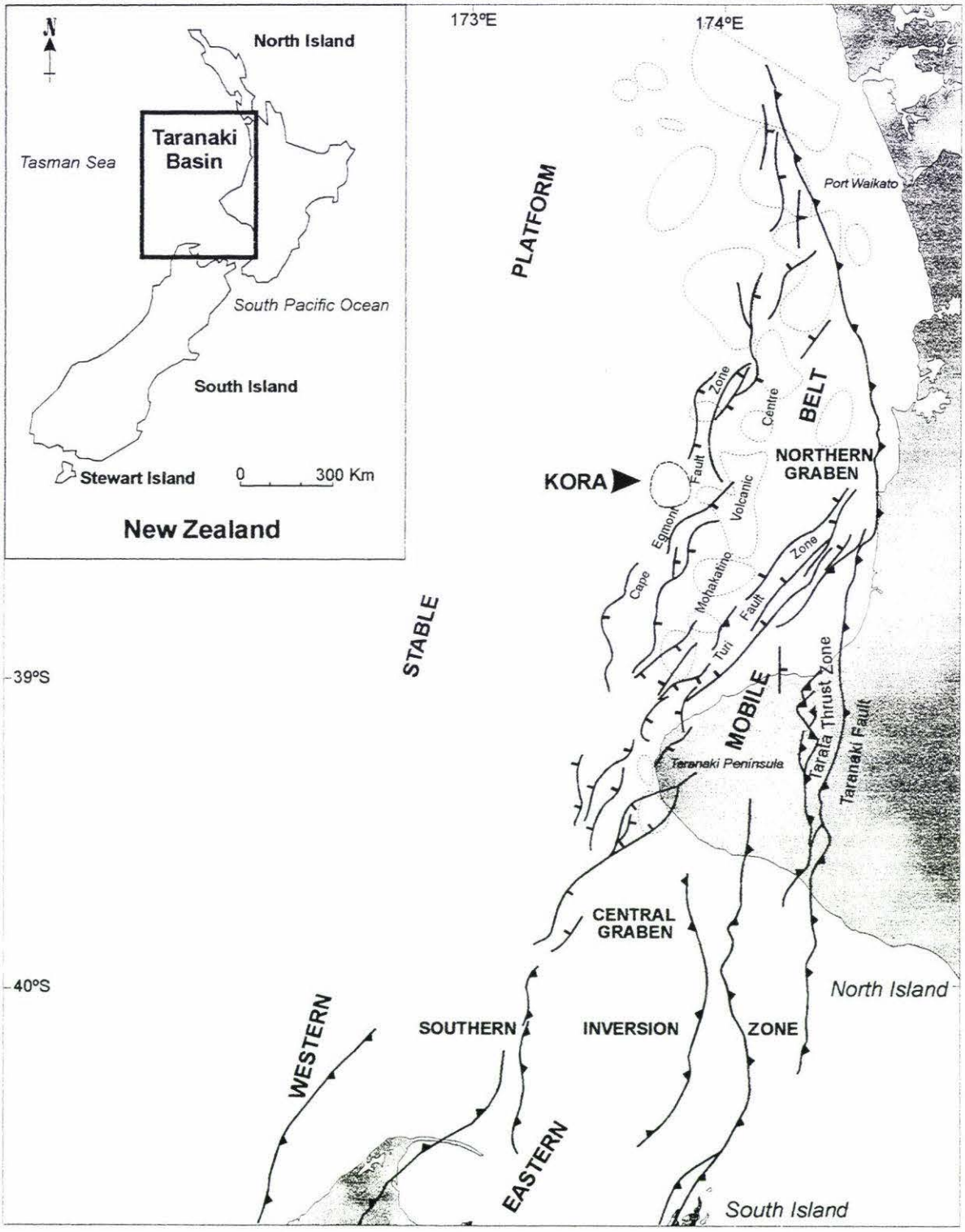

Figure 1.1

Location map showing Kora and the main structural features of the Taranaki Basin (After King and Thrasher, 1997)

the preserved nature of the Kora edifice, provide a good example of a submarine arc-volcano. Consequently results from this research will contribute new information to the global database for submarine arc-volcanism, as well as contributing to the record of Late Cenozoic volcanism in New Zealand.

1.2 GEOLOGICAL SETTING – TARANAKI BASIN

Taranaki Basin is presently New Zealand's primary oil and gas producing region. This Cretaceous and Tertiary sedimentary basin constitutes an offshore and onshore area of some 100 000 km^2 (King, 1994), and embraces most of the western margin of the North Island of New Zealand. The basin is bounded in the east by the Taranaki Fault, and extends west to where Neogene sediments prograde on to the Challenger Plateau. The southern limits of Taranaki Basin are thought to merge with the basin and range province of Northwest Nelson, while the northern part of Taranaki Basin is contiguous with the offshore Northland Basin (King, 1994), however, a latitude of 37°S is designated the boundary between these two sedimentary basins (Isaac *et al.*, 1994).

1.2.1 Structural Components

Taranaki Basin is subdivided in to two structural provinces; the Western Stable Platform, and the Eastern Mobile Belt (Fig. 1.1). The easternmost part of the Western Stable Platform occurs where Neogene depositional sediments prograde on to the regionally subsiding sea floor (King and Thrasher, 1997), while the Eastern Mobile Belt consists of a northern sector consisting of the Northern Graben and Central Graben, and a southern sector which includes the Southern Inversion Zone and Tarata Thrust Zone (King, 1994). The boundary between the Eastern Mobile Belt and the Western Stable Platform is defined by the eastern limit of plate boundary deformation on the overriding Australian plate (King, 1994).

1.2.2 Stratigraphy and Geological History

Taranaki Basin contains up to 9 km of Cretaceous and Tertiary sedimentary fill (Palmer, 1985). The stratigraphy is presented in Fig. 1.2. The Cretaceous - Cenozoic geological history of Taranaki Basin is well documented in a number of papers, for example King and Thrasher (1992; 1997), King (1994), Stern and Holt (1994), and

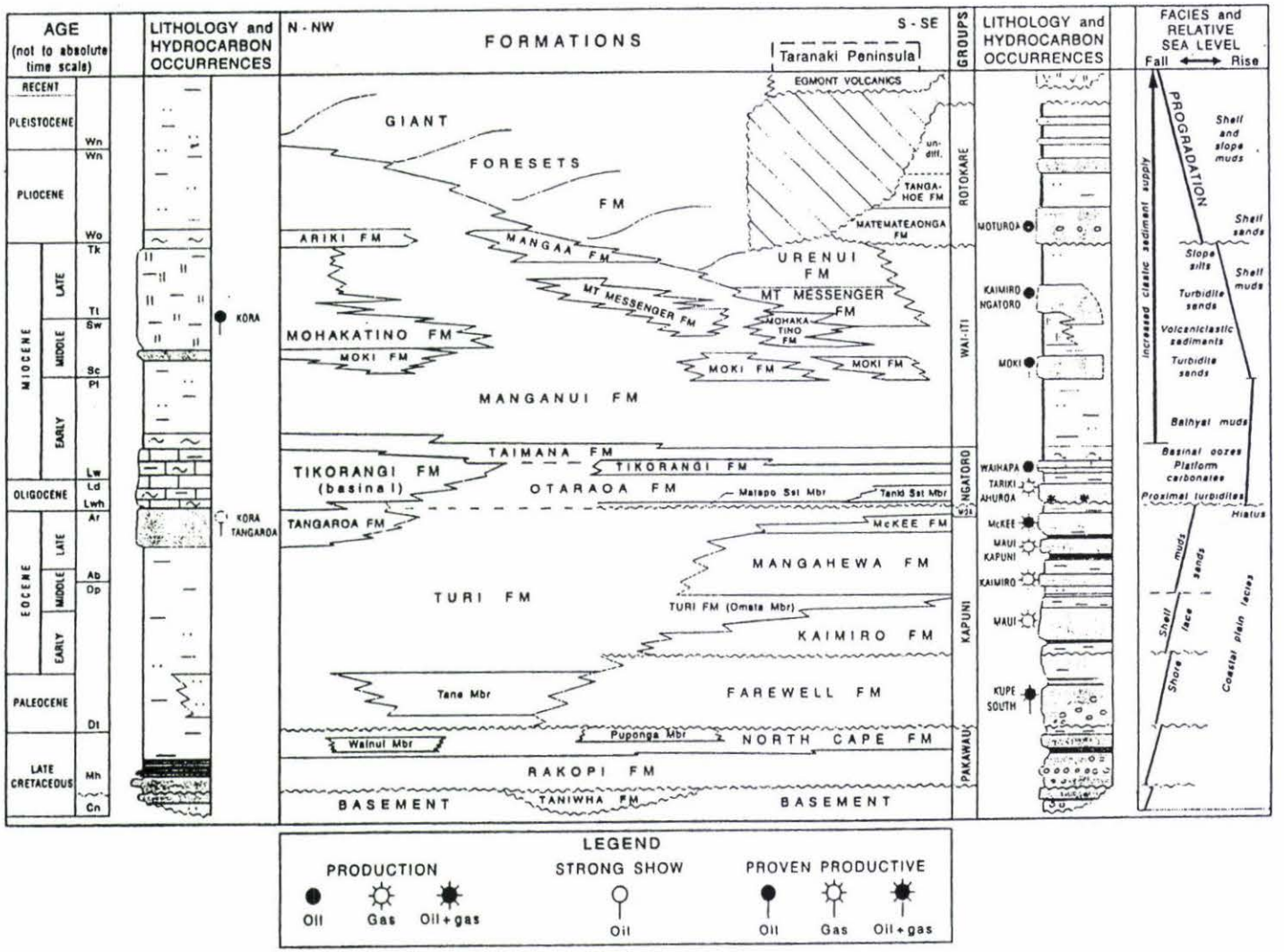

Figure 1.2
Cretaceous-Cenozoic stratigraphic framework for Taranaki Basin (from King and Thrasher, 1997)

Palmer and Andrews (1993). Most authors recognize four intervals that have played a key role in the geological development of Taranaki Basin.

1. From 80 Ma to 53 Ma the Tasman Sea opened in response to extension along the eastern margin of Gondwanaland.
2. The Late Cretaceous and Paleocene Taranaki Basin was largely emergent and sedimentation included deposition of coal measures and coastal plains deposits (Palmer, 1985).
3. From the Eocene Taranaki Basin gradually submerged, and by Early Oligocene a passive margin had developed in association with subduction along the Australian/Pacific plate boundary northeast of New Zealand. (King and Thrasher, 1997).
4. The final period of basin development occurred from Oligocene to Recent when convergent tectonics related to the present day Australian/Pacific plate boundary caused deformation of the basin fill as it is seen today (King and Thrasher, 1997).

1.2.3 Miocene Volcanism in the Taranaki Basin – The Mohakatino Volcanic Centre

Within the stratigraphic framework outlined above, Kora is one of 25 recognized Miocene intra-arc stratovolcano complexes buried in the Northern Taranaki Basin (Bergman *et al.*, 1992). These stratovolcano complexes were originally identified from magnetic anomalies (Hatherton, 1968) and collectively form the Mohakatino Volcanic Centre. The volcanic centres form a NE-SW trending lineament along the axis of the Northern Graben (King and Thrasher, 1997) between Cape Egmont in the south and Port Waikato farther north. Here the Mohakatino volcanics converge on the NW-SE trending western belt of the Early Miocene Northland Arc. The Northern Graben is mostly a post-Mohakatino feature which formed predominantly during the Plio-Pleistocene in response to fault activity along the west bounding Cape Egmont Fault Zone and the east bounding Turi Fault Zone (King and Thrasher, 1997). The Kora Structure is buried within the western rim of the Northern Graben in the Cape Egmont Fault Zone and is one of the most westerly volcanoes within the Mohakatino Volcanic Centre.

The onset of volcanism in the Mohakatino centre began in the late Early Miocene with intra-basement intrusion, followed by extrusive submarine volcanic eruptions which peaked between 14 and 11 Ma (King and Thrasher, 1997). This phase of volcanism coincided with pronounced tectonism associated with the developing Australian/Pacific plate boundary and migration of the instantaneous pole of rotation away from New Zealand between 21 Ma and 10 Ma (Walcott, 1987). For example, convergent plate motion first became evident between 23 Ma and 20 Ma when basement rocks were overthrust in a westerly direction along the Taranaki Fault (King and Thrasher, 1997). Mohakatino volcanism finally ceased at approximately 7-8 Ma (e.g. Bergman *et al.*, 1992), although some of the buried volcanics adjacent to the Egmont Peninsula may be younger (King and Thrasher, 1997).

1.3 KORA VOLCANIC CENTRE

1.3.1 Distribution of Exploration Wells and Drilling Results

In 1988, Arco Petroleum NZ Inc. commenced a hydrocarbon exploration programme in which 5 wells (Kora-1, Kora-1A, Kora-2, Kora-3 and Kora-4) were drilled in to the Kora volcanic edifice (Fig. 1.3). Extensive core and electric log data were collected. The general drilling results and stratigraphy for each well are described below and summarised in Fig. 1.3. A more detailed description of the lithologies encountered in the Kora wells is covered in Chapter 2.

Kora-1 drilled the southeastern flank of the volcanic edifice. The top 1631.6 m of this well "along hole (AH)" consists of Plio-Pleistocene Giant Foresets Formation - a succession of siltstones and mudstones deposited as the shelf-break migrated westward and northward (Beggs, 1990; King and Thrasher, 1997). Underlying the Giant Foresets Formation, Miocene volcanics occur between 1781 m bkb and 2581 m bkb, and beneath these volcanics the well intersected 320 m of Early Miocene, Manganui Formation 'deep-water' mudstones (King and Thrasher, 1997). The Manganui Formation is underlain by Tikorangi Formation between 2899 m bkb and 3128 m bkb. These sediments are highly calcareous outer-shelf and upper-slope carbonates that were deposited during the Late Oligocene and Early Miocene (King and Thrasher, 1997). Beneath the Tikorangi Formation from 3128 m bkb to 3242 m bkb, deep marine sandstones comprising the Tangaroa Formation occur. This formation contains deep marine sandstones that were emplaced during the Late

Figure 1.3

Composite stratigraphic columns for Kora wells
(adapted from McManamon, 1993)

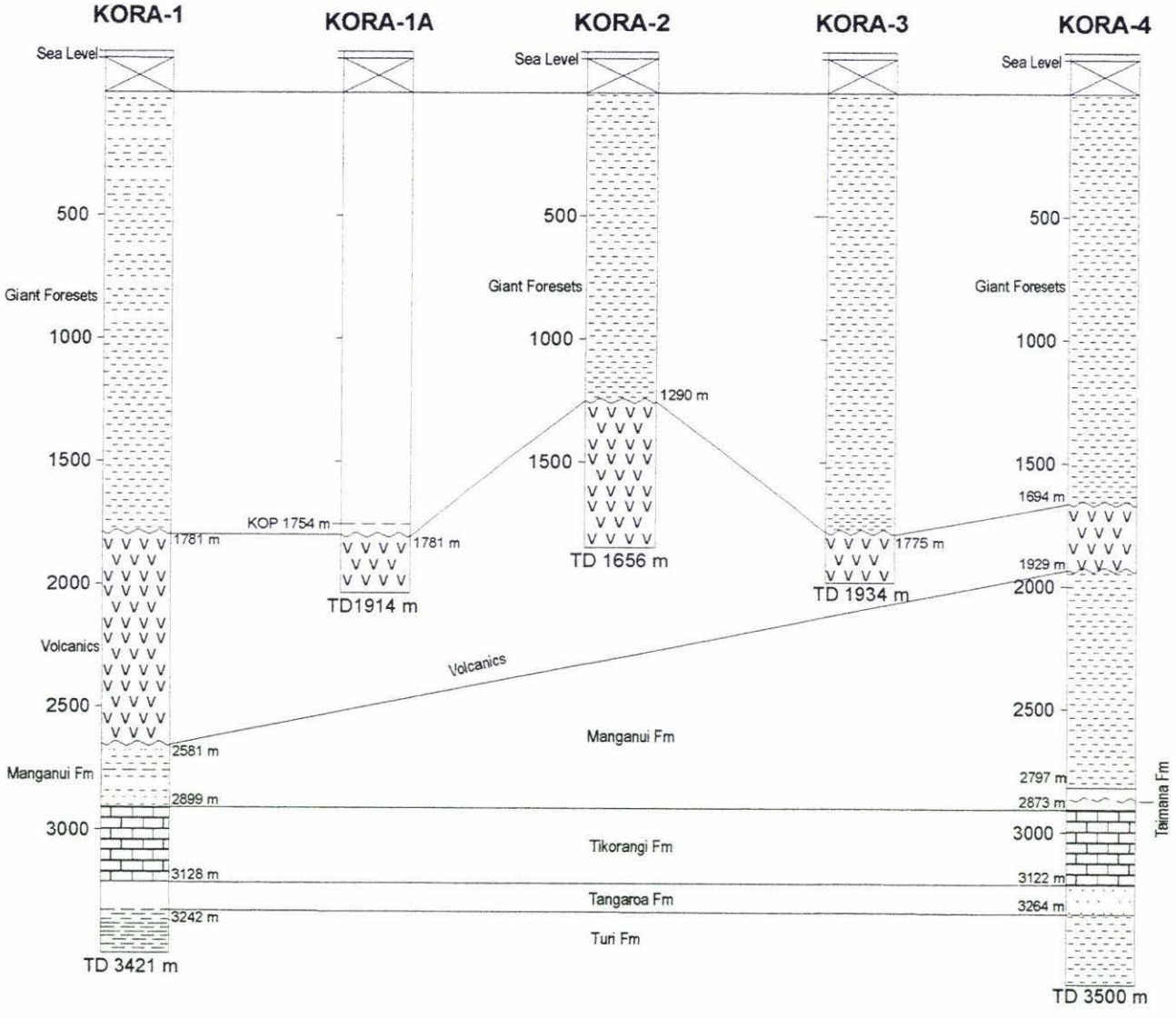

Eocene and Early Oligocene as debris flows, liquified flows and turbidity currents (King and Thrasher, 1997). From the base of the Tangaroa Formation to 3421 m bkb (total well depth) Turi Formation sediments form the final metres of the Kora-1 well. This formation contains shelf and bathyal calcareous marine mudstones that were deposited from the Paleocene to late Eocene (King and Thrasher, 1997).

Kora-1A was a deviated well, drilled from a window in Kora-1 between 1754 m bkb and 1761.5 m bkb. This well was drilled entirely within the volcanics between 1781 m bkb and 1914 m bkb (McManamon, 1993). Kora-2 location is 2.5 km NNW of Kora-1 and that well drilled to a total depth of 1656 m bkb. Giant Foresets Formation account for the uppermost 1130 m and terminate directly above the volcanics at a depth of 1290 m bkb. The well terminated within the volcanic interval (McManamon, 1993). Kora-3, located 1 km NNW of Kora-1, drilled to a total depth and terminated at 1934 m bkb within the volcanics. The upper 1622.5 m of Kora-3 comprises of Giant Foresets Formation while the top of the volcanics occurs at 1775 m bkb (McManamon, 1993).

Kora-4 is located 4.5 km WSW of Kora-1 and drilled to a total depth of 3500 m bkb. The upper 1500 m comprises Giant Foresets Formation, with the volcanics spanning the interval between 1694 m bkb and 1929 m bkb. Directly beneath the volcanics, the Manganui Formation extends to a depth of 2797 m bkb, and below Manganui Formation, is 76 m AH of early Miocene marl, Taimana Formation. This formation represents a depositional hiatus which occurred in the Early Miocene as clastic sedimentation slowed. The Taimana Formation is underlain by Tikorangi Formation to a depth of 3122 m bkb and below this, Tangaroa Formation occurs until 3264 m bkb. Kora-4 reached a total well depth of 3500 m bkb within the Turi Formation.

1.3.2 Previous Studies

Analyses of the lithological and well data were summarised in a single comprehensive paper published by Bergman *et al.,* (1992). Other than the unpublished well reports this has been the only significant paper dealing specifically with the volcaniclastics at Kora. Other workers who have investigated Kora include McManamon (1993) who published a brief summary of the drilling results and petroleum geology of the Kora prospect, Reed (1992) who has studied the

geochemistry of the oil from Kora, and Hayward and Strong (1988) who reported on the foraminiferal faunas in Kora-1. Since this initial work no other research referring specifically to Kora has been published. The work by Bergman *et al.,* (1992) provides an excellent summary of the "stratigraphy, volcanic facies, petrology, geochemistry, age and evolution" of Kora and its encompassing volcaniclastic sediments. The main points from this paper relevant to this study are detailed below.

The volcanic rocks erupted from Kora are subduction-related arc-andesites derived from depleted mantle based on major and trace element geochemistry. The absolute ages of the volcanic rocks vary between 20 Ma and 8 Ma with the earliest ages (*between 20 Ma and 19 Ma*) corresponding to a pre-eruptive intrusive event. The inception of eruptive volcanism began some time between 15 Ma and 17 Ma and the volcanism ended as late as 8 Ma (Bergman *et al.,* 1992).

The biostratigraphic and palaeoecological evidence (Hayward and Strong, 1988), indicates that the volcaniclastics drilled by the Kora wells were deposited under fully marine conditions. Further evidence to support this interpretation is the lack of vesiculated volcanic clasts in the lithologies cored from Kora. The top of the volcanic interval contains benthonic foraminifera indicative of upper bathyal water depths (i.e. Hayward, 1986; Hornibrook *et al.,* 1989; in Bergman *et al.,* 1992). Likewise, benthonic foraminifera within the overlying Giant Foresets Formation sediments and samples from deeper within the volcanics also indicate middle and uppermost bathyal water depths.

Some 40 seismic profiles were acquired across the Kora feature (Bergman, pers comm). These show that the Kora edifice has up to 1000 m of relief with 8°-15° slopes and a basal diameter of some 10 km. The lithologies cored from Kora include "bioturbated, calcite-cemented tuffs; tuffs, lapilli tuffs, hyaloclastite tuffs, lapillistones and tuff breccias; volcanic sandstones and reworked tuffs; and volcanic conglomerates and breccias" (Bergman *et al.,* 1992).

The mineralogy and petrography indicates that the lithologies are predominantly andesitic (Bergman *et al.,* 1992). The primary minerals are plagioclase (andesine –

labradorite), hornblende, clinopyroxene (augite), quartz, and Fe-Ti oxides (titanomagnetite and ilmenite). Many of the lithologies have altered to clays that were derived from glass as well as plagioclase and hornblende. For example smectite (after glass, plagioclase, and hornblende), quartz (after plagioclase and hornblende), zeolites (after glass, plagioclase and hornblende), illite (after glass and plagioclase), analcite, corrensite, biotite, pyrite, calcite, and hematite are the prevalent alteration phases (Bergman *et al.,* 1992).

The work of Bergman *et al.,* (1992) and the other industry related studies present a comprehensive, broad range of analyses from Kora. These have characterised the Kora Structure from a hydrocarbon reservoir perspective. The objective of this study is to place Kora within its volcanological setting.

2.0 Fabric Characteristics of Lithologies from Kora

2.1 INTRODUCTION

The fabric of a sedimentary rock provides information about the geological processes that produced that particular rock (Lapidus, 1987). In this study the fabric of the volcaniclastics have been described and interpreted from core material collected from the Kora-1A, Kora-2 and Kora-3 exploration wells. The objective of this work is to identify the depositional slope processes operational during the formation of the Kora edifice.

2.2 METHOD

2.2.1 Data Acquisition

The open file reports for the Kora-1A, Kora-2 and Kora-3 wells were inspected at the Ministry of Commerce in Wellington and the final well reports containing the detailed well logs for Kora-1A (Arco Petroleum NZ Inc., 1988a), Kora-2 (Arco Petroleum NZ Inc., 1988b) and Kora-3 (Arco Petroleum NZ Inc., 1988c) were acquired. These three wells were chosen specifically because they had core cut from the volcanic interval.

The core from Kora-1A, Kora-2 and Kora-3 were inspected and described at the Ministry of Commerce 'Core Store' located on Gracefield Road in Lower Hutt. Textural fabric including clast orientation, shape, size, matrix support, sorting, clast density and proportions of matrix were recorded. Lithologic descriptions follow the terminology used by Arco Petroleum NZ Inc.

The long and short axes of individual clasts in the slabbed core were measured using callipers and a standard metric ruler. The shape of each individual clast was discerned using a visual comparison aid (*after* Powers, 1953; and Shepard, 1963; In: Andrews, 1982) (Appendix 1.1). Sorting estimates were obtained using a verbal scale (*after* Compton, 1962; *in* C. King, 1992) (Appendix 1.2) as were the component proportions (*after* Folk et al., 1970 *in* Andrews, 1982) (Appendix 1.3). The relative orientation of the long axis for each clast was also measured using a Rotring azimuthal protractor to identify possible clast imbrication. And as a final descriptive procedure photographs were taken of the representative core lithologies.

In the fine-grained lithologies such as tuff, and the matrix of the conglomerates and tuff breccias, the individual clasts were too small to be measured using the unaided eye. These were described from thin sections. The sampling strategy was constrained by the core recovered. There were a large number of gaps in the cored interval, the result of poor core recovery in some places. A consistent strategy of taking one or two samples (no more than ~3cm^3) from each lithological change through the core was followed. This avoided destroying the well-preserved nature of the core while at the same time maintaining a representative sample distribution.

2.2.2 Thin Section Analysis

In the lab, thin sections were prepared using the method described for 'non-friable, insoluble rocks' after Lewis (1981) (Appendix 1.4). When describing the thin-sections, the same descriptive parameters used for hand specimen description at the core store (section 2.2.1) were applied to the thin sections. Photomicrographs were taken from representative thin sections to illustrate aspects of the rocks.

2.2.3 Textural Analysis

The grainsize for individual clasts and crystals from both hand specimen and thin section were measured and the combined lengths and breadths of each clast averaged using the calculation (L+B)/2 (after Schneiderhöhn, 1954). These data were then converted from millimetres to Phi units (ϕ=-log$_2$ *d*) and the grainsize parameters of Folk and Ward (1957) calculated to describe the graphic mean (a measure of mean grain size), inclusive graphic standard deviation (a measure of sorting), inclusive graphic skewness, and graphic kurtosis for both thin section data and hand specimen data (see Appendix 2). The results provide quantitative data that will be directly comparable with future textural studies on submarine arc volcanoes. These data also assist qualitative description of the textures and fabric in lithologies from Kora. As a final procedure, the 'elongation ratio' (after Schneiderhöhn, 1954) was calculated to illustrate the sphericity of the clasts in the volcaniclastics.

2.2.4 XRD Analysis

X-ray diffraction analysis was performed on samples that were too fine grained for thin section analysis and samples that were not prepared as thin sections. Whole-

rock analysis, with minimal sample treatment, was carried out using the Soil Science X-ray Diffraction Laboratory at Massey University. This procedure served to confirm the identity of heavy minerals observed in thin section and their relative proportions (wt %) including the predominant clays present in the samples analysed. Further treatments and analysis were not performed because Bergman *et al.,* (1992) had previously undertaken extensive clay mineralogy.

2.3 RESULTS

2.3.1 Core Logs and Distribution of Observations and Sample Data

The locations of the exploration wells Kora-1A, Kora-2 and Kora-3 are illustrated in Fig. 2.1. Kora-1A is located in the middle of the downthrown southeastern portion of the edifice, Kora-2 is positioned 2.5 km NNW from Kora-1A closer to the crest of the volcanic edifice while Kora-3 is located 1 km NNW from Kora-1A between Kora-1A and Kora-2 (McManamon, 1993). The lithologies represented in each of the three wells are summarised in Figs. 2.2, 2.3 and 2.4 respectively. Each of these figures illustrates the location of samples taken for thin section analysis (e.g. TS1, TS2) and the location of cored intervals that were measured directly with the unaided eye (e.g. OB1, OB2). The lithologic summaries are a combination of observations made by Arco Petroleum NZ Inc (1988a,b,c), Bergman *et al.,* (1992) and personal observations made for this study (see Appendix 3.1, 3.2 and 3.3).

2.3.2 Kora-1A Core Observations

The lithologies identified in Kora-1A (Arco Petroleum NZ Inc., 1988a) include volcanic conglomerates, tuff breccias, lapilli tuff, tuffs, hyaloclastite tuffs, and lapillistones. Where core has not been cut, lithologies have been inferred (Arco Petroleum NZ Inc., 1988a) using geophysical well logs.

Conglomerates

In Kora-1A the conglomerates occur within core at 1793 m bkb to 1798 m bkb, and 1818 m bkb to1830 m bkb (Fig. 2.2). Conglomerate is also inferred at 1852 m bkb -

Figure 2.1

Surfer image of Kora and the location of exploration wells used in this study

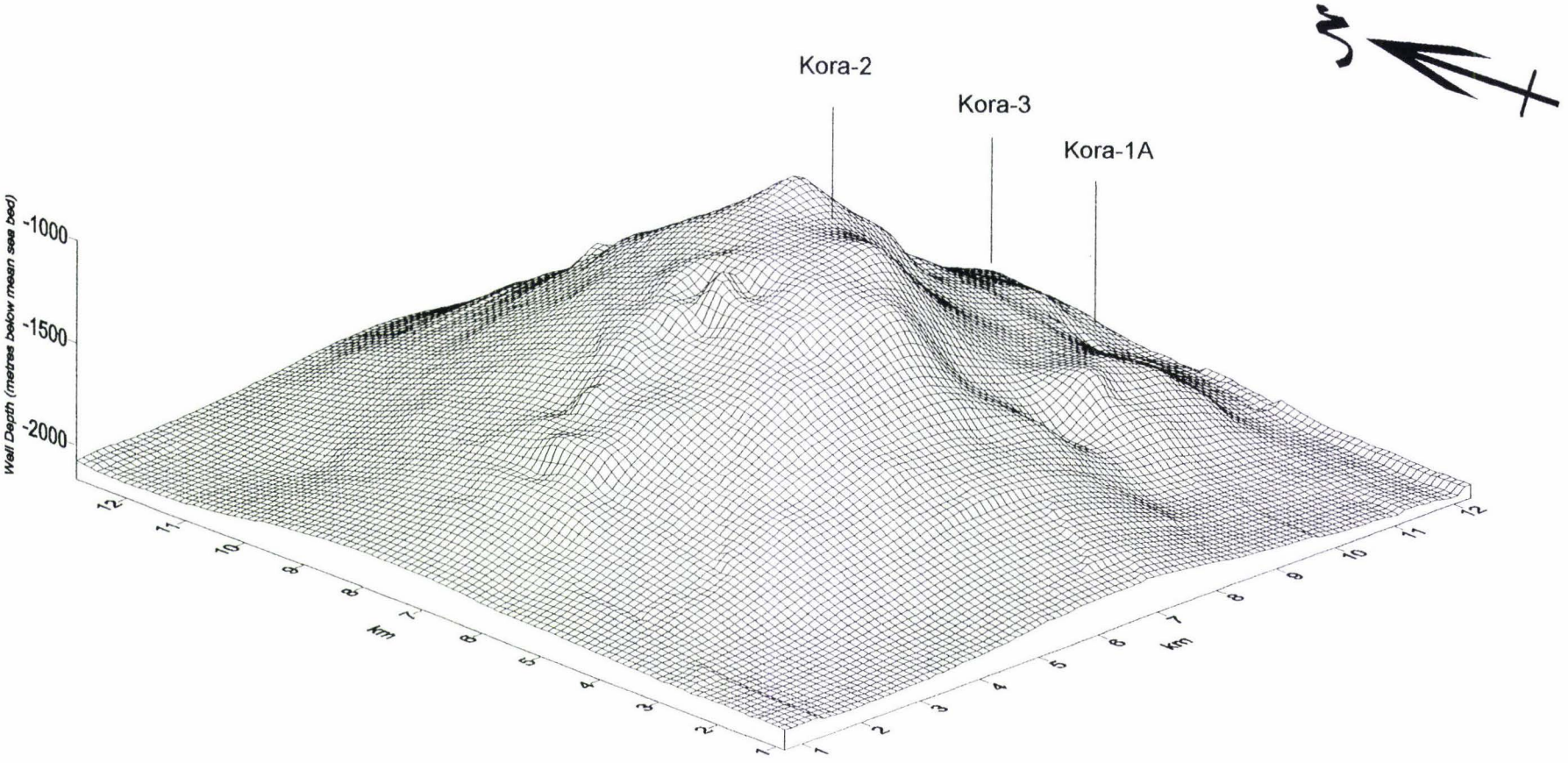

Figure 2.2
Kora-1A Lithologic Log
(After: ARCO Petroleum NZ Inc, 1988a; Bergman *et al.*, 1992; and this study)

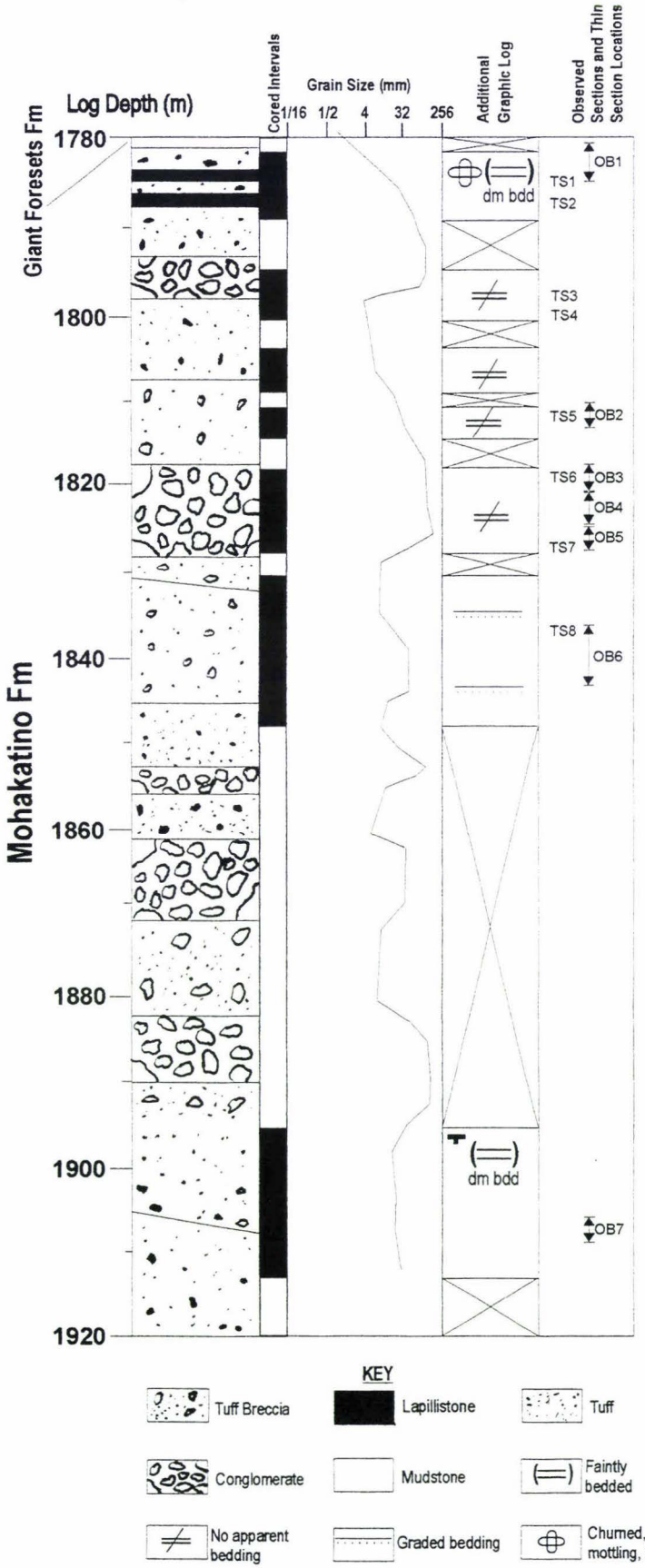

Core Descriptions

1783 - 1787 m bkb
Hard to moderately soft, moderately sorted, burrowed and bored, interbedded tuffs and lapillistone. The contacts between these faintly bedded lithological units is mostly gradational, although rare contacts are ripped up. The framework components include fine sand and medium sized pebble, subrounded to subangular clasts of andesite, and broken crystals of weathered plagioclase and hornblende. The matrix consists of fine ash to very coarse sand sized crystals, and clay. In thin section the framework components consist of fine to medium sand, moderately sorted, crystals of plagioclase, hornblende, augite, and the minerals glauconite and magnetite. The matrix is clayey and comprises up to 50 % of the rock.

1793 - 1807 m bkb
Unconsolidated volcanic conglomerate and volcanic sands. The framework clasts in the conglomerate include very hard, rounded and well rounded, green and red, porphyritic textured pebbles and boulders of andesite. The matrix in the volcanic conglomerate contains fine clay, andesite fragments, and crystals of plagioclase and hornblende. The whole rock minerals include plagioclase, and lesser amounts of amphibole, calcite, and clays. In thin section the unit contains poorly sorted, fine sand sized crystals and a matrix of clay and silt sized crystal fragments.

1818 - 1829 m bkb
Red, green, grey often pitted and subrounded, non-vesicular andesitic porphyritic textured clasts vary in size from 20 mm to >160 mm. Clasts are mainly poorly sorted and vary between matrix supported and clast supported. Clasts are often broken *in situ*, with dissaggregated rock fragments remaining close to source and contributing to the surrounding matrix. The matrix content also varies between tuff and lapilli tuff. In thin section, the unit contains poorly sorted, very fine sand sized crystals of plagioclase (up to 50 %), hornblende (up to 20 %), and lesser augite, clay, and quartz.

1831 - 1846 m bkb
Weakly graded, poorly sorted, moderately soft to hard lithological unit. The framework clasts are angular to subangular andesite grits and very coarse pebbles. The clasts are more closely packed as the well depth increases, and the proportion of matrix material decreases with increasing well depth. The matrix consists of fine sand and grit sized crystals. In thin section, the rock comprises poorly to moderately sorted, fine sand sized crystals of plagioclase, augite, hornblende, and opaques. The crystals are broken and pitted, and have a holocrystalline and clay matrix.

1895 - 1907 m bkb
Variably spherical, angular to subangular coarse sand and cobble sized clasts of andesite, and non-porphyritic pale grey andesite clasts. The coarse sand size material typically consists of subhedral hornblende crystals. The dominant whole rock minerals include plagioclase, amphibole, quartz, hematite, clay, and lesser magnetite and zeolite.

Figure 2.3
Kora-2 Lithologic Log
(After: ARCO Petroleum NZ Inc, 1988b; Bergman *et al.*, 1992; and this study)

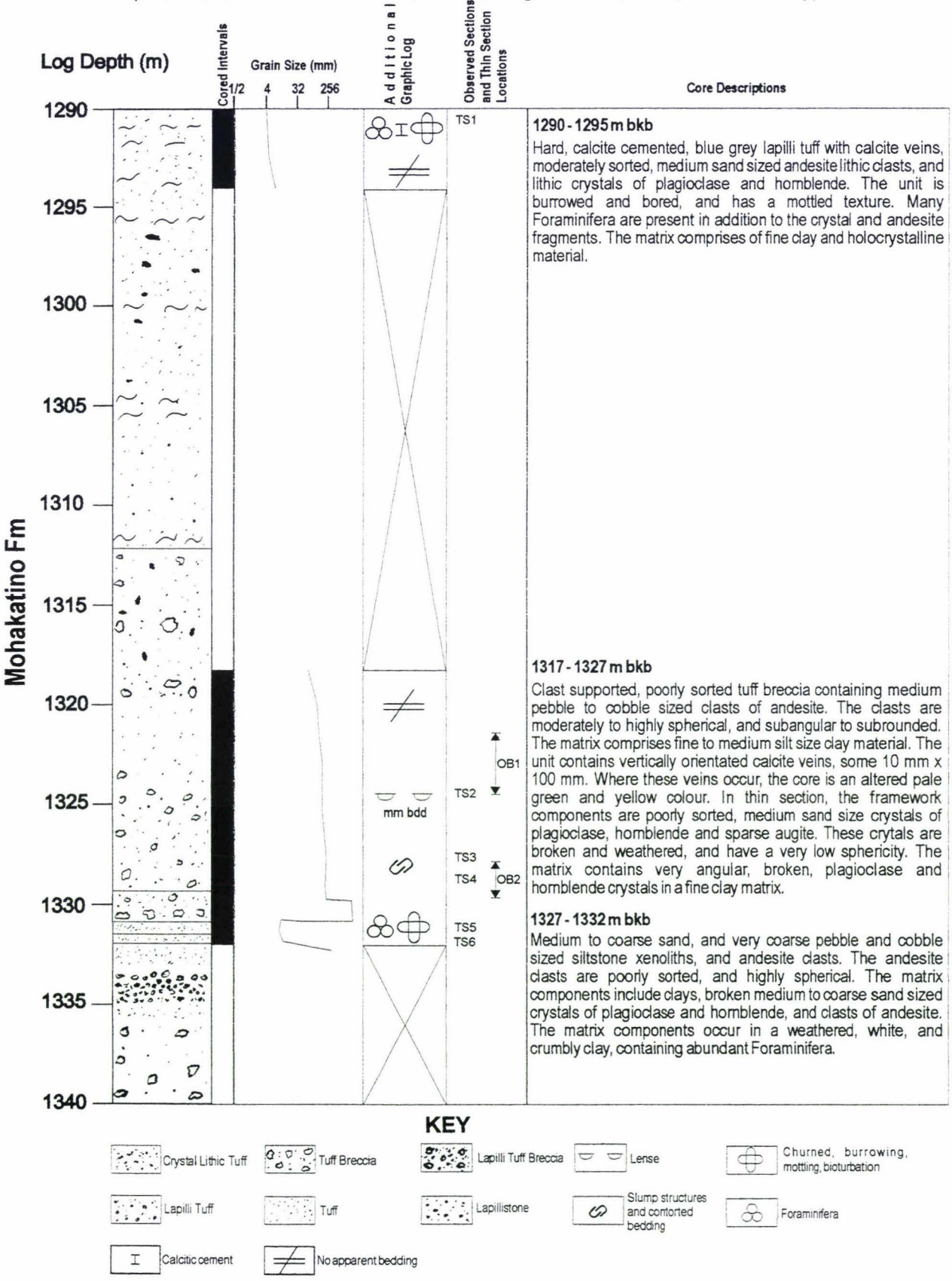

Figure 2.4
Kora-3 Lithologic Log
(After: ARCO Petroleum NZ Inc, 1988c; Bergman *et al.*, 1992; and this study)

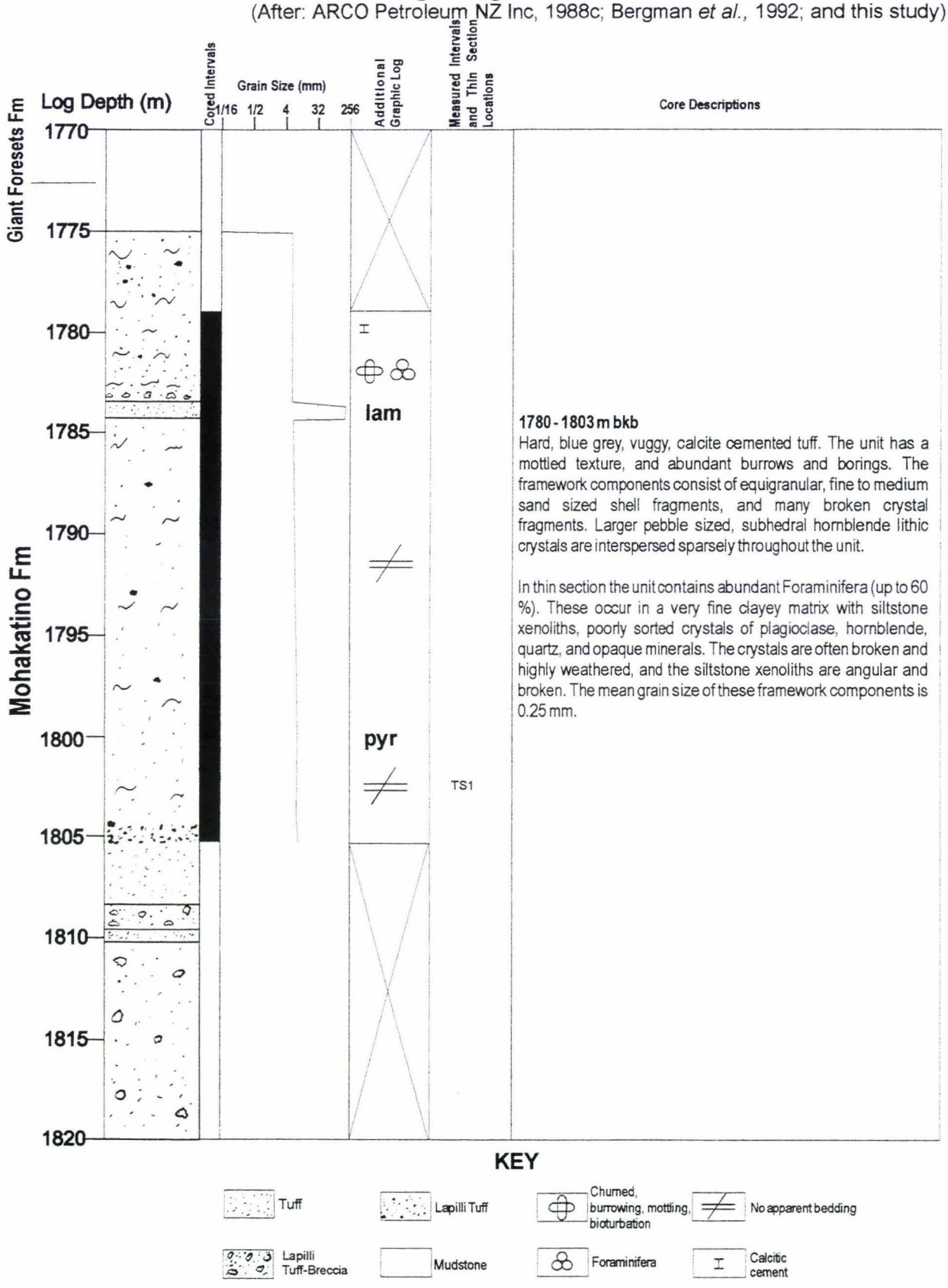

1856 m bkb and 1882 m bkb -1890 m bkb based on well log interpretation (Arco Petroleum NZ Inc., 1988a). The thickness of each conglomeratic unit in Kora-1A varies between 5 and 10 metres and these units are generally bounded above and below by tuff breccias. Conglomerates are notably absent in Kora-2 and Kora-3.

The framework clasts comprising the conglomerate are heterolithic, red, green and grey hematite altered, porphyritic andesite clasts with a 'lapilli tuff and tuff' matrix (Bergman *et al.,* 1992) (e.g. Plate 1 and Plate 2). The mean grain size for the framework clasts in OB3, OB4 and OB5 (see Table 2.1) varies between 10.26 mm and 19.69 mm, although the largest observed clasts are up to 80 mm in size. The framework clasts are poorly to moderately sorted, rounded to subrounded, and moderately spherical (elongation ratio is 1.51). The grainsize distribution for the conglomerate framework clasts also varies with depth, for example skewness values are nearly symmetrical in OB3 and OB4 while OB5 is negatively skewed. Kurtosis values also vary between platykurtic, very platykurtic, and leptokurtic for all well depths, which suggests that the dominant clast size populations measured occur in subequal proportions.

The percentage of matrix in the conglomerate varies randomly with well depth. For example the observed core interval OB3 (Fig. 2.2) contains up to 50 % matrix. The matrix in OB4 varies between 40 % and 30% of the rock. In contrast the matrix in OB5 comprises approximately 70% of the core and consists of much coarser gravelly material mixed with a very fine silt sized component (i.e. lapilli tuff). The matrix contains weathered and broken plagioclase crystals, hornblende crystals, and secondary opaque mineral growths (Appendix 4). These crystals and minerals are supported in very fine clay. For example, TS6 contains up to 30 % hornblende, 30 % plagioclase, and 5 % of the thin section is comprised of opaque minerals. The crystal components are mainly subhedral in form, and often fractured. Similarly, TS7 contains subangular and subrounded crystals of hornblende (5 %), plagioclase (30 %), and opaque minerals (2-5 %). The crystals and minerals are supported in a clay matrix, mixed with numerous 0.01 mm x 0.06 mm, plagioclase crystal fragments.

The textural characteristics of the conglomerate matrix varies little with well depth (see Table 2.2). For example, TS3 has a mean grain size of 0.13 mm and is poorly

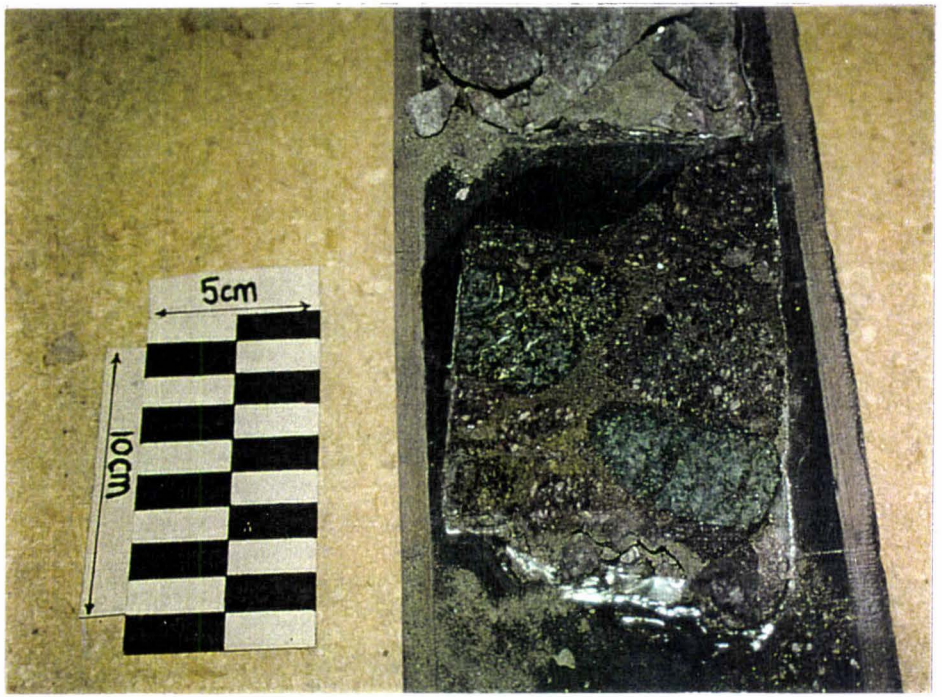

Plate 1

Kora-1A 1820.26 m

Plate 1 illustrates the distinct colouring of the framework clasts in the conglomerate, and the smooth, well rounded clast profiles.

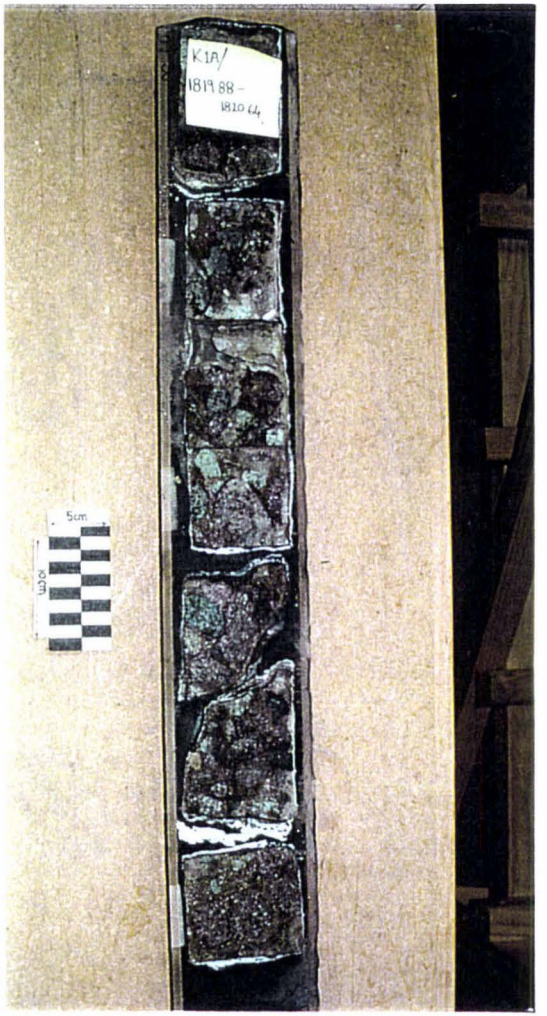

Plate 2

Kora-1A 1819.88 m - 1820.64 m

Plate 2 demonstrates the poor sorting, clast to clast contact, and typical size of the framework clasts in the conglomerate.

Table 2.1

Statistical Results from Textural Analysis of Kora-1A Hand Specimens

	Depth (m)	Mz	δ	Sk1	Kg	Mean vector	Roundness	L:B (Sphericity)	n	
OB1	1783-1785	-1.90	0.82 (*moderately sorted*)	-0.29 (*negatively skewed*)	1.03 (*mesokurtic*)	271	*subrounded to subangular*	1.62 (moderate)	65	Lapillistone
OB2	1811-1812	-2.73	0.94 (*moderately sorted*)	0.17 (*positively skewed*)	1.47 (*leptokurtic*)	59	*subangular*	1.42 (high)	30	Tuff breccia
OB3	1818-1820	-4.30	1.33 (*poorly sorted*)	-0.04 (*nearly symetrical*)	0.82 (*platykurtic*)	290	*subrounded to rounded*	1.51 (moderate)	70	
OB4	1823-1825	-3.76	1.74 (*poorly sorted*)	0.02 (*nearly symmetrical*)	0.65 (*very platykurtic*)	41	*subrounded*	1.51 (moderate)	16	Conglomerate
OB5	1826-1830	-3.36	0.90 (*moderately sorted*)	-0.27 (*negatively skewed*)	1.21 (*leptokurtic*)	59	*subrounded*	1.51 (moderate)	98	
OB6	1838-1843	-3.30	0.76 (*moderately sorted*)	0.10 (*nearly symmetrical*)	1.08 (*mesokurtic*)	270	*subangular-angular*	1.50 (moderate)	87	Tuff breccia
OB7	1907-1908	-4.56	0.93 (*moderately sorted*)	0.08 (*nearly symmetrical*)	1.08 (*mesokurtic*)	40	*subangular-angular*	1.47 (high)	35	

Statistical Results from Textural Analysis of Kora-2 Hand Specimens

	Depth (m)	Mz	δ	Sk1	Kg	Mean vector	Roundness	L:B (Sphericity)	n=	
OB1	1322-1324	-3.3	0.75 (*moderately sorted*)	-0.05 (*nearly symmetrical*)	0.93 (*mesokurtic*)	98	*subrounded to well rounded*	1.3 (very high)	24	Lapilli tuff
OB2	1328-1329	-3.93	1.11 (*poorly sorted*)	0.12 (*positively skewed*)	0.77 (*platykurtic*)	76	*subrounded to rounded*	1.45 (high)	29	

Table 2.2

Statistical Results from Textural Analysis of Kora-1A Thin Sections

	Depth (m)	Mz	δ	Sk1	Kg	Mean vector	Roundness	L:B (Sphericity)	n	
TS1	1784	2.90	1.04 (*moderately sorted*)	-0.13 (*negatively skewed*)	0.97 (*mesokurtic*)	2.60	*subrounded to rounded*	1.70 (moderate)	210	Tuffs, hyaloclastite tuffs and lapillistones
TS2	1786	2.30	0.94 (*moderately sorted*)	-0.59 (*negatively skewed*)	6.35 (*extremely leptokurtic*)	2.60	*subrounded to rounded*	1.72 (moderate)	222	
TS3	1797.5	2.97	1.17 (*poorly sorted*)	-0.14 (*negatively skewed*)	1.01 (*mesokurtic*)	66.52	*subrounded to subangular*	1.95 (low)	202	Conglomerate matrix
TS4	1803		(grain mount)				*subrounded to rounded*	1.57 (moderate)	98	Pyroclastic sand
TS5	1812.8	2.83	1.16 (*poorly sorted*)	0.06 (*nearly symmetrical*)	0.94 (*mesokurtic*)	24.30	*subrounded to rounded*	1.93 (low)	103	Tuff breccia matrix
TS6	1820	2.63	1.71 (*poorly sorted*)	0.03 (*nearly symmetrical*)	1.01 (*mesokurtic*)	331.79	*subrounded to rounded*	1.6 (moderate)	180	
TS7	1829	3.20	1.39 (*poorly sorted*)	-0.11 (*negatively skewed*)	0.95 (*mesokurtic*)	321.77	*subrounded to subangular*	1.80 (low)	190	Conglomerate matrix
*	1837	3.03	0.72 (*moderately sorted*)	-0.13 (*negatively skewed*)	1.13 (*leptokurtic*)	36.49	*subrounded to rounded*	1.90 (low)	350	
TS8	1839	2.96	1.48 (*poorly sorted*)	-0.02 (*nearly symmetrical*)	0.93 (mesokurtic)	56.12	*subrounded*	1.90 (low)	189	Tuff breccia matrix

* Not illustrated in Figure 4.2

Statistical Results from Textural Analysis of Kora-2 and Kora-3 Thin Sections

	Depth	Mz	δ	Sk1	Kg	Mean vector	Roundness	L:B (Sphericity)	n	
TS1	1290	2.71	0.71 (*moderately sorted*)	-0.14 (*negatively skewed*)	0.86 (*platykurtic*)	21.60	*subrounded to rounded*	1.81 (low)	44	Crystal lithic tuff
TS2	1324	1.96	1.51 (*poorly sorted*)	-0.31 (*very negatively skewed*)	0.96 (*mesokurtic*)	81.70	*subrounded to rounded*	2.03 (low)	136	
TS3	1327	2.26	1.05 (*poorly sorted*)	-0.30 (*negatively skewed*)	0.83 (*platykurtic*)	43.56	*subrounded to subangular*	1.89 (low)	64	
TS4	1332.5a	2.06	0.99 (*moderately sorted*)	-0.03 (*nearly symmetrical*)	0.84 (*Platkykurtic*)	81.20	*subrounded and rounded*	1.95 (low)	193	Tuff breccia matrix and lapilli tuff
TS5	1332.5b	2.30	1.09 (*poorly sorted*)	-0.14 (*negatively skewed*)	0.94 (*mesokurtic*)	59.93	*subrounded and rounded*	1.89 (low)	235	
TS6	1328	1.98	1.04 (*poorly sorted*)	-0.80 (*nearly symmetrical*)	0.21 (*very platykurtic*)	71.14	*subrounded and rounded*	2.02 (very low)	164	
TS1	Kora-3/1803	2.16	1.13 (*poorly sorted*)	-0.20 (*negatively skewed*)	0.89 (*platykurtic*)	301	*subrounded*	1.89 (low)	89	Crystal lithic tuff

sorted. The matrix components are subrounded to subangular, and have a mean elongation ratio of 1.95, demonstrating a low sphericity. TS6 has a mean grain size of 0.16 mm, the matrix is poorly sorted, and the clasts are more spherical than for TS3, as shown by the smaller elongation ratio of 1.60. The grain size distribution of the framework components in the matrix is also relatively uniform. For example, the framework components of TS4 and TS7 are negatively skewed and mesokurtic, and similar to TS6, which is nearly symmetrical and mesokurtic.

Whole-rock XRD analyses (Table 2.3 and Fig. 2.5) indicate that andesine, amphibole, augite, magnetite, calcite, zeolites, hematite, pyrite, quartz and clay minerals dominate the conglomerate matrix. The proportion of quartz is greater in the conglomerate is than in the other lithologies, and the total clay content is lower in the conglomerate than in the finer grained tuffs and hyaloclastite tuffs.

The mean vector for both the framework clasts and the matrix components in the conglomerate, show that the clasts generally display a lack of imbrication. However, because the number of clasts measured is limited, and the orientation of the sections of core unknown, it is not possible to unequivocally establish whether there is clast imbrication.

The fabric of the framework clasts within the conglomerate in Kora-1A is best illustrated in Figs. 2.6, 2.7, 2.8, and Plates 1, 2, 3 and 4. The sketches and photographs show that the larger conglomerate clasts are very rounded, with varying degrees of matrix support and sorting, and are commonly fractured (e.g. Plate 4).

Tuff Breccia

The tuff breccias are the most common lithology in the cored interval of Kora-1A (Arco Petroleum NZ Inc., 1988a). They occur at 1788 m bkb to 1794 m bkb, 1809 m bkb to 1818 m bkb, 1830 m bkb to1844 m bkb, 1895 m bkb to 1912 m bkb. They are also inferred at 1850 m and 1895 m based on geophysical logs (Arco Petroleum NZ Inc., 1988a). The tuff breccias vary in thickness between 10 m and 15 m, with the thickest unit located between 1830 m bkb and 1845 m bkb and the smallest unit located between 1788 m bkb and 1794 m bkb. These units are generally bounded

Table 2.3
Major Mineralogical Components (wt %) derived from XRD of Lithologies from Kora-1A, Kora-2 and Kora-3

Exploration Well and Depth of Sample	Quartz	Feldspar	Calcite	Analcite	Vermiculite	Magnetite	Hornblende	Illite	Zeolite	Total %
Kora-1A										
1788.24 m (bkb)	18	58			15		9			100
1803 m (bkb)		48.48			9.09	24.2	18.23			100
1812.8 m (bkb)	12.4	66.8					20.8			100
1839 m (bkb)	14	50			5	10	14	7		100
1905.25 m (bkb)		48.4			10.38	17.32	23.9			100
Kora-2										
1290.7 m (bkb)		24.19	41.39						34.42	100
1324.2 m (bkb)		66.86	11.3		4.04		17.8			100
1327.2 m (bkb)	32.5	40.4						7.1	20	100
1327.7 m (bkb)	9.47	24.1	18.65			11.43	27.9	8.45		100
1332.5 m (bkb)	16.9	43.4			8.2		17.5		14	100
Kora-3										
1783.6 m (bkb)	3	4	6	84	3					100
1803.5 m (bkb)	16	20.6	22.5		6.9				34	100

Figure 2.5 (Bergman *et al.*, 1992)

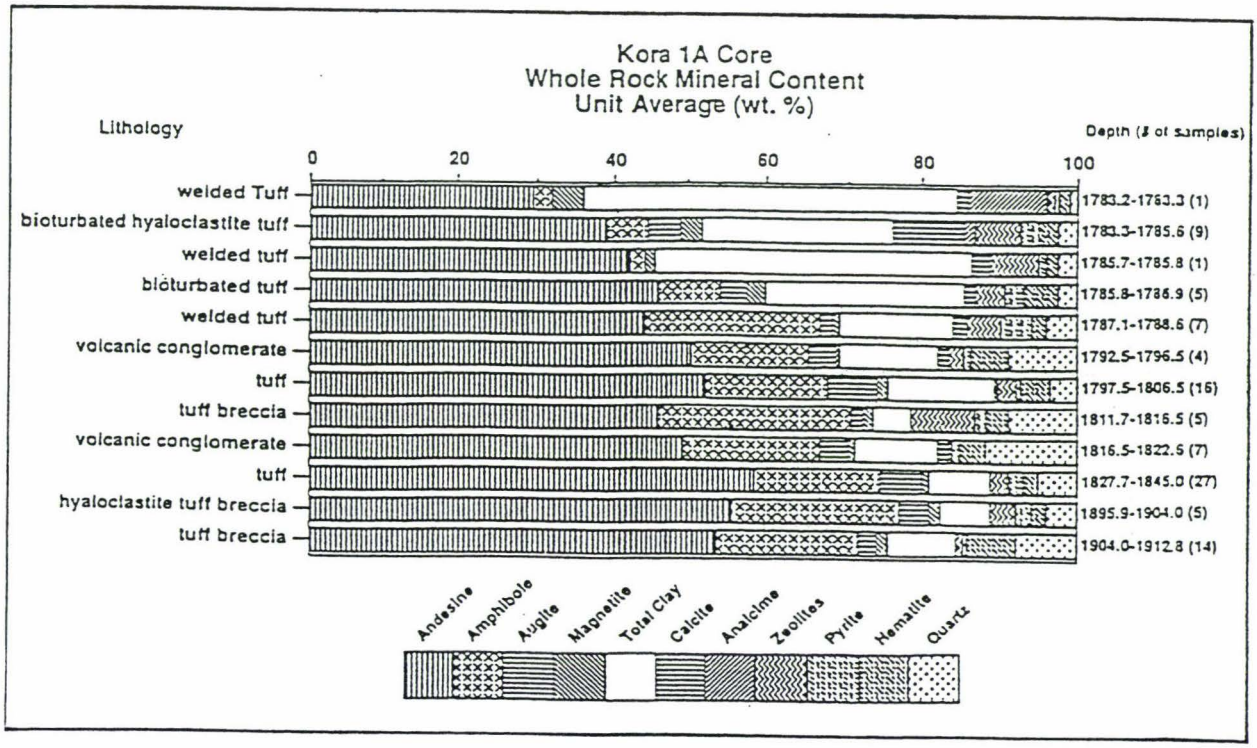

Figure 2.6

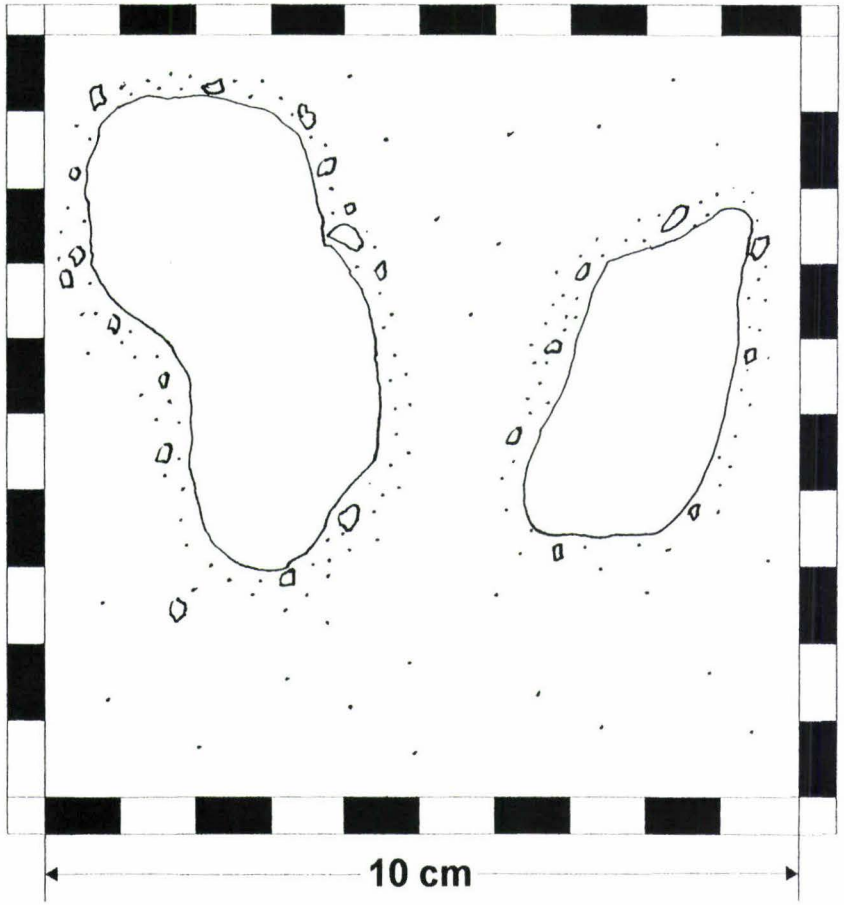

Kora-1A 1821.93 m - 1825.15 m

A sketch of two large, cobble sized, subrounded, porphyritic textured, clasts of andesite. The clasts are surrounded by a halo of angular, andesite pebbles. The larger clasts and encompassing halo are supported by a matrix of fine hornblende rich, volcaniclastic sand.

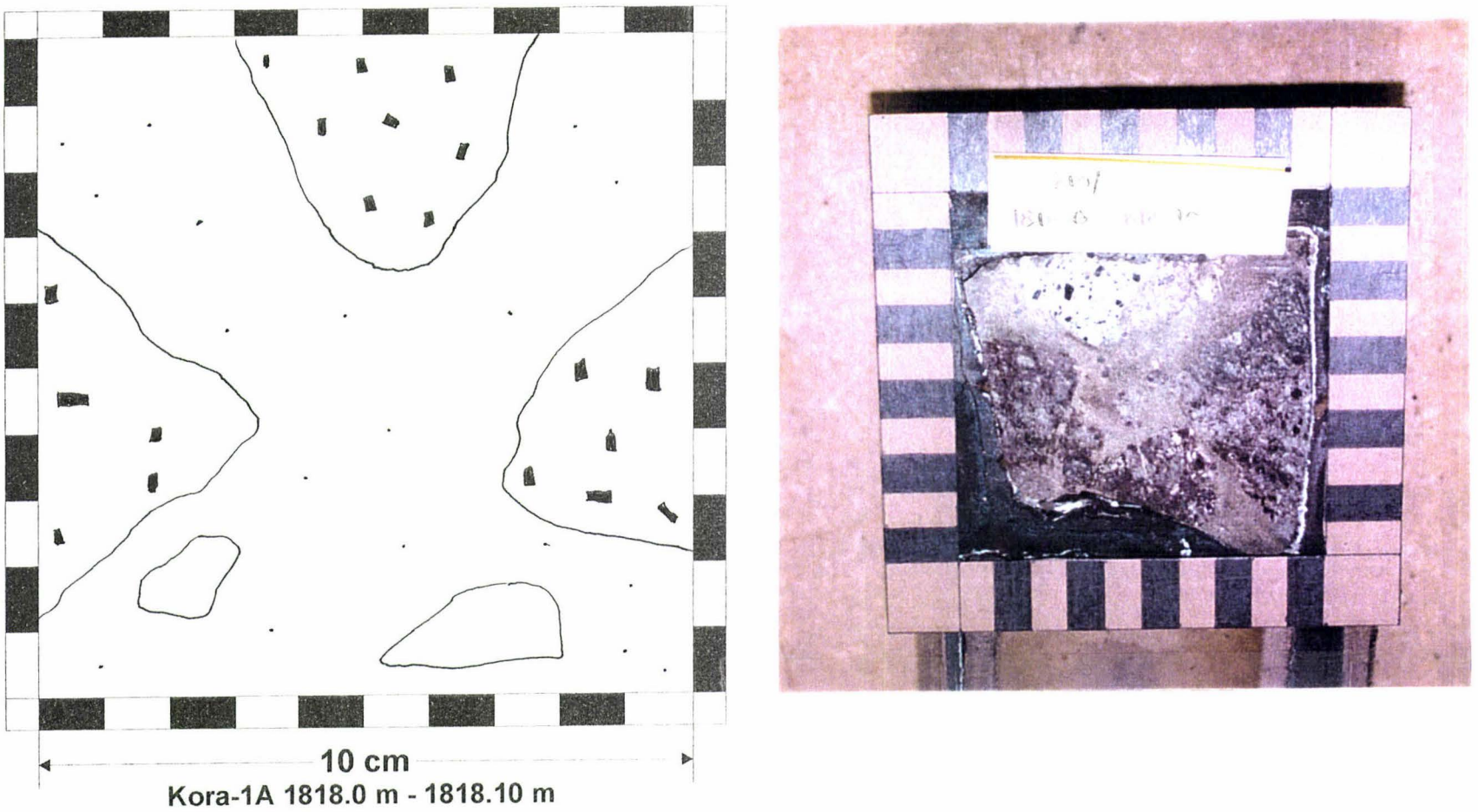

Figure 2.7

A sketch and photograph illustrating cobble sized, subrounded, red and grey, porphyritic textured clasts of andesite. The clasts are supported by a sandy matrix and surrounded by subangular pebbles.

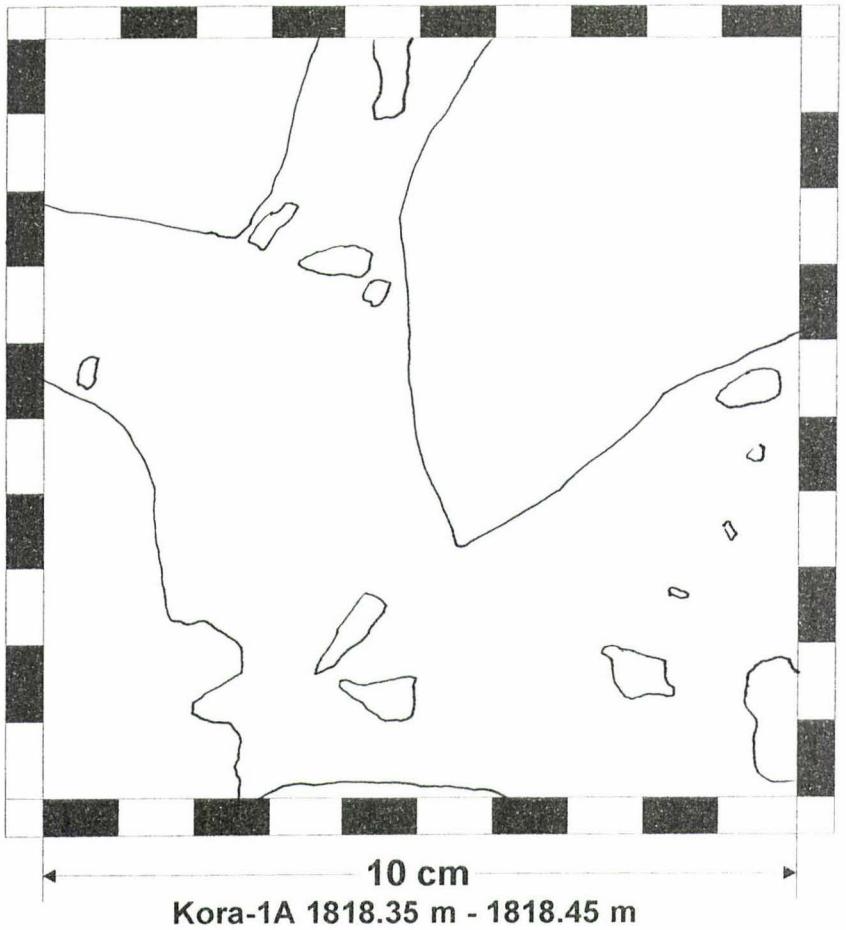

Figure 2.8

This sketch and photograph show smooth, rounded, red porphyritic clasts, and small angular to very angular, red porphyritic clasts. The matrix consists of medium to coarse, equigranular volcaniclastic sand. Note that the small angular clasts are derived from the large, rounded framework clasts.

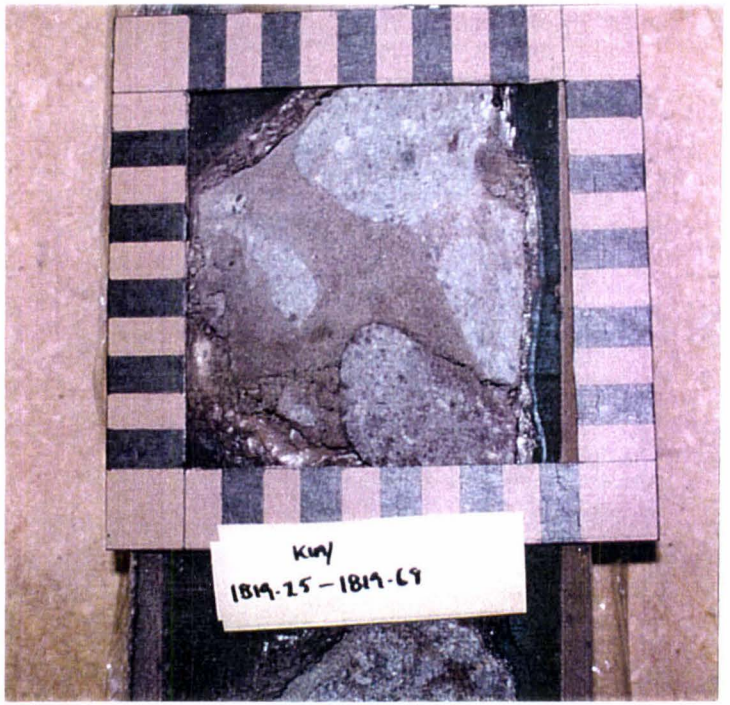

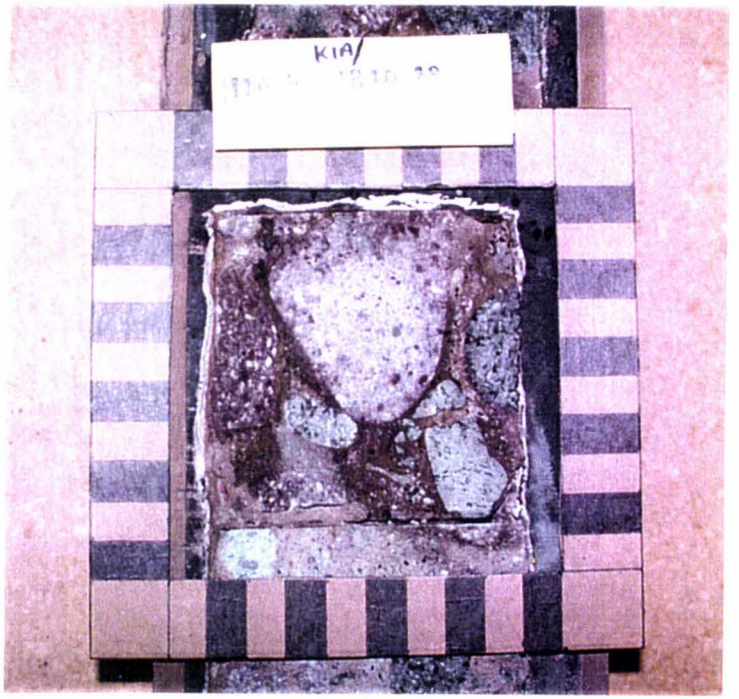

Plate 3

The square grid shown for scale in Plate 3 and Plate 4 is 10 cm x 10 cm

Plate 4

Plate 3 and Plate 4

Plates 3 and 4 illustrate the fractured framework clasts in the conglomerate in Kora-1A. The distance between the broken pieces of the fractured,greeny grey, clast, in the bottom right hand corner of plate 4, is no more than 4 mm. Plate 3 and plate 4 also illustrate the variation in the proportion of matrix that comprises the conglomerate in Kora-1A. The conglomerate in plate 3 contains up to 40 % matrix, while the conglomerate in plate 4 contains approximately 10 - 15 % matrix.

above and below by conglomerates and are more prevalent in Kora-1A than either Kora-2 or Kora-3.

The framework clasts in the tuff breccias include angular to subangular pebbles and very coarse pebbles of andesite. The clasts are highly spherical to moderately spherical fragments of andesite, similar to the red, green and grey porphyritic textured clasts in the conglomerates, and other equigranular textured, pale grey clasts. The mean size of the clasts varies between 6.63 mm and 22.62 mm, and the whole rock is moderately sorted. The general distribution of the grain sizes varies, for example skewness is positive to nearly symmetrical and kurtosis is leptokurtic to mesokurtic.

The percentage of matrix in the tuff breccia varies in Kora-1A. For example OB2 comprises 75 % matrix and 25 % clasts, with the clast density only increasing slightly to nearly 40 % near the base of OB2. This proportion is similar to the matrix in OB6, which comprises 60-70 % of the observed core. In contrast, the matrix in OB7 constitutes 10 % of the core.

In thin section the framework components in the tuff breccia matrix have a mean grain size between 0.12 mm and 0.14 mm. The matrix components include subrounded to rounded, poorly to moderately sorted, crystal fragments and lithic clasts of andesite. The clasts have a low sphericity; the elongation ratio of the crystals and clasts is 1.9, notably higher than the framework components in the conglomerate matrix (see Table 2.2). For example, the framework clasts in TS5 are supported by many small <.02 mm lithic crystal fragments and a very fine clay component, which comprises 40 % of the thin section (see thin section descriptions in Appendix 4). Grain size statistics for TS5 show that the mean grain size for the framework crystals and lithic clasts is 0.14 mm. The crystals and lithics are poorly sorted, subrounded to rounded and have a low sphericity (the elongation ratio is 1.93). The distribution of grain sizes in the tuff breccia matrix at all depths sampled, is nearly symmetrical to negatively skewed, and mesokurtic to leptokurtic.

The whole-rock composition of the tuff breccia consists of andesine, amphibole, augite, magnetite, calcite, zeolites, pyrite, hematite and quartz (Table 2.3, and Fig. 2.5). This assemblage does not change significantly in tuff breccias at other

stratigraphic levels in Kora-1A; like the conglomerate, the tuff breccia is depleted in total clay content, and slightly more enriched in quartz relative to the other lithologies in Kora-1A.

The clast fabric in the tuff breccias is illustrated in plates 5, 6, 7, 8, and in Figs. 2.9 and 2.10. The illustrations show that the textural fabric in the tuff breccia is more diverse than the statistical data indicate. That is to say, the grain size and fabric variations in Kora-1A occur gradually, although in places abrupt changes do occur. For example, at 1897.75 m bkb (see Plate 8) there is an abrupt, change. The upper unit contains closely packed/clast supported, 30 mm x 30 mm subangular, moderately spherical clasts. The lower unit is fine grained and matrix supported, containing smaller 5 mm x 2 mm subangular, moderately spherical clasts. The exact thickness of each unit is difficult to discern because sections of core are missing. However, based on the thickness of the next deepest lithological unit, the unit beneath the contact is probably no more than one metre thick. The tuff breccia is also variably sorted throughout Kora-1A. For example, visual estimates (Compton, 1962; *in* C.King, 1992) show the tuff breccias units at 1811.8 m bkb (Plate 5) and 1830.9 m bkb (Plate 6) are poorly sorted, whereas at depths of 1845.21 m bkb and 1898 m bkb the tuff breccias are moderately to well sorted.

Tuffs, Hyaloclastite Tuffs, and Lapillistones

The top 7 m of Kora-1A between 1781 m bkb and 1788 m bkb, consist of interbedded tuffs, hyaloclastite tuffs and lapillistone (Fig. 2.2). The framework components in these units (OB1) include clasts of andesite and broken crystals of plagioclase and hornblende. These clasts and crystals are sub-rounded to subangular, moderately spherical (elongation ratio is 1.62), moderately sorted, and have a mean grain size of 3.73 mm. The grain size distribution is also negatively skewed and mesokurtic (Table 2.1).

In thin section (TS1 and TS2), the crystal components include hornblende (10 %), plagioclase (30 %), augite (5 %), glauconite (5-15 %) and opaques (5-10 %) (Appendix 4). The matrix comprises 50 % of TS1 and consists of poorly sorted, clast supported, andesite lithics, and clay. The whole-rock mineralogy of the tuffs, hyaloclastite tuffs and lapillistone (Fig. 2.5), is dominated by the same mineral

Plate 5

Kora-1A 1811.8 - 1812 m

The tuff breccia between 1811.8 m and 1812 m in Kora-1A, contains angular andesite framework clasts, the high percentage of matrix (up to 80 %), the coarse gritty texture of the matrix, and vertically orientated fractures in a framework clast near the bottom right hand corner of the core.

The square grid shown for scale in Plate 5 is 10 cm x 10 cm

Plate 6

Kora-1A 1830.9 m

The tuff breccia at 1830.9 m in Kora-1 contains the same coarse lapilli tuff matrix, and angular framework clasts as observed in plate 5. Note also, that the framework clasts observed in both plate 5 and plate 6 consist of similar porphyritic textured lithologies, and the average size of these framework clasts is also very similar.

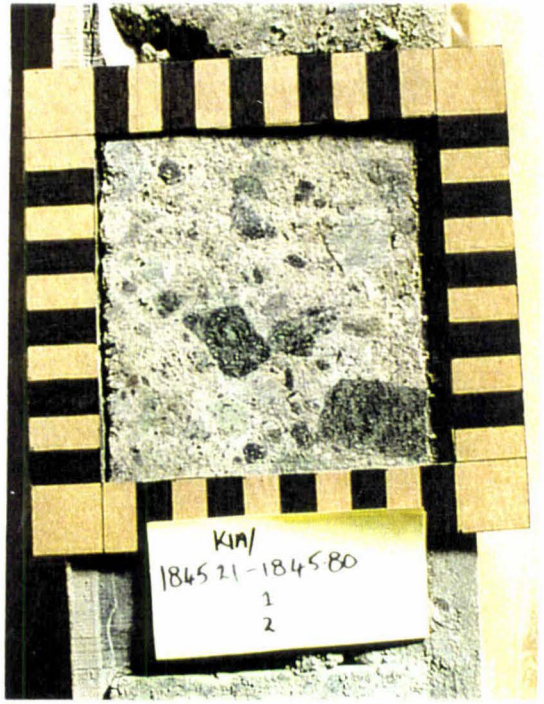

Plate 7

Kora-1A 1845.21 - 1845.8 m

In this portion of the tuff breccia between 1845.21 m and 1845.8 m in Kora-1A the variable textural character of the tuff breccias is apparent. This tuff breccia consists of closely spaced subangular framework clasts, and a fine clay and tuffaceous matrix. The matrix contributes up to 30 % of the core.

The square grid shown for scale in Plate 7 and Plate 8 is 10 cm x 10 cm

Plate 8

Kora-1A 1897.75 - 1898.5 m

Plate 8 displays a sharp textural change between 1897.75 m and 1898.5 m in Kora-1A. The lithology above the contact is a clast supported breccia, and the framework clasts in the unit are very coarse subangular and sub rounded pebbles. The lithology below the contact is a lapilli tuff. The matrix in the tuff breccia is the same as the lapilli tuff in the lower unit. The contact between the two lithologies is slightly rippled.

Figure 2.9

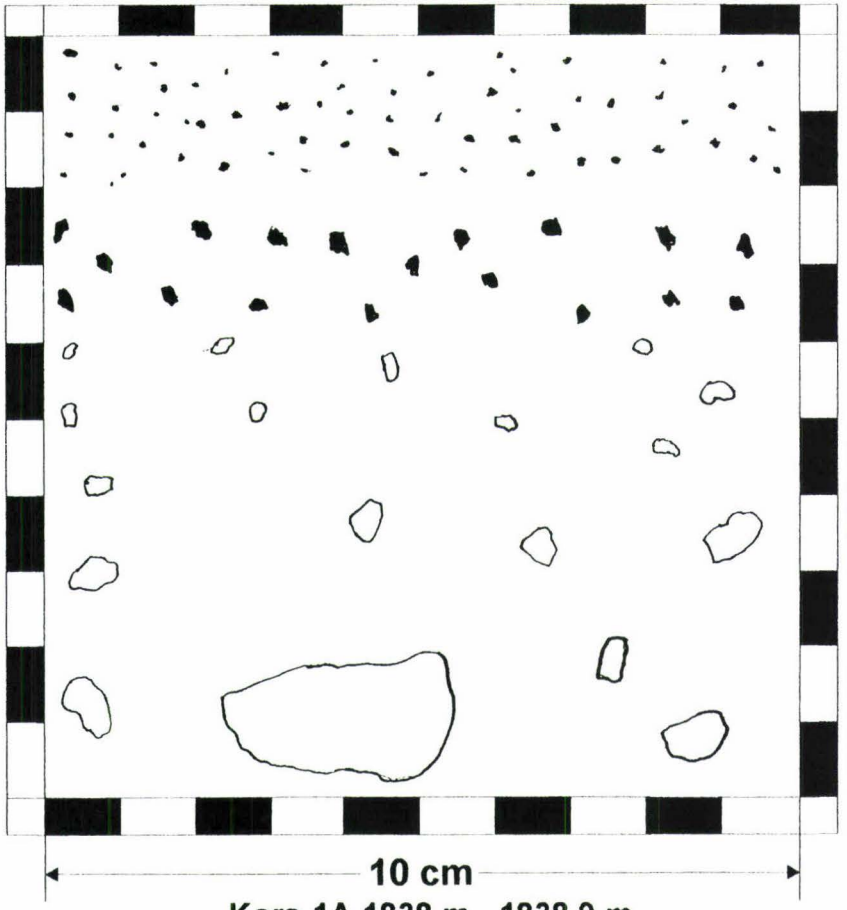

Kora-1A 1838 m - 1838.9 m

A sketch illustrating the size grading of clasts in the tuff breccia at this well depth. The smaller clasts are more densely packed than the larger clasts located near the base of this sketch.

Figure 2.10

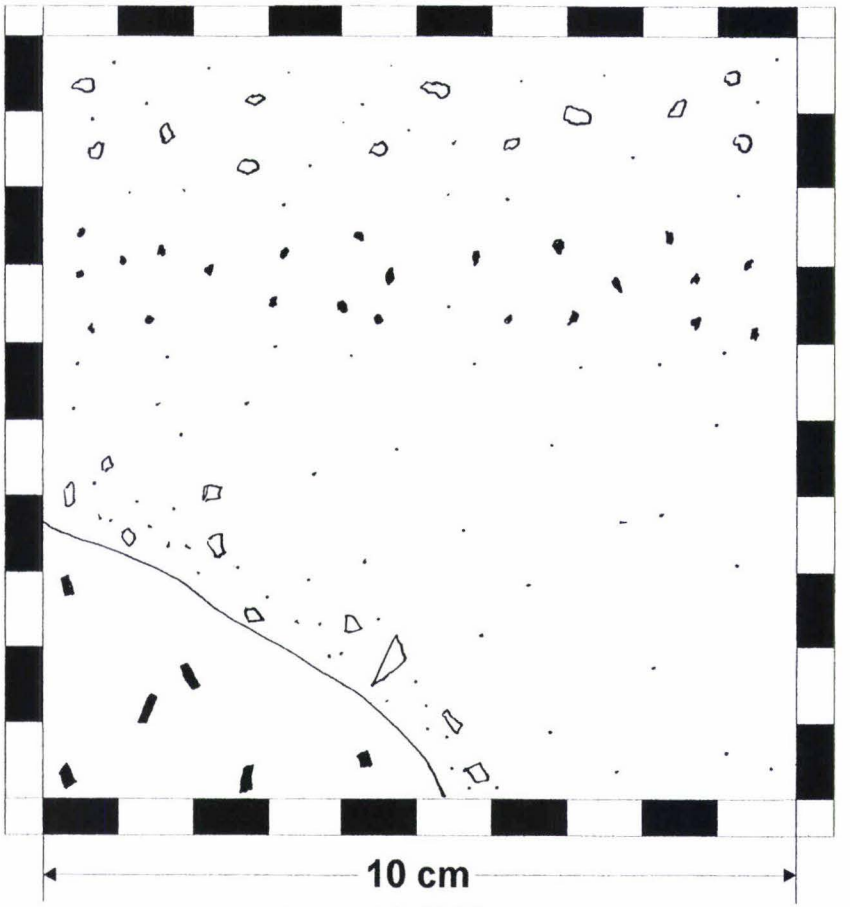

Kora-1A 1899.4 m

This sketch illustrates a halo of angular gravel fragments surrounding a large round porphyritic clast in the lower left corner of the sketch. The upper portion of the sketch shows two pebbly lenses separated by a matrix of fine sandy and clayey volcaniclastic sediment

assemblage as the tuff breccias and conglomerate in Kora-1A, i.e. andesine, amphibole, augite, magnetite, calcite, analcime, zeolite, pyrite, hematite and quartz. However, the relative proportion of minerals varies between lithologies. For example, the tuffs, hyaloclastite tuffs and lapillistone all contain a greater proportion of clays, with lesser andesine (30 – 40 wt%) and quartz (up to 5 wt%), compared to the tuff breccias and conglomerates (andesine 40 – 50 wt%; quartz 5 – 10 wt%).

The arrangements of the framework clasts in the tuffs, hyaloclastite tuffs and lapillistone are complex. Plates 9 to 14 illustrate small-scale 100 mm -200 mm thick units, containing burrows and borings. Plate 12 illustrates a typical section of core between 1784.21 m bkb and 1785.03 m bkb, and the visual variations in textural fabric. Plates 14A to 14D illustrate the fabric of the tuffs in thin section.

2.3.3 Kora-2 Core Observations

The lithologies in Kora-2 include crystal lithic tuffs and intermixed tuff and lapilli tuff breccias (Arco Petroleum NZ Inc., 1988b; Bergman *et al.*, 1992; and in this study) (see Fig. 2.3) (Plates 15 to 19). These lithologies are predominantly fine grained, compared with the lithologies of Kora-1A and have been subjected to more intense bioturbation. Consequently most of the primary depositional structures in Kora-2 have not been preserved (Bergman *et al.*, 1992).

Crystal Lithic Tuffs

The cored interval containing the crystal lithic tuff is located between 1290 m bkb and 1294 m bkb. A summary of lithologies from this interval is presented in Fig. 2.3.

The framework components comprising the crystal lithic tuffs (TS1) include crystals of plagioclase (5-10 %), hornblende (2 %), and secondary mineral growths of opaques (5 %) and glauconite, which occurs as a secondary mineral around the framework grains (Appendix 4). The crystals of the lithic tuff are on average 0.15 mm in size, moderately sorted, negatively skewed and platykurtic. They are subrounded to rounded and have a moderate to low sphericity (elongation ratio is 1.81).

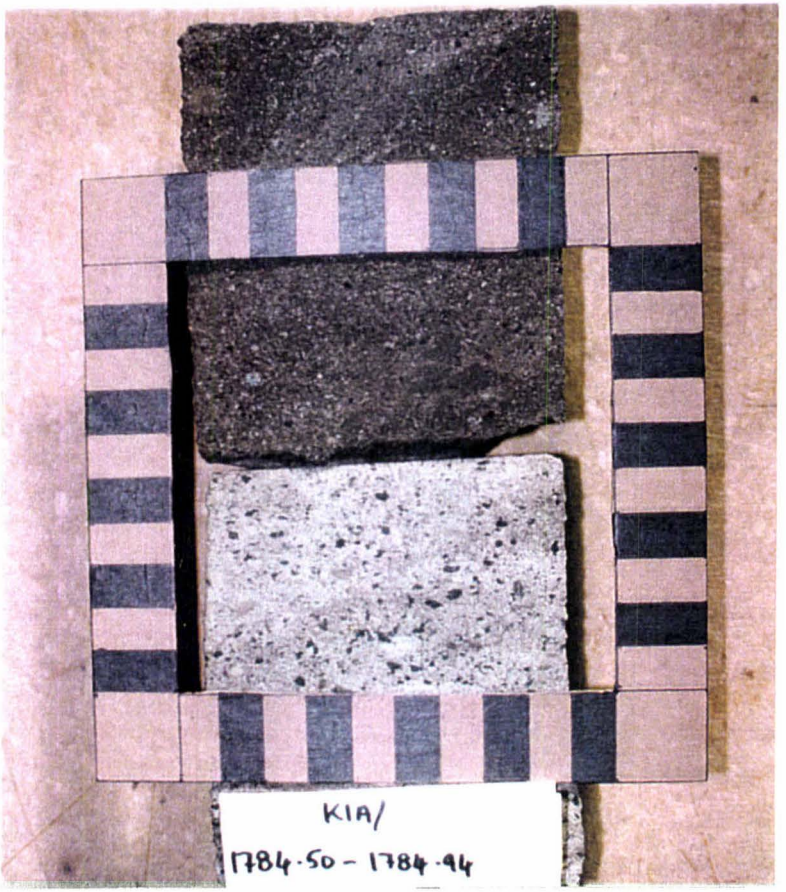

Plate 9
Kora-1A 1784.5 - 1784.94 m

A section of core from between 1784.5 m and 1784.94 m in Kora-1A illustrating two lithologic units. The upper unit is a dark coloured equigranular tuff, and the lower unit is a pale, mottled, calcareous tuff, containing angular, pebble sized crystals, and clasts of andesite. The exact nature of the contact between these two units is unclear because the section of core containing the contact is absent.

Plate 10
Kora-1A 1783 - 1783.98 m

Plate 10 depicts a section of core between 1783 m and 1783.98 m in Kora-1A. The photograph illustrates the subtle grading from tuff to lapilli tuff and back to tuff over a depth of no more than 150 mm.

The square grid shown for scale in Plate 9 and Plate 10, is 10 x 10 cm

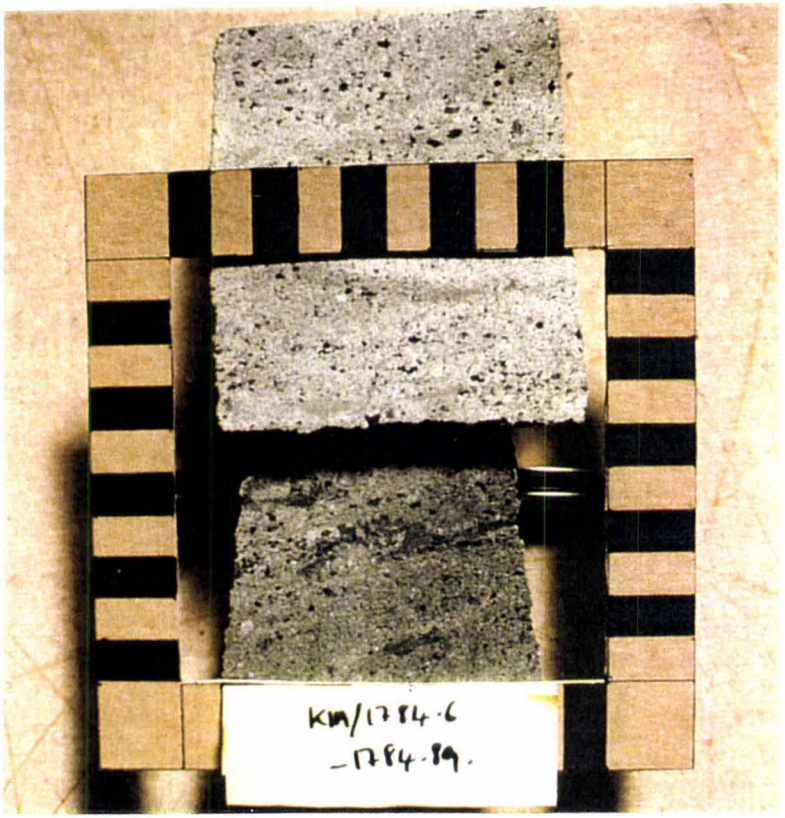

Plate 11

Kora-1A 1784.6 - 1784.89 m

Plates 11 and 12 illustrate the rapid transition between tuff and lapilli tuff units between 1784.2 m and 1785 m in Kora-1A. Note the mottled/?bioturbated texture of the pale coloured units.

The grid shown for scale in Plate 10 is 10 cm x 10 cm

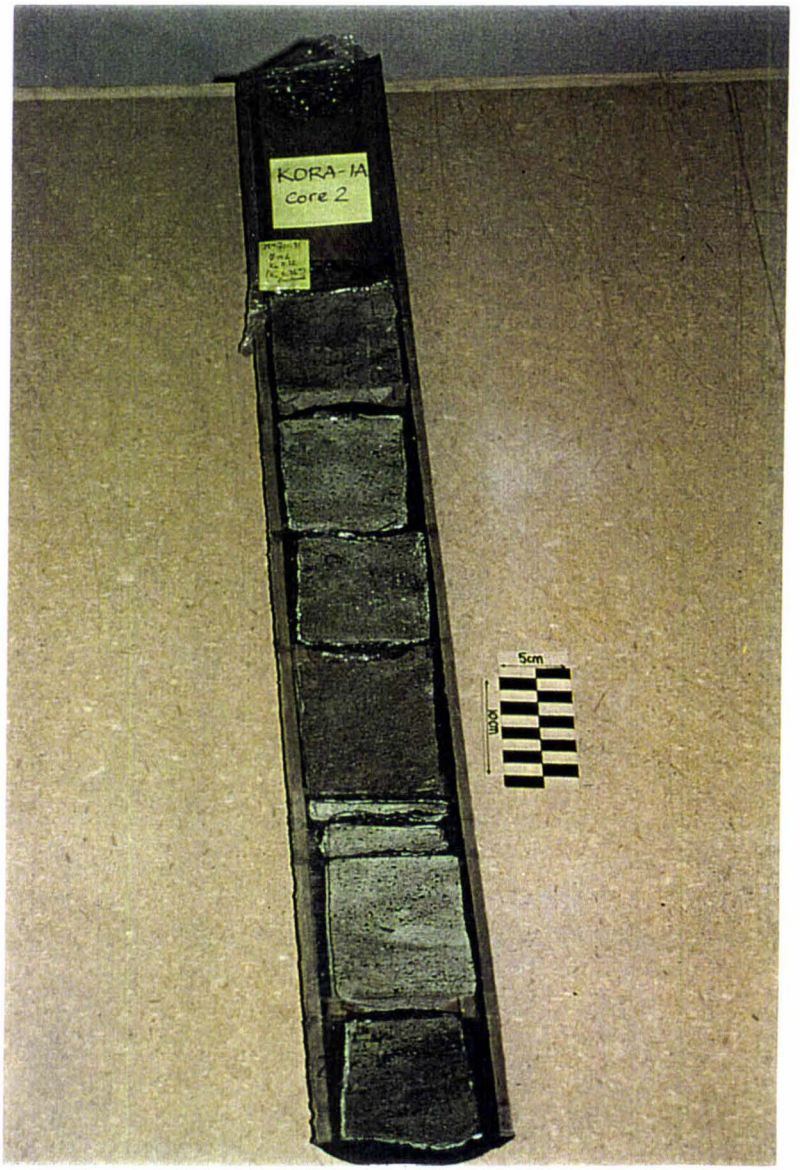

Plate 12

Kora-1A 1784.2 - 1785 m

Plate 13

Kora-1A 1785.72 - 1785.82 m

A fine ash unit between 1785.72 m and 1785.82 m in Kora-1A contains poorly sorted, subangular and angular clasts of andesite, and calcite lined vugs.

The grid shown for scale in Plate 13 and Plate 14 is 10 cm x 10 cm

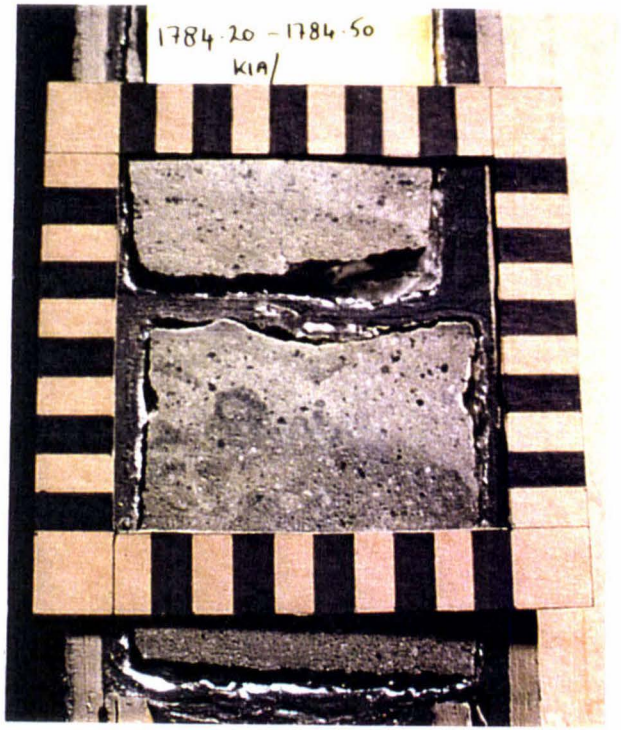

Plate 14

Kora-1A 1784.2 - 1784.5 m

A bioturbated contact between 1784.2 m and 1784.5 m in Kora-1A. The upper lithology is a crystal rich, light coloured lapilli tuff, and the lower lithology is a darker, crystal depleted tuff. The contact between these two units is burrowed and bored.

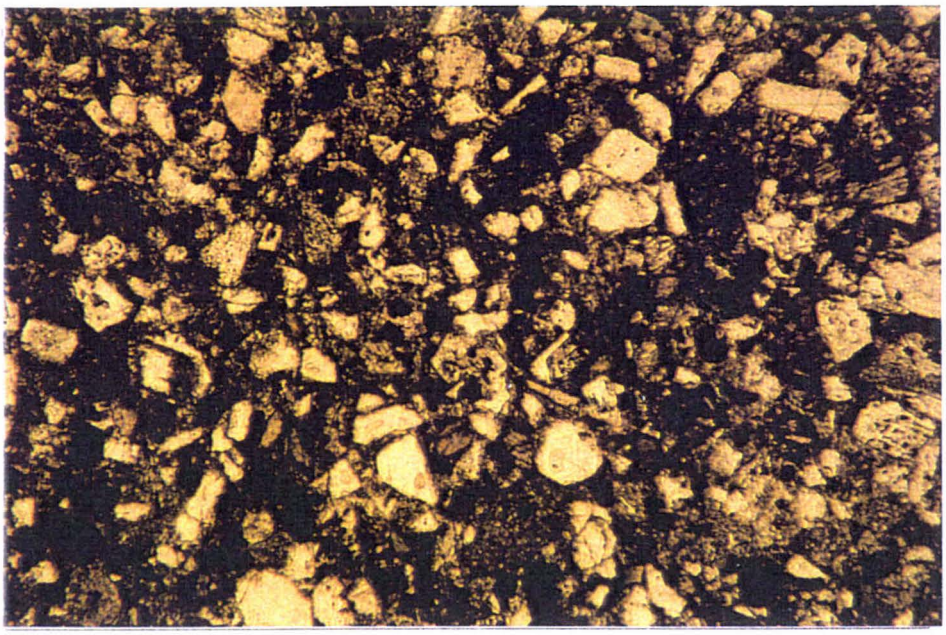

Plate 14A

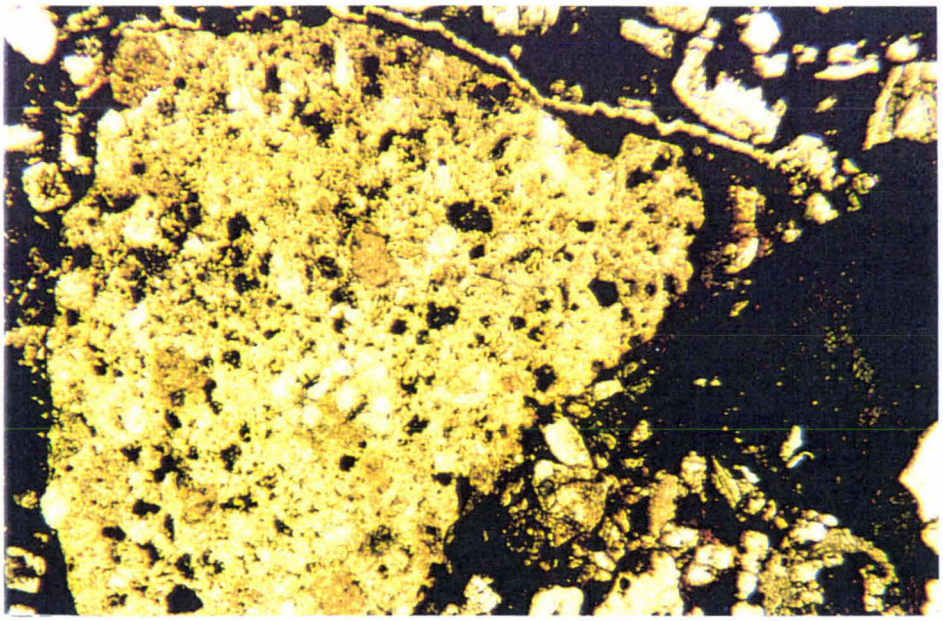

Plate 14B

Plate 14A and Plate 14B

Plates 14A and 14B are photomicrographs of the tuff located at 1784.3 m in Kora-1A. The photomicrographs illustrate densely packed, angular and subangular plagioclase crystal fragments and lithic clasts of andesite. The lithic clasts and crystal fragments are supported in a clay matrix. Plate 14B contains larger lithic clasts, and many smaller, angular, crystal fragments.

All photomicrographs were taken in plane polarized light with the magnification set on 25x

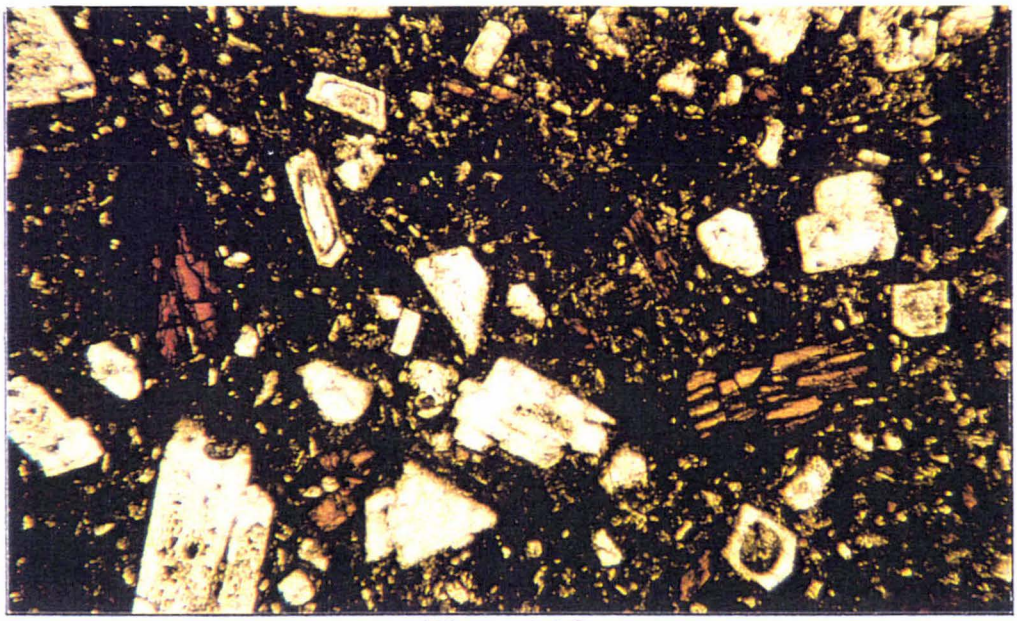

Plate 14C

Plate 14C is a photomicrograph of the welded lapillistone (Arco Petroleum NZ Inc., 1988a) at 1786.96 m in Kora-1A. The dominant components in plate 14C are crystal fragments of hornblende and plagioclase. Some of the crystal cores are dissolving, for example the large plagioclase crystal near the bottom left hand corner of the plate. The matrix surrounding the crystals is comprised of calcite and many smaller (< 0.1 mm) crystal fragments.

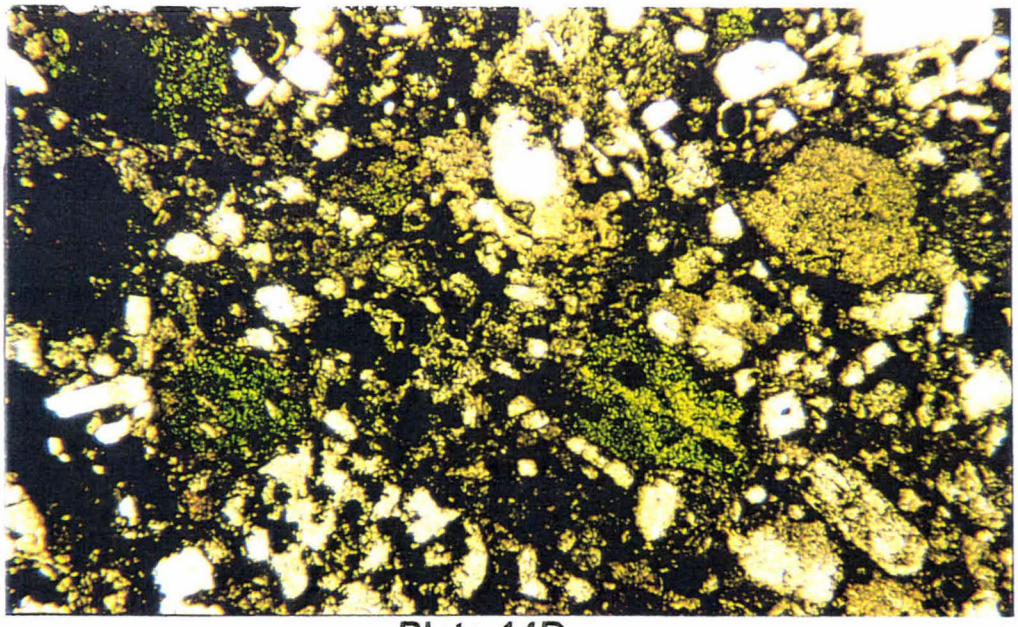

Plate 14D

Plate 14D is a photomicrograph of the tuff at 1797.5 m in Kora-1A. The plate illustrates a densely packed, poorly sorted clast fabric with a minor matrix component. The dominant components in the photomicrograph are subhedral plagioclase crystals and andesite lithics. The matrix contains glauconite, opaque minerals and many small (<0.5 mm) crystal fragments.

All photomicrographs were taken in plane polarized light with the magnification set on 25x

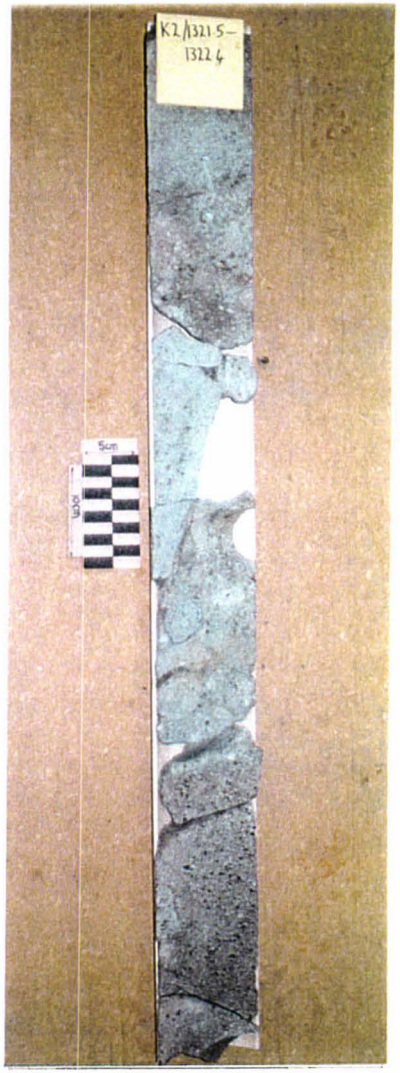

Plate 15

Kora-2 1321.5 - 1322.4 m

Plate 15 illustrates the hard, grey, homogenous, clay altered, andesitic lapilli tuff, between 1321.5 m and 1322. 4 m in Kora-2.

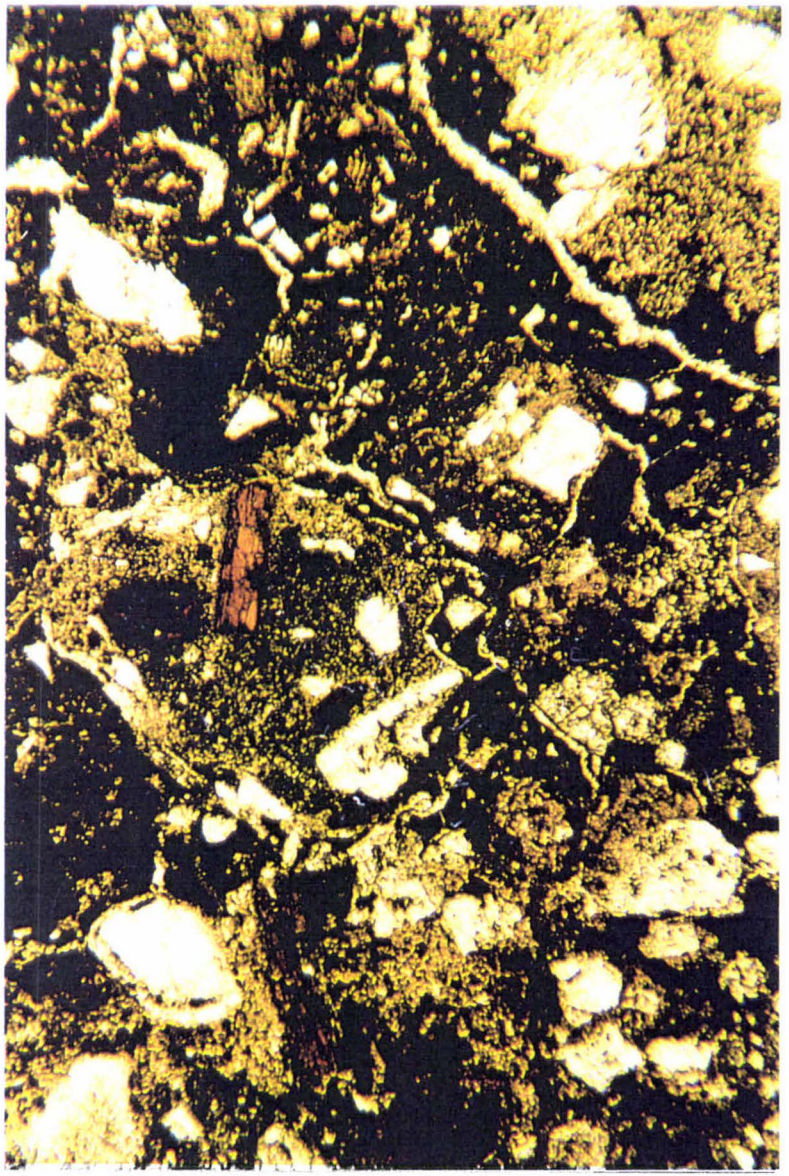

Plate 15A

Plate 15A is a photomicrograph of the calcite cemented, bioturbated, crystal lithic tuff (Arco Petroleum NZ Inc., 1988c) at 1290 m in Kora-2. The plate illustrates the calcite cement that forms a lining around each of the lithic clasts and crystals in the rock.

Plate 16

Kora-2 1326.9 m

Plate 16 depicts an erosional lithological contact at 1326.9 m in Kora-2. The upper lithology is an equigranular, clay altered, lapilli tuff, and the lower lithology contains very angular siltstone slump blocks, and clasts of andesite in a fine tuffaceous matrix. The contact between the upper and lower lithologies is very uneven and abrupt.

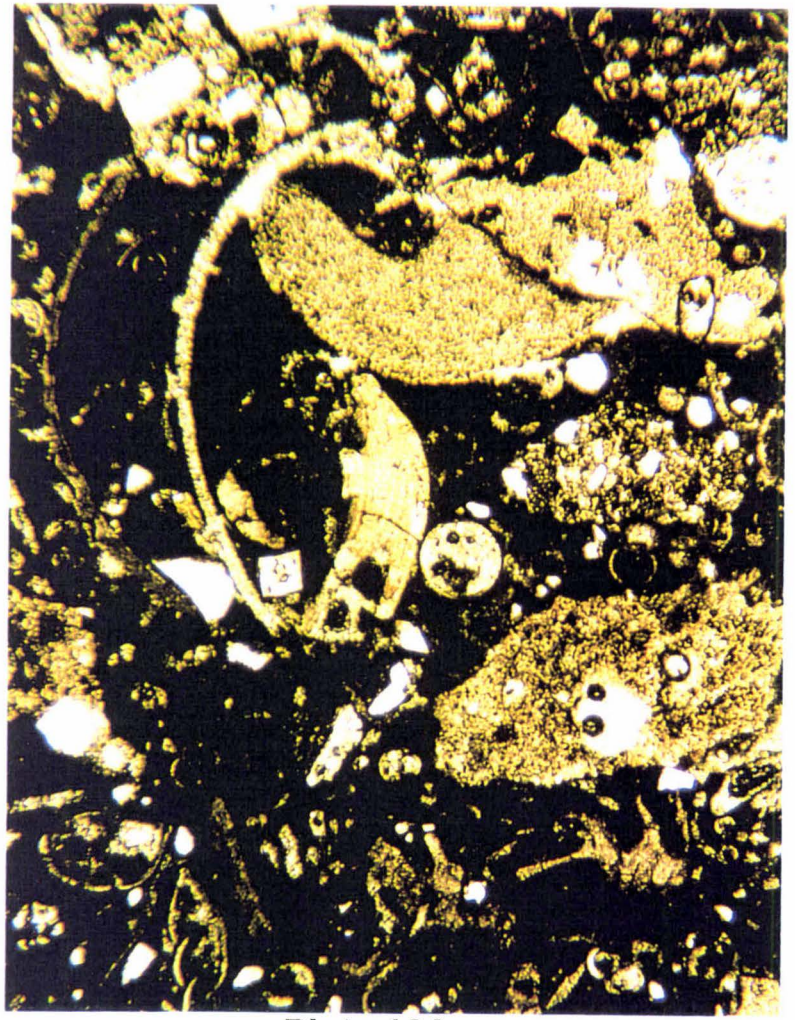

Plate 16A

Plates 16A and 16B are photomicrographs of the clay altered lapilli tuff at 1327 m in Kora-2. The most prominent features in these two plates are the high proportion of pelagic foraminifera (up to 85 %), the occurrence of subangular andesite lithic clasts, and the lack of crystals and crystal fragments.

All photomicrographs were taken under plane polarized light with the magnification set on 25x

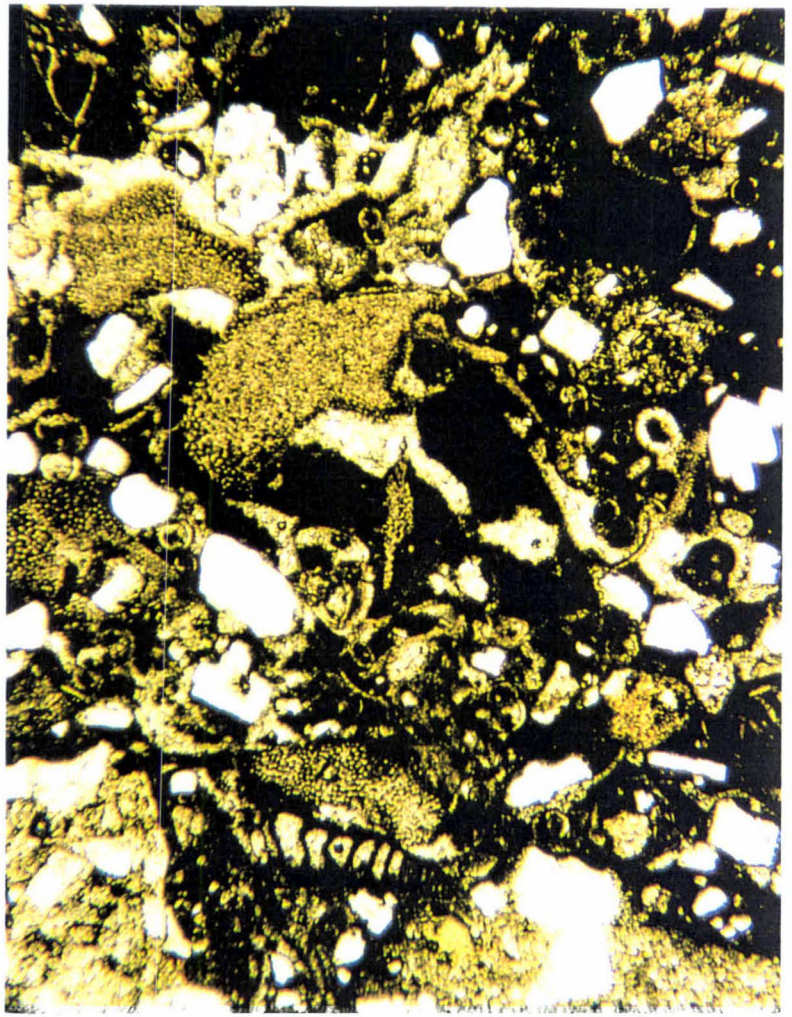

Plate 16B

Plates 16A and 16B are photomicrographs of the clay altered lapilli tuff at 1327 m in Kora-2. The most prominent features in these two plates are the high proportion of pelagic foraminifera (up to 85 %), the occurrence of subangular andesite lithic clasts, and the lack of crystals and crystal fragments.

All photomicrographs were taken under plane polarized light with the magnification set on 25x

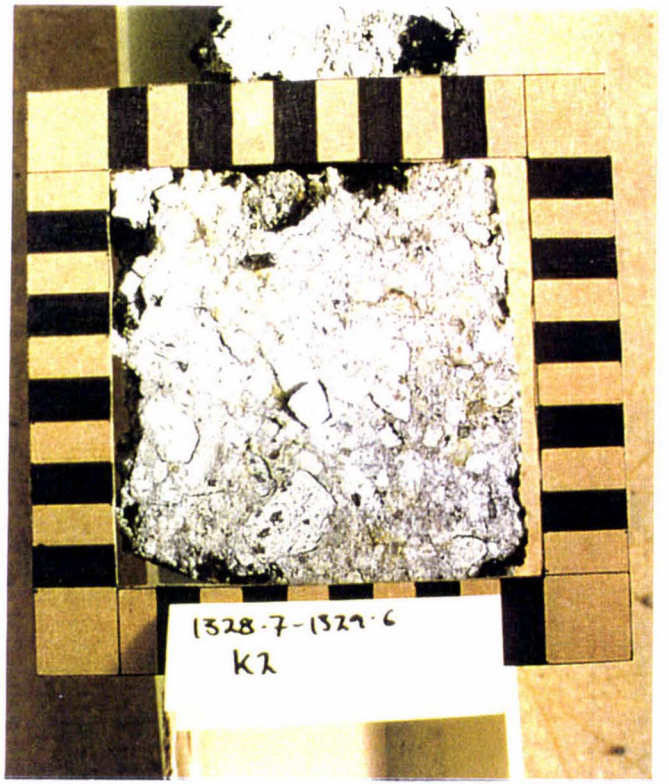

Plate 17

Kora-2 1328.7 - 1329.6 m

Plates 17 and 18 illustrate a clast supported tuff breccia located between 1328.7 m and 1329.6 m in Kora-2. Note the fine clay matrix, the high sphericity of the framework clasts, and the overall equigranular texture of the unit.

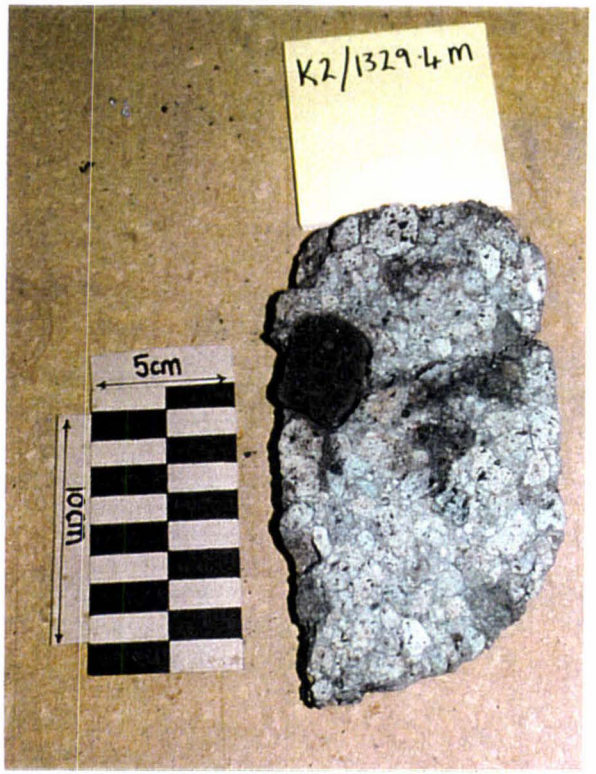

Plate 18

Kora-2 1329.4 m

Plates 17 and 18 illustrate a clast supported tuff breccia located between 1328.7 m and 1329.6 m well depth in Kora-2. Note the fine clay matrix, and the high sphericity and roughly equigranular texture of the framework clasts.

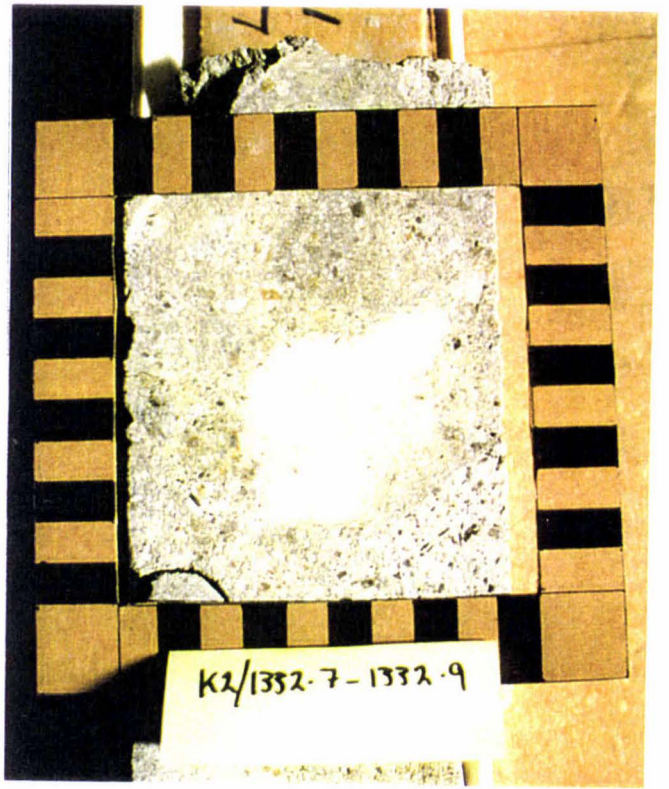

Plate 19

Kora-2 1332.7 - 1332.9 m

Plate 19 illustrates a tuff breccia containing angular, block sized clasts, supported in a lapilli tuff matrix between 1332.7 m and 1332.9 m in Kora-2. Note the ragged edges of the clast in the centre of the photograph.

The matrix in the crystal lithic tuff comprises fine clay. Foraminifera make up to 50 % of TS1 (e.g. Plate 16A and 16B). In TS1, the whole-rock mineralogy is dominated by calcite (42 wt%) and zeolite (34 wt%), and the unit is generally depleted in heavy minerals (see Table 2.3). The fine grainsize and obliterated fabric caused by pervasive bioturbation preclude any description of the original depositional fabric.

Tuff Breccias and Lapilli Tuffs

The tuff breccias and lapilli tuffs in Kora-2 occur between 1318 m bkb and 1333 m bkb (Arco Petroleum NZ Inc., 1988b). The description and location of these lithologies is presented in Fig. 2.3.

The framework components in the lapilli tuffs are grey, equigranular textured clasts of andesite. The clasts are moderately sorted and angular to subangular. The clasts also have an elongation ratio of 1.3 (Table 2.1), making these clasts the most spherical in the Kora wells. The mean grain size of the clasts is 10.0 mm (OB1), and the grain size distribution is nearly symmetrical and mesokurtic.

In thin section the framework crystals in the lapilli tuff matrix (TS2, TS3 and TS4) include hornblende (30 %), plagioclase (35 - 40 %), augite (<1 %) and opaques (5 %). The finer matrix components consist of smaller, more angular, weathered and broken plagioclase crystals and fine clay size material. These matrix components contribute to 40 % of the thin section. Textural analysis of the framework components in the matrix shows that the mean grain size of crystals varies between 0.21 mm and 0.25 mm. The crystals are poorly sorted, negatively skewed, mesokurtic to platykurtic, and the clasts are rounded to subangular. The elongation ratio varies between 2.03 and 1.89, suggesting that the clasts forming the matrix forming clasts have a very low sphericity compared to the framework clasts that the matrix supports (Table 2.2).

The mineralogical composition from whole-rock XRD analysis of the lapilli tuff consists of quartz, feldspar, calcite, vermiculite, hornblende, illite and zeolite. For example, at 1324.2 m bkb (Table 2.3) the main mineralogical abundances are feldspar (66.86 wt%), calcite (11.3 wt%), vermiculite (4.04 wt%), and hornblende (17.8 wt%).

The framework clasts in the lapilli tuff breccia are subangular, poorly sorted, moderately spherical (elongation ratio 1.45) (Table 2.1), clasts of andesite. The mean grain size of the clasts is 14.9 mm, and the grain size distribution is positively skewed and platykurtic. In thin section the lapilli tuff breccia matrix (TS5 and TS6) contains framework crystals of plagioclase (30 %), hornblende (25 %), opaques (10 - 15 %). These crystals are supported in fine clay, which contributes up to 40 % of the thin section. Whole-rock XRD results show that mineralogy consists of feldspar (43 wt%), hornblende (17.5 wt%), quartz (16.9 wt%), zeolite (14.0 wt%) and vermiculite (8.2 wt%) (Table 2.3). For example, the mean grain size of the crystals and clasts in the matrix in TS6 varies between 0.26 mm – 0.20 mm. The clasts are moderately to poorly sorted, skewness is nearly symmetrical to negative, and kurtosis is mesokurtic to very platykurtic. The matrix clasts are subrounded to rounded and have a low sphericity (elongation ratio 1.89 - 2.02), which is similar to the matrix components at shallower depths in Kora-2, for example TS2 and TS3 (Table 2.2).

The arrangement of the framework clasts in the lapilli tuff and lapilli tuff breccia in Kora-2 are illustrated in plates 15, 16, and 17. The most distinctive features illustrated in the plates are the erosional contact at 1326.9 m bkb (Plate 16), and the close juxtaposition of poorly sorted and well sorted units between 1321.5 m bkb and 1332.9 m bkb. The low sphericity of the larger clasts between 1327 m bkb and 1332.9 m bkb, and the large contrast in grainsizes with depth are other significant features of the lithologies in the Kora-2 well.

2.3.4 Kora-3 Core Observations

The lithologies in Kora-3 include tuffs and tuff breccias (Arco Petroleum NZ Inc., 1988c; Bergman *et al.*, 1992) (see Fig. 2.4). These lithologies are represented in approximately 25 m of slabbed core from 1780 m bkb to 1805 m bkb. Like Kora-2, Kora-3 has been intensively burrowed and bored, and few of the original depositional structures or fabric remain intact.

Tuffs

The tuffs in Kora-3 are massive, grey, calcite rich and mottled, with numerous burrows and borings, and few obvious lithological variations in the cored interval

(Plates 20, 21, 22, and 22A). At 1803 m bkb (e.g. Plate 22A) angular andesite lithic clasts form approximately 10 –15 % of the total thin section. The remaining framework components include crystals of hornblende, quartz and opaque minerals. The groundmass/matrix of the thin section contains up to 60 % foraminifera, and the remaining matrix material is clay. XRD analysis of the crystal lithic tuff at 1803.5 m bkb, shows that the dominant mineral components are zeolite (34 wt%) %), calcite (22.5 wt%), feldspar (20.6 wt%), quartz (16 wt%), and vermiculite (6.9 wt%) (Table 2.3). This general composition is similar to the samples analysed from Kora-1A and Kora-2.

In hand specimen, the lithological units in Kora-3 are evenly textured and equigranular. However, lithic clasts of andesite occur at irregular, sparse intervals in the core. For example, at 1783 m bkb (Plate 20). In thin section, the andesite lithic clasts are more abundant. For example, plate 22A depicts andesite lithics mixed with subhedral crystals and crystal fragments of plagioclase, and pelagic foraminifera.

2.4 IINTERPRETATION OF RESULTS

2.4.1 Interpretation of the Tuff Breccias and Conglomerates in Kora-1A

The tuff breccias and conglomerates are interpreted as medium to low energy, density modified grain flows. The conglomerates form the basal traction component of the flows, and the tuff breccias represent suspension settling of fine volcaniclastics. This interpretation is based on the stratigraphic distribution of the tuff breccias and conglomerates in Kora-1A, the composition, distribution of the framework clast shapes in each unit, and the composition and amount of matrix in the tuff breccias and conglomerates in Kora-1A.

The tuff breccias and conglomerates occur at relatively frequent intervals in Kora-1A, from approximately 1790 m bkb to total well depth at 1915 m bkb, and the conglomerates are generally bounded above and below by tuff breccias. For example, the conglomerates occur in the intervals 1793 m bkb – 1798 m bkb, and 1818 m bkb – 1830 m bkb, and the tuff breccias are located between 1788 m bkb – 1793 m bkb, 1809 m bkb – 1818 m bkb, and 1830m bkb – 1845 m bkb (Fig. 2.2). The cyclic or alternating occurrence of tuff breccia and conglomerate throughout Kora-1A

Plate 20
Kora-3 1783.6 m

Plate 20 illustrates a blue/grey, calcareous tuff breccia located at 1783.6 m in Kora-3. Note the angular, lithic clast of andesite in the centre of the photograph, and the oil stains at the base of the core unit.

Plate 21
Kora-3 1791 m

Plates 21 and 22 illustrate the lithologies typically encountered between 1791 m and 1803.5 m in Kora-3. The lithologies are hard, blue/grey, oil stained, calcite cemented, bioturbated (burrowed and bored), crystal lithic tuffs, and hyaloclastite tuffs.

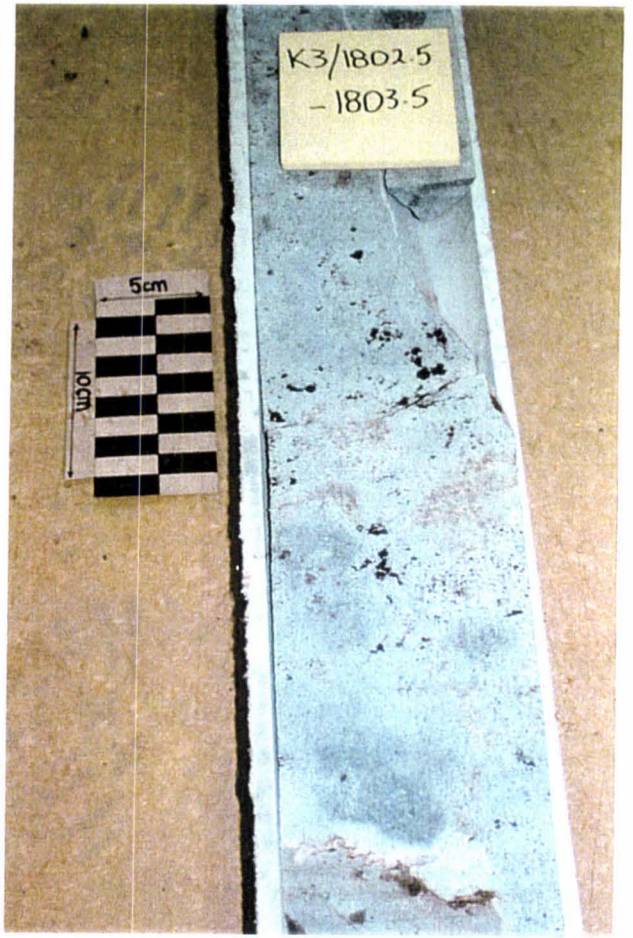

Plate 22

Kora-3 1802.5 - 1803.5 m

Plates 21 and 22 illustrate the typical lithologies located between 1791 m and 1803.5 m in Kora-3. The lithologies are hard, blue/grey, oil stained, calcite cemented, bioturbated (burrowed and bored), crystal lithic tuffs, and hyaloclastite tuffs.

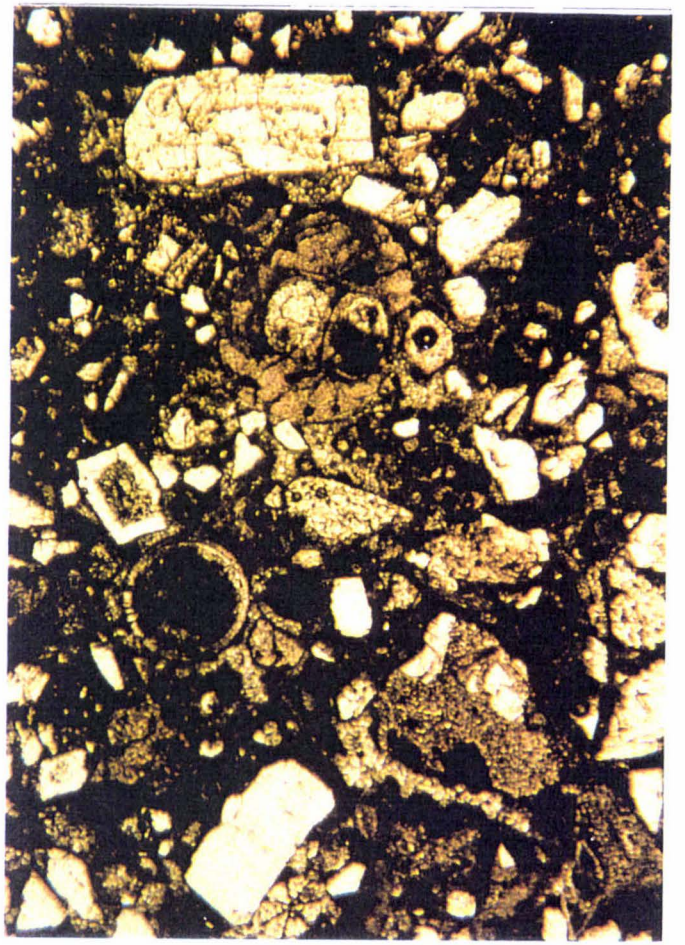

Plate 22A

Plate 22A depicts the bioturbated, calcite cemented, crystal lithic tuff at 1803 m in Kora-3. The sample is a poorly sorted mixture of plagioclase crystal fragments, subhedral plagioclase crystals, and pelagic foraminifera.

indicate the tuff breccias and conglomerates share similar depositional processes, depositional events occurred relatively frequently, and the magnitude of flows were relatively uniform.

The framework clasts in the tuff breccias of Kora-1A are the fragmented equivalent of the red, green, and grey, porphyritic clasts, and andesite lithic clasts observed in the conglomerates. The matrix composition in the conglomerates is roughly the same composition as the matrix in the tuff breccias. Similarities in the composition of framework clasts and matrix indicate the volcaniclastics comprising the tuff breccias and conglomerates came from the same eruptive source.

Lithological contacts between the conglomerates and tuff breccias in Kora-1A are rare due to inconsistent core recovery, however, the well rounded framework clasts that comprise the conglomerate become more fragmented at the upper boundary of each conglomeratic unit and the base of each tuff breccia. For example, the tuff breccia located between 1809 m and 1818 m (Fig. 2.7) contains the same red, green and grey, heterolithic, porphyritic clasts that comprise the top of the conglomerate located between 1818 m bkb and 1830 m bkb (Plate 1 and 2). The contact between the two units at 1818 m bkb appears to be gradational, suggesting the tuff breccia and conglomerate between 1809m bkb and 1830 m bkb represent a single depositional unit. If lithological contacts between tuff breccias and conglomerates throughout the rest of Kora-1A are gradational, then the conglomerates probably represent the base of each depositional unit, and the tuff breccias probably represent the upper part of each depositional unit.

The framework clasts in the conglomerate near the top of Kora-1A (e.g. 1795.4 m bkb) are some of the oldest rocks dated from the Kora edifice (i.e. 17.6 Ma; Bergman *et al.,* 1992). The clasts are well rounded considering their hardness, and position on the edifice – no more than two or three kilometres from the main vent and less than one kilometre from a satellite vent on the southeastern flank of the edifice. The rounded shape of the clasts cannot be accounted for by wave action because foraminifera above and below the volcanics indicate that Kora existed between 200 m and 500 m water depth (Bergman *et al.,* 1992). Therefore, the rounded and subrounded, red, green and grey, hard, porphyritic andesite framework clasts in the

conglomerate probably attained their shape during primary submarine eruptions. The clasts were probably plucked from deep in the volcanic conduit during eruptions and shaped during the ascent through the conduit to the sea floor (S.Bergman pers comm.).

Fractured framework clasts presumably caused by clast to clast collisions are common in the conglomerates in Kora-1A. The fractured clasts are most prevalent near the top of each conglomeratic unit, and do not occur in the tuff breccias. For example, the green/grey clast in the bottom right hand corner of plate 4 has been fractured. The fractured clasts are less abundant in the main body of the conglomerates (e.g. Kora-1A 1824-25 m bkb) where the clast sizes increase and the percentage of matrix varies between 30 % and 70 %. The fractured clasts in the conglomerate are unlikely to be the result of faulting, because fractures do not propagate throughout the tuff breccias and conglomerates, cored from Kora-1A. The distribution of fractured clasts in the conglomerates in Kora-1A, and lack of imbrication support the interpretation that the lower and middle part of the conglomerates travelled down the slopes of the edifice as a cohesive gravity slide or flow. The 'soupy' nature of the flow would have supported the clasts resulting in fewer clast to clast collisions. The upper part of the conglomerate, with increased fractured clasts, and overlain by tuff breccias, travelled down the edifice slope as a more turbulent subaqueous gravity flow. Turbulent flow probably developed because of the resistant shear stress between the subaqueous gravity flow surface and surrounding seawater (Norem *et al.,* 1990; Hampton and Locat, 1996; Mohrig *et al.*, 1998). For example, the density of a fluid relative to debris is close to 1:2 (Mohrig *et al.,* 1998). In contrast, in subaerial conditions, the density of air relative to debris is smaller than 1:1000 (Mohrig *et al.,* 1998). The overlying tuff breccias therefore represent the suspended load that settled out of the water column above the conglomerates.

The polymodal matrix in the tuff breccias and conglomerates can be compared to the coarse-grained matrix conglomerates in the Onyx Cave Member of the Richmond slice in the central Appalachian mountains (Lash, 1984). The Onyx Cave Member conglomerates are 0.6 – 2 m thick compared to 5 m – 10 m at Kora, and contain a poorly sorted, sandy and gravelly matrix. The framework clasts in the Onyx Cave Member conglomerates are tabular and up to 350 mm, and the matrix consists of 10

– 15 % mud, in addition to the sand and gravel size components. A modified density grain flow is the inferred depositional mechanism for the Onyx Member conglomerate based on the presence of inverse grading, tabular clasts orientated at high angles to the bedding, the presence of a poorly sorted, gravelly matrix, and the small amount of matrix mud (Lash, 1984).

Modified density grain flows are intermediate between a true grain flow and a debris flow, and the dependant variable is the amount of mud in the flow. Slope angles are usually 9 degrees or less for flow initiation to occur, and for the flow to maintain its energy. The density of the interstitial fluids must also be greater than that of the ambient fluid (Lowe, 1976).

The lithologies at Kora have a volcanogenic origin, compared to the middle shelf sediments of the Onyx Cave Member conglomerates, however, the conglomerates and tuff breccias in Kora-1A are inferred to have a similar depositional mechanism. The upper and basal portions of the conglomerates in Kora-1A lack the planar clast fabric, and cohesive mud matrix, typical of debris flows (Middleton and Hampton, 1976), and are too thick to be classified as 'true grain-flows', (typically < 5 cm thick; Lowe, 1976). Like the Onyx Cave Member conglomerates, the conglomerates and tuff breccias in Kora-1A contain framework clasts that are orientated at high angles, a poorly sorted gravelly matrix, and a small amount of clay sized material – features more typical of the density modified grain flow described by Lash (1984) and Lowe (1976).

2.4.2 Interpretation of the Tuffs, Hyaloclastite Tuffs and Lapillistone

The interbedded tuff, hyaloclastite tuffs and lapillistone located between 1781 m bkb and 1788 m bkb, form a prominent cap on the tuff breccias and conglomerates in Kora-1A, and represent a final phase of edifice construction at Kora. The faint, 100 mm – 200 mm, beds of moderately sorted, medium pebble sized and coarse sand sized lenses, and pebble trains occur frequently throughout the tuffs, hyaloclastite tuffs and lapillistone. The beds were probably deposited in a combination of low energy grain flows, and suspension settling. If high-energy gravity flows were responsible for the units, then bedding would be more distinct, the units would be

thicker, and lithological contacts would be ripped up. For example, Mc Phie (1995) has interpreted laminated and thinly bedded lenses < 2m thick, as 'principle lithofacies' in the Nakorotubu Basalt. The lithofacies contains planar, even, continuous beds, the thickest of which are internally massive. The lithofacies also contains volcanic lithic and crystals (pyroxene and feldspar), and sparse single pebbles or trains of pebbles and cobbles. The depositional processes inferred responsible for this lithofacies is 'suspension and turbidity current sedimentation below the wave base' (Mc Phie, 1995).

Where the tuffs, hyaloclastite tuffs and lapillistone have been burrowed and bored (e.g. Plate 14 Kora-1A 1784.2 m bkb – 1784.5 m bkb) deposition of the tuffs, hyaloclastite tuffs, and lapillistone probably happened in periodic pulses. A depositional hiatus occurred between each pulse, allowing worm colonies and other burrowing biota to establish and thrive in the fine subaqueous volcaniclastic debris.

The moderately sorted crystal fragments, subhedral crystals, and lithic clasts of andesite that comprise the framework components in the tuffs, hyaloclastite tuffs and lapillistone confirm an entirely volcanic source, and a high degree of fragmentation and granulation associated with primary subaqueous eruptions. The matrix in the tuffs, hyaloclastite tuffs and lapillistone is a similar composition to the matrix in the conglomerates and tuff breccias in Kora-1A. However, the former lithologies contain up to 50 % clay (Fig. 2.5), nearly twice the percentage of clay in the tuff breccias and conglomerates. The relatively large amount of clay indicates the erupted volcaniclastics contained a high proportion of andesitic glass at the time of deposition. The overall composition of the matrix in the tuffs, hyaloclastite tuffs, and lapillistone is the same as the matrix in the tuff breccias and conglomerates. This suggests the tuffs, hyaloclastite tuffs and lapillistone that were derived from primary subaqueous eruptions, were the source for the matrix in the conglomerates and tuff breccias in Kora-1A.

2.4.3 Interpretation of the Tuffs in Kora-2 and Kora-3

The crystal rich, lithic tuffs in Kora-2 between 1290 m bkb and 1295 m bkb, and the tuffs in Kora-3 between 1780 m bkb and 1805 m bkb contain randomly orientated,

subhedral crystals and fine sand sized lithic andesite clasts. These indicate the tuffs were deposited as unconsolidated volcaniclastic debris, prior to precipitation of the calcite cement. Pervasive burrowing and boring and abundant pelagic foraminifera indicate deposition of the tuffs occurred infrequently, like the interbedded tuffaceous units in the upper 7 m of the cored interval in Kora-1A. Sparse, angular, cobble sized and pebble sized andesite lithic clasts in the tuffs in Kora-2 and Kora-3 (e.g. Plate 20; Kora-3 1783.6 m bkb) indicate that primary subaqueous eruptions released enough energy to rip up clasts from the eruptive vent. The angular shape of the clasts may also suggest the flows of tuffaceous, volcaniclastic debris travelled down the edifice slopes as a cohesive flow, entraining the lithic clasts, and preventing the rolling required to shape the clasts. Alternatively, the angular lithic clasts may indicate the flows of tuffaceous volcaniclastic did not travel far from source before settling on the edifice slopes.

The tuff units in Kora-2 and Kora-3 are generally between 5 m and 20 m thick (Arco Petroleum NZ Inc., 1988b;1988c). The thickness of the tuffs in Kora-2 and Kora-3, and the lack of cored pristine lavas suggests a very high level of granulation at the water-magma interface during primary subaqueous eruptions. The mechanisms required for such fragmentation would be a fuel coolant interaction, typical of hydrovolcanism (e.g. Sheridan and Wohletz, 1983). Smith and Batiza (1989) have suggested cooling-contraction granulation as a possible mechanism for seamount hyaloclastites at water depths of 1250 m – 2300 m in the Pacific. The seamount hyaloclastites contain abundant blocky, sliver and fluidal glass shards, plagioclase crystal fragments, and lithics. The seamount hyaloclastites are also 'weakly normally graded', and contain a matrix of pelagic sediment. Given the high level of fragmentation in the tuffs in Kora-2 and Kora-3, the abundance of foraminifera, and clays altered from andesitic glass, cooling-contraction was probably a significant cause for fragmentation of the volcaniclastic debris comprising the tuffs.

The rate of eruption would have played a key role in the style of the depositional processes at work on Kora during eruptive episodes. If eruptions from Kora were highly effusive, then the burrowing and boring in Kora-2 and Kora-3 would not be as pervasive in the tuffs, and pelagic foraminifera would not be as abundant. An increased eruption rate would also result in more continuous grain flows, and without

bioturbation depositional structures would probably have remained intact. The high degree of fragmentation in the tuffs in Kora-2 and Kora-3, suggest numerous small-scale (<5 cm) 'particulate grain flows' were the depositional mechanism. The fine, crystal rich and glass rich volcaniclastics probably settled from suspension on to the slopes of the volcanic edifice as each subaqueous eruption proceeded. As the volcano slopes steepened, the unconsolidated glassy, crystal rich, and lithic rich, volcaniclastics would slide or flow down the edifice slopes to re-establish a slope angle below the angle of repose. For continuous deposition of sand sized material in grain flows that occur in a subaqueous environment, the static angle of repose must have existed between 18° and 28° (Middleton and Hampton,1976., Lowe, 1973; in Lowe, 1982). Furthermore, Lowe (1982) suggests that deposits of grain flows are typically thin, inversely graded and inclined at the angle of repose. The intense bioturbation of volcaniclastic units in Kora-2 and Kora-3 precludes the ability to resolve such details. However, because the slopes of Kora are in the order of 15° (Bergman *et al.,* 1992), and volcaniclastics were highly fragmented at the time the tuffs in Kora-2 and Kora-3 were deposited, particulate grain flows are the most likely depositional mechanism for the tuffs. The older eruptive units would have altered to clays prior to the emplacement of the younger, glassy, and crystal rich volcaniclastics. This would increase the likelihood of larger scale slope instabilities, caused in part, by the thixotropic character of clays such as montmorillonite (e.g. Lonsdale and Batiza, 1980). Such a scenario could account for the slump features identified in Kora-2 and Kora-3 (Arco Petroleum NZ Inc., 1988b,1988c).

2.4.4 Interpretation of the Tuff Breccias in Kora-2

The tuff breccias in Kora-2 contain smaller, well sorted, more spherical, and densely packed clasts compared to the tuff breccias in Kora-1A. The greater sphericity and smaller size of the andesite clasts in Kora-2 suggest the tuff breccia in Kora-2 was transported a greater distance from source, than the tuff breccias in Kora-1A. The closely packed clasts, a smaller percentage of matrix in Kora-2, and siltstone slump blocks (Plate 16), may also indicate a higher flow velocity.

However, the variably coarse matrix, small thickness of the tuff breccia units, and lack of a planar clast fabric in the Kora-2 tuff breccias, suggests a 'density modified grain flow' mechanism deposited the tuff breccias in Kora-2.

2.5 Summary of Interpretations

a) Interpretation of volcaniclastic core lithologies from the Kora volcano indicate that suspension settling from subaqueous eruptions, particulate grain flows, and density modified grain flows, were the prevalent depositional mechanisms associated with the developing volcaniclastic apron at Kora (Fig. 2.11). The conglomerates and tuff breccias in Kora-1A were deposited together as one depositional unit in entirely subaqueous conditions. The conglomerates forming the lower part of the unit were emplaced by density modified grain flows, and the tuff breccias comprising the upper part of the unit were emplaced from suspension settling. The tuff breccia in Kora-2 was also emplaced as a density modified grain flow.

b) Interbedded tuffs, hyaloclastite tuffs, and lapillistone located in the upper cored interval of Kora-1A were deposited in a combination of grain flows and suspension settling. Deposition occurred following primary subaqueous eruptions, which forced large concentrations of fine glass, and crystals into suspension around the volcanic edifice.

c) The tuffs in Kora-2 and Kora-3 were emplaced from secondary grain flows, grain flows following subaqueous eruptions. As the edifice slopes oversteepened past the angle of repose, the loose, highly fragmented volcaniclastic debris became unstable and travelled down the edifice slopes coming to rest on slopes below the angle of repose.

d) Depositional volcaniclastic events were also infrequent. There was enough time between eruptions for burrowing and boring organisms to establish colonies in the fine volcaniclastics, and for pelagic foraminifera to become mixed with the volcaniclastics.

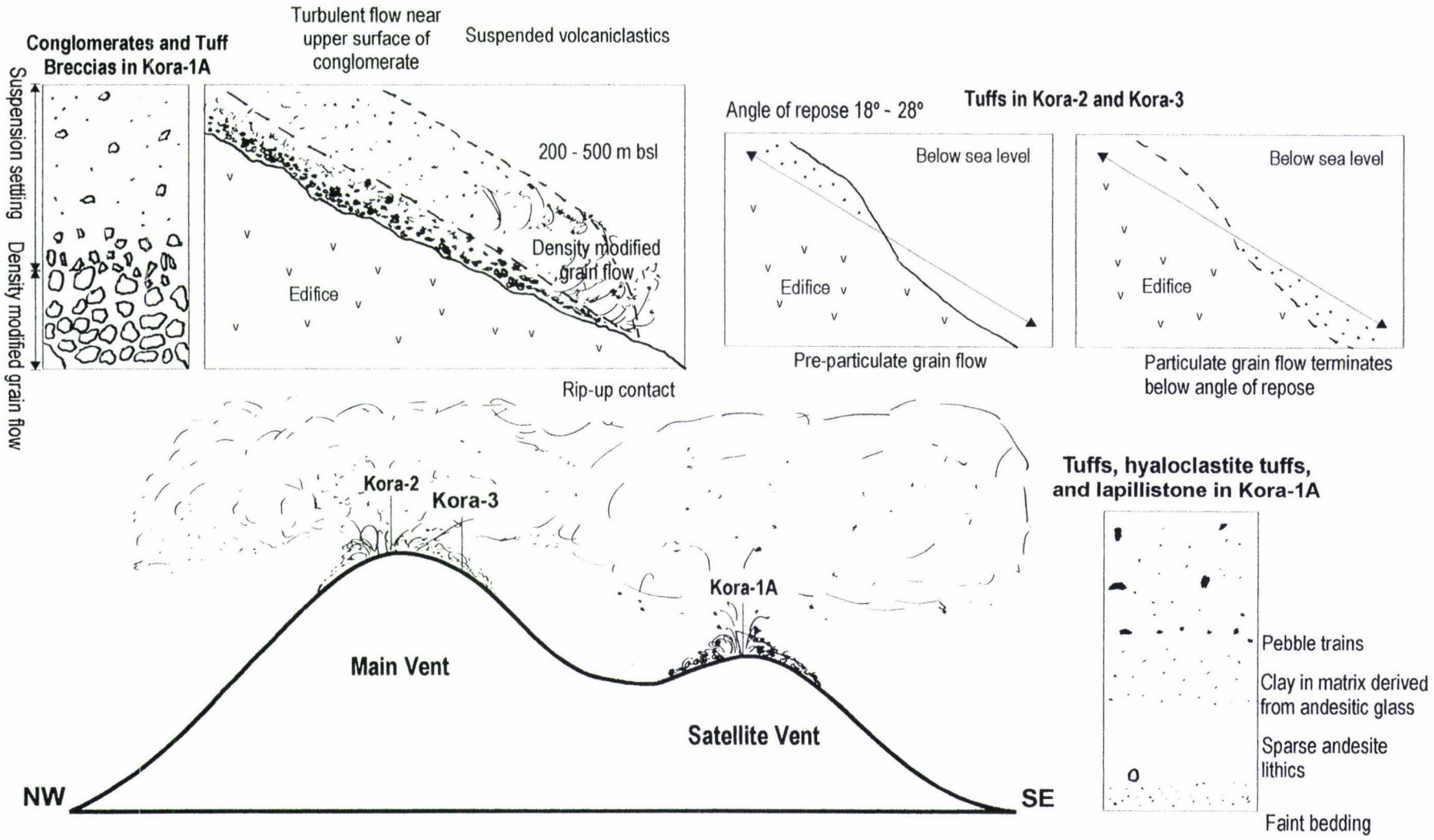

Figure 2.11
Stylized interpretation of the main depositional volcaniclastic processes at Kora

3.0 Seismic Analysis

3.1 INTRODUCTION

The aim of this study is to identify the types of slope processes that have been responsible for the construction of the Kora edifice. Using seismic reflection profiles, the seismic facies comprising the volcaniclastic apron at Kora have been identified. These facies have been used to identify the scale, extent and style of medium and large-scale volcaniclastic depositional processes.

3.2 METHOD

Seismic reflection profiles HF 1094, 81-SY-07BG, HF 540, 81-SY-09BG, 81-SY-03, and AR88 107A/AR88-M107, were selected for this seismic facies study. The above profiles provide effective, cross-sectional profiles across the volcaniclastic apron enclosing the Kora edifice (Fig. 3.1). The seismic facies were determined by defining the main body, the volcaniclastic apron, and the ring plain after the method described by Herzer (1995). Reflection patterns associated with the core of the volcanic edifice are termed "main body facies" reflectors. Reflectors that offlap the volcanic edifice and onlap surrounding ocean floor reflectors are interpreted as "apron facies reflectors", and ocean floor reflectors which onlap apron facies reflectors are termed "ring plain facies" reflectors. The seismic facies were then placed in their relative chronological context by determining time equivalent seismic reflectors for the top Eocene, top Early Miocene, top Middle Miocene and top Late Miocene with assistance from V. Stagpoole (pers comm, 11/1997). These reflectors were then used to identify the relative position of the volcanic interval (i.e. mostly Middle and Late Miocene) so that the shape, amplitude, continuity, and acoustic impedance of the reflectors comprising seismic facies within the volcanic interval could be identified and described.

Figure 3.1

Location of seismic reflection profiles used in this study.
(after Bergman *et al.*, 1992).

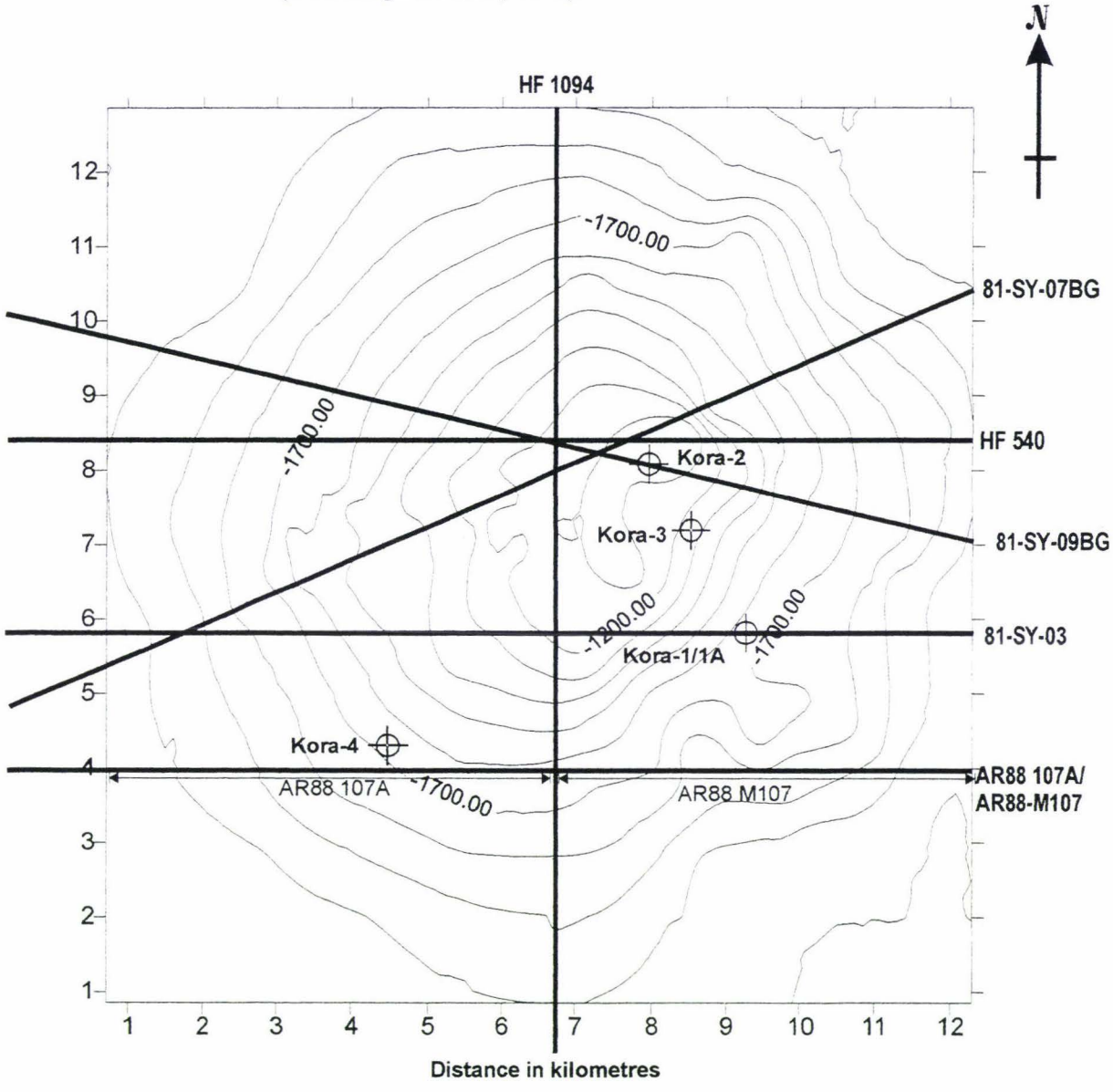

3.3 DESCRIPTION OF INDIVIDUAL SEISMIC REFLECTION PROFILES

3.3.1 Seismic reflection profile AR88 107A/AR88-M107

Seismic lines *AR88-107A* and *AR88-M107* (Fig. 3.2) were acquired by Western Geophysical for Arco International in 1988. These two 48 channel sections form a composite profile orientated west – east across the southern flank of the Kora edifice (Fig. 3.1).

The apron facies on the southern aspect of Kora appear as sigmoidal wedges draped either side of the edifice crest. They extend some 1.5 km westward and 2 km eastward respectively. The apron facies vary in thickness from approximately 50 m at the high point of the apron to approximately 420 m on eastern flanks. The reflectors within the apron facies that comprise this thickness contain continuous high amplitude reflectors up to 1 km in length, and discontinuous lenticular shaped reflectors, which descend east and west away from the highest point in the profile. The reflection pattern directly beneath the high point contains discontinuous, high and low amplitude reflectors that are 100 – 150 m long.

3.3.2 Seismic reflection profile 81 SY 07BG

Seismic line *81 SY 07BG* (Fig. 3.3) was acquired by Geco N.Z. in 1982 for Shell BP and Todd Oil Services Ltd. This 96 channel 48 fold CDP stacked section is orientated southwest - northeast across the summit of the edifice (Fig. 3.1).

The individual reflectors comprising the internal apron facies are typically hummocky, continuous (as long as 1 km), and high to medium amplitude. The apron facies is nearly 480 m at its thickest point and contains numerous downlapping wedge shaped reflectors. These become more apparent in the upper and medial slopes on both sides of the edifice, where they extend as far as 3.5 to 4 km from the edifice summit on to the lower slopes. The volcaniclastic apron is thinnest near the summit and gradually thickens towards the middle edifice slopes where the apron steps into main body facies, giving the contact between apron facies and main body facies a concave-upwards appearance (Fig. 3.3). The top bounding apron facies reflectors on the medial northeastern slopes bulge out above the mean slope angle and these reflectors are straight and sub-parallel, lacking the hummocky shape of underlying reflectors.

Figure 3.2
Seismic reflection profile and line drawing for part of AR 88 107A and AR88-M107

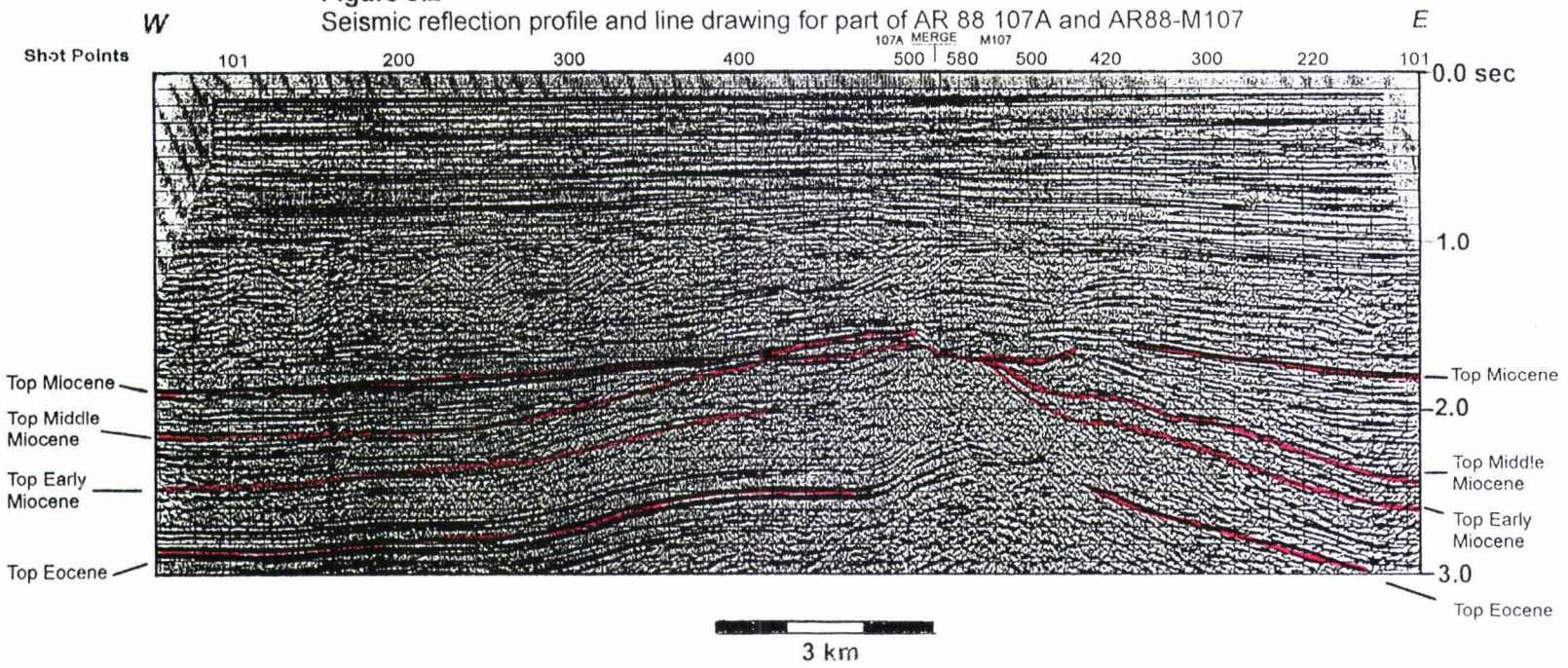

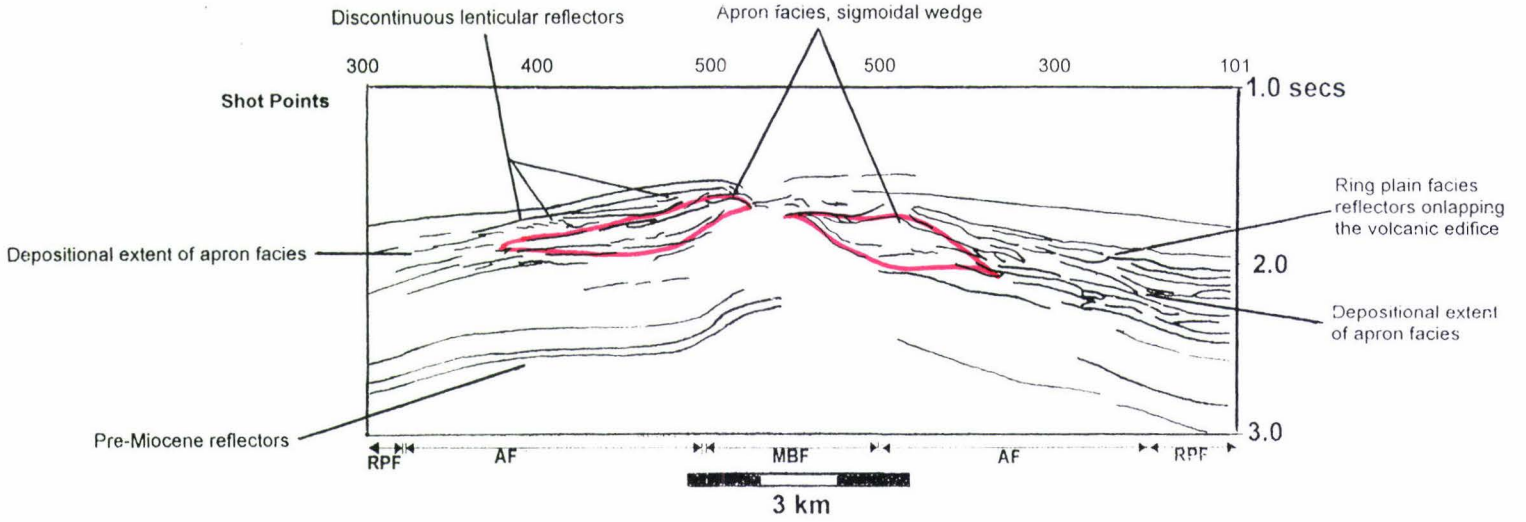

Figure 3.3
Seismic reflection profile and line drawing for part of 81-SY-07BG

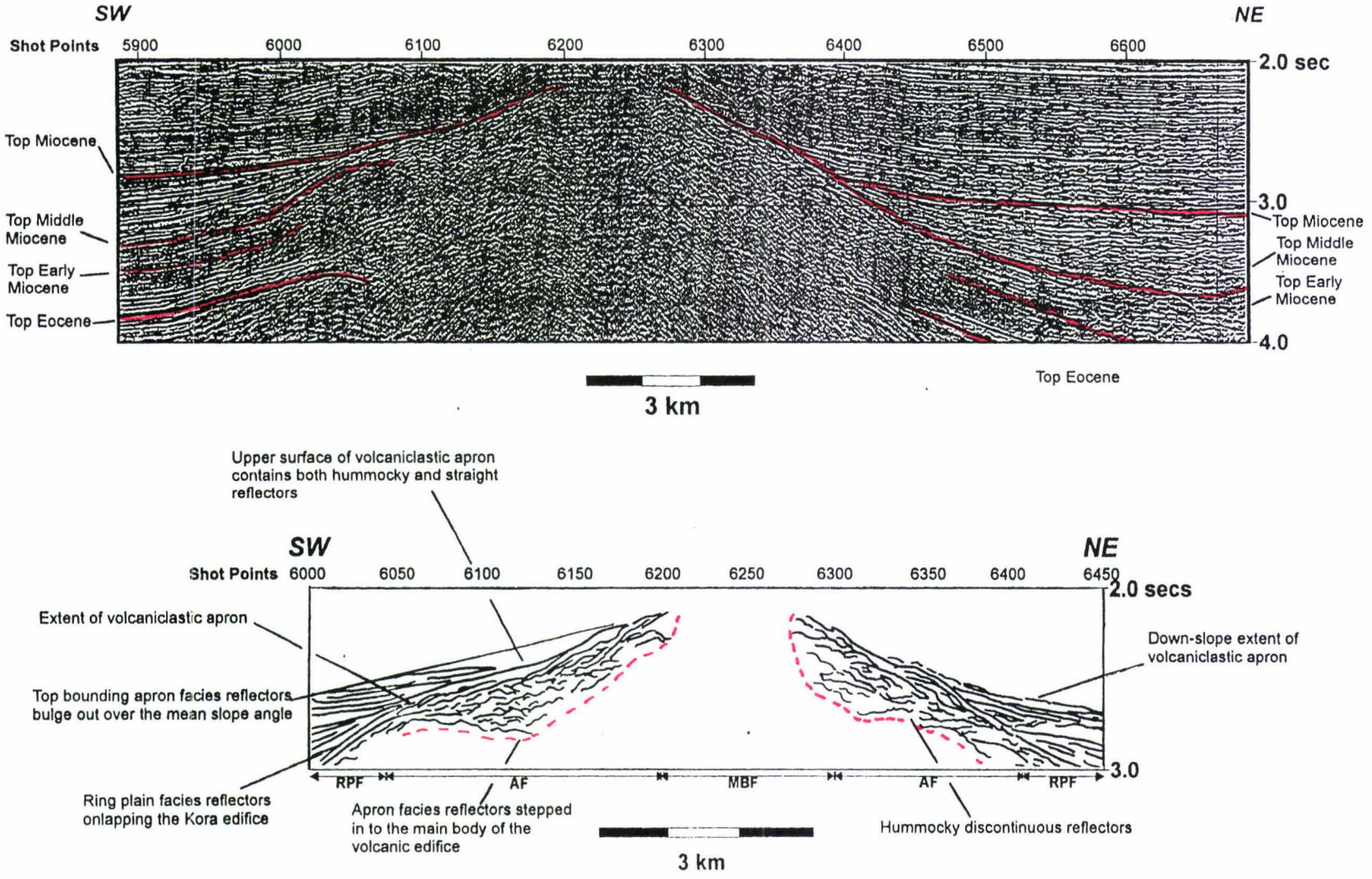

3.3.3 Seismic reflection profile 81 - SY - 03

Seismic reflection line *81 - SY - 03* (Fig. 3.4) was acquired by GECO A.S in 1982 and reprocessed by Entropic Geophysical for Arco International. This 96 channel 48 fold CDP stacked section is orientated west - east across the Kora edifice immediately south of the summit (Fig. 3.1).

The volcaniclastic apron facies are up to 420 m thick, and the internal reflection characteristics vary from west to east. The western reflectors are dominantly continuous (approx 2.8 km), sub-parallel, wedge shaped, and downlap onto ring plain facies. The amplitude of individual reflectors varies systematically, for example the terminal wedge reflectors have high amplitude, straight, sub-parallel tails and the area between the tail and terminal wedge contains typically low amplitude and hummocky reflection patterns (Fig. 3.4). Near the summit, reflectors are short, of variable amplitude with a common horizontal extent of approximately 100m, while east of the summit the reflectors are dominantly short to medium length (up to 500 m in length). The eastern aspect of the edifice is also down-faulted and a possible satellite vent forms a prominent knoll halfway down the edifice (Fig. 3.4).

3.3.4 Seismic reflection profile HF 1094

Seismic reflection line *HF 1094* (Fig. 3.5) was acquired by Prakla Seismo in 1976 and reprocessed by Entropic Geophysical for Arco International. This 48 channel 24 fold CDP stacked section is orientated south - north through the summit of the Kora edifice (Fig. 3.1).

The overall morphology of apron facies reflectors is very similar to 81-SY-03 with apron facies comprising numerous downlapping wedges that are draped over the crest of the Kora edifice. Unlike the other profiles however, the volcaniclastic mantle overlying the summit and main body facies away from the summit is relatively thick, i.e. approximately 160 m. The apron thickens up to approximately 260 m, and extends for some 3.5 km. The basal apron facies reflector is hummocky and is stepped in to the main body of the edifice (Fig. 3.5). Internally the apron facies reflectors vary with slope aspect. The southern slopes generally contain discontinuous high to low amplitude reflectors. Individual reflectors never exceed 1 km in length, and thickness never exceeds 40 m. There are few obvious clinoform

Figure 3.4
Seismic reflection profile and line drawing from part of 81 SY 03

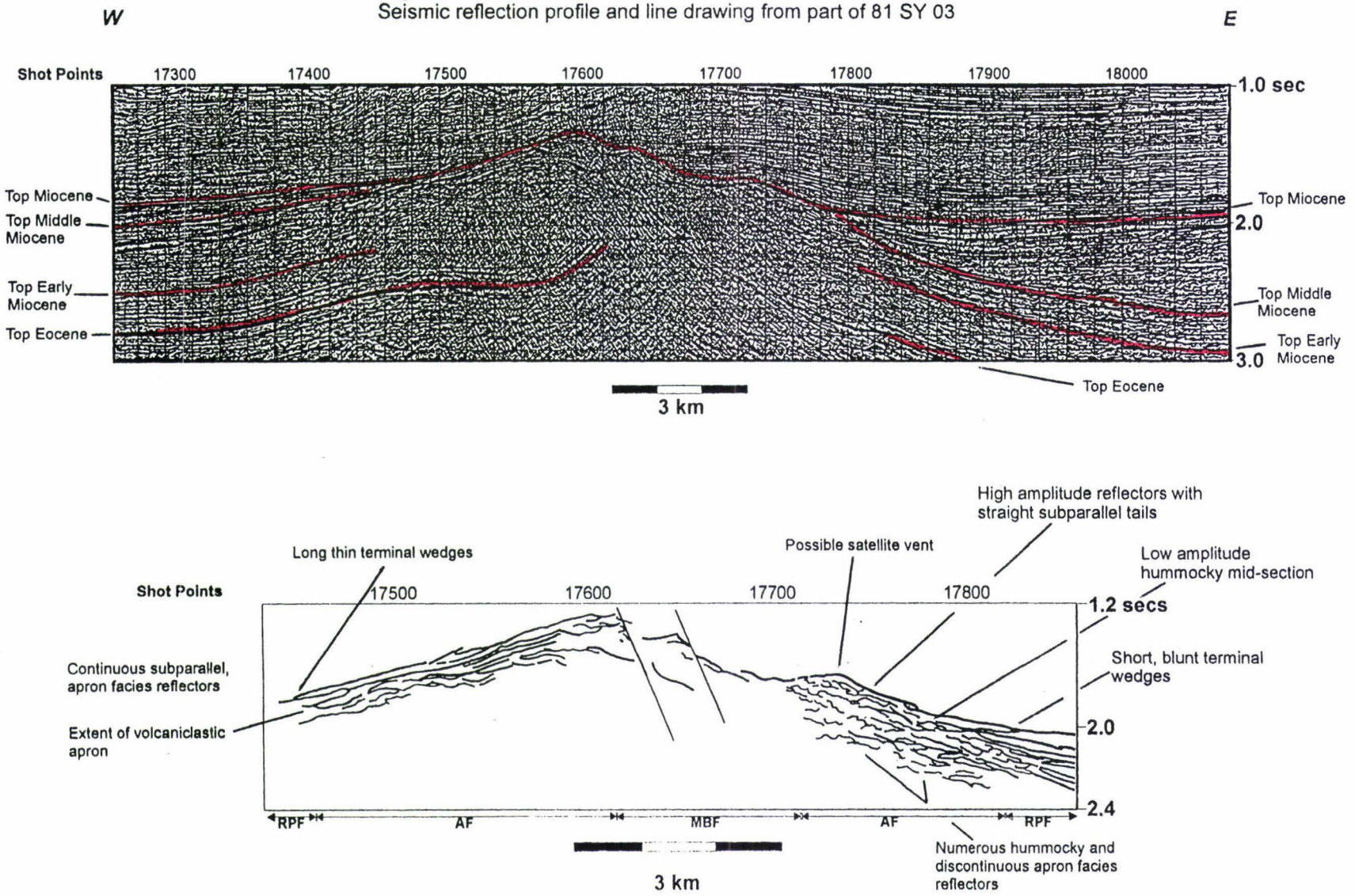

Figure 3.5

Seismic reflection and line drawing of HF 1094

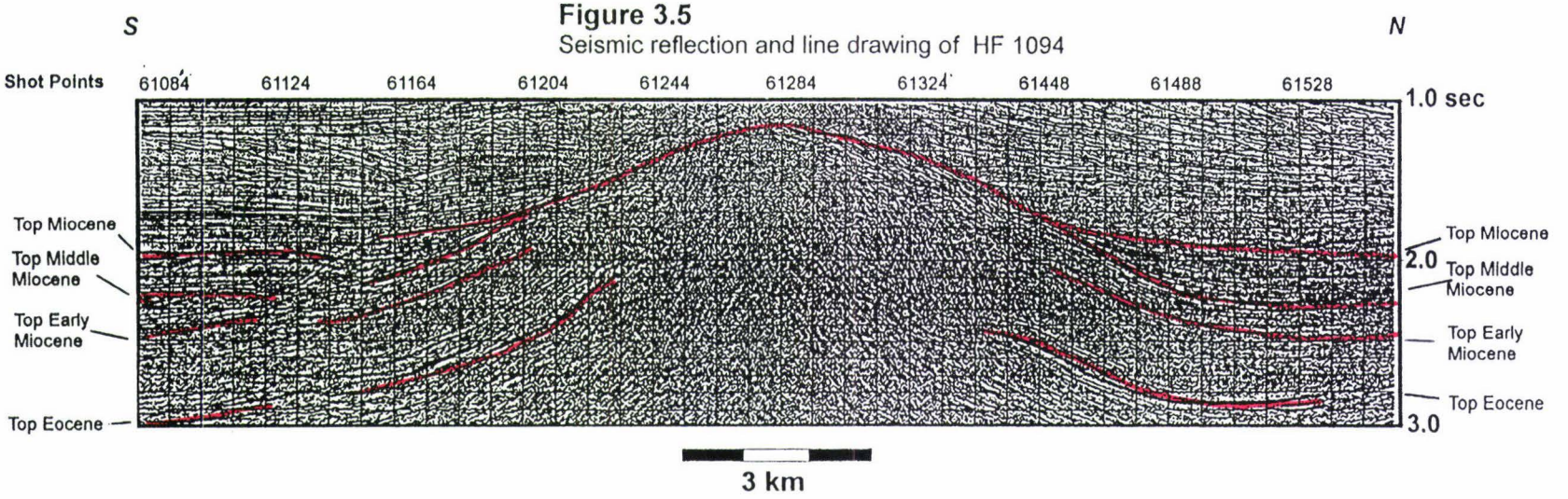

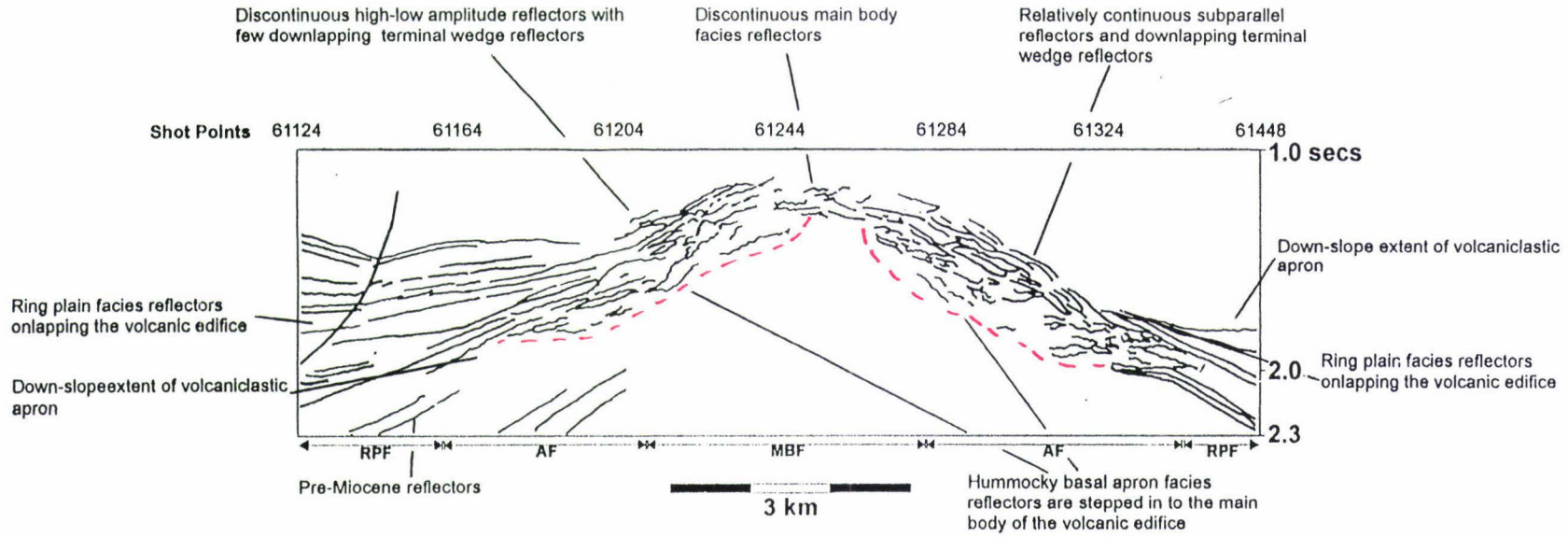

"wedge shaped" reflectors in the distal portion of the volcaniclastic apron. The apron facies on the northern aspect are more continuous, sub-parallel reflectors up to 2 km in length and approximately 210 m to 420 m in thickness. Numerous intertwined downlapping, wedge shaped apron facies reflectors which have variable amplitudes are also present (Fig. 3.5).

3.3.5 Seismic reflection profile 81 - SY – 09BG

Seismic reflection line *81 - SY – 09BG* (Fig. 3.6) was acquired by Geco, N.Z. in 1982 for Shell BP and Todd Oil Services Ltd. This 96 channel 48 fold CDP stacked section is orientated northwest - southeast through the summit of the Kora edifice (Fig. 3.1).

The volcaniclastic apron facies consists of a downlapping apron wedge located on either side of the edifice summit. The thickest part of the apron either side of the summit is approximately 100 m on medial edifice slopes, and the lateral extent of the apron either side of the summit is nearly 4.5 km on the northwest and up to 5 km on the southeastern aspects. The basal apron reflector is also stepped in to the main body of the edifice, especially near the summit on northwestern slopes (Fig. 3.6). Internally the apron facies reflectors vary with slope aspect. On the northwestern slopes there are 3 km of long, continuous, high amplitude reflectors which represent units that are approximately 60 m in thickness. The wedge shaped reflectors are long, straight, and well developed. Near the summit, reflectors are less continuous and merge with the chaotic reflection patterns of underlying main body facies.

On the southeastern slopes the reflectors are relatively continuous and very hummocky. They vary in amplitude and lateral extent. The longest reflectors are some 1 or 2 km in length – much shorter than on the northwestern slopes. However, the apron is thicker to the SE of the edifice and numerous wedge shape reflectors downlap on to the underlying apron and ring plain facies. Another distinctive feature on seismic line 81 – SY – 09 is a large slump structure on middle northwestern edifice slopes which has been overlain by younger apron facies reflectors.

Figure 3.6
Seismic reflection profile and line drawing for part of 81 SY 09BG

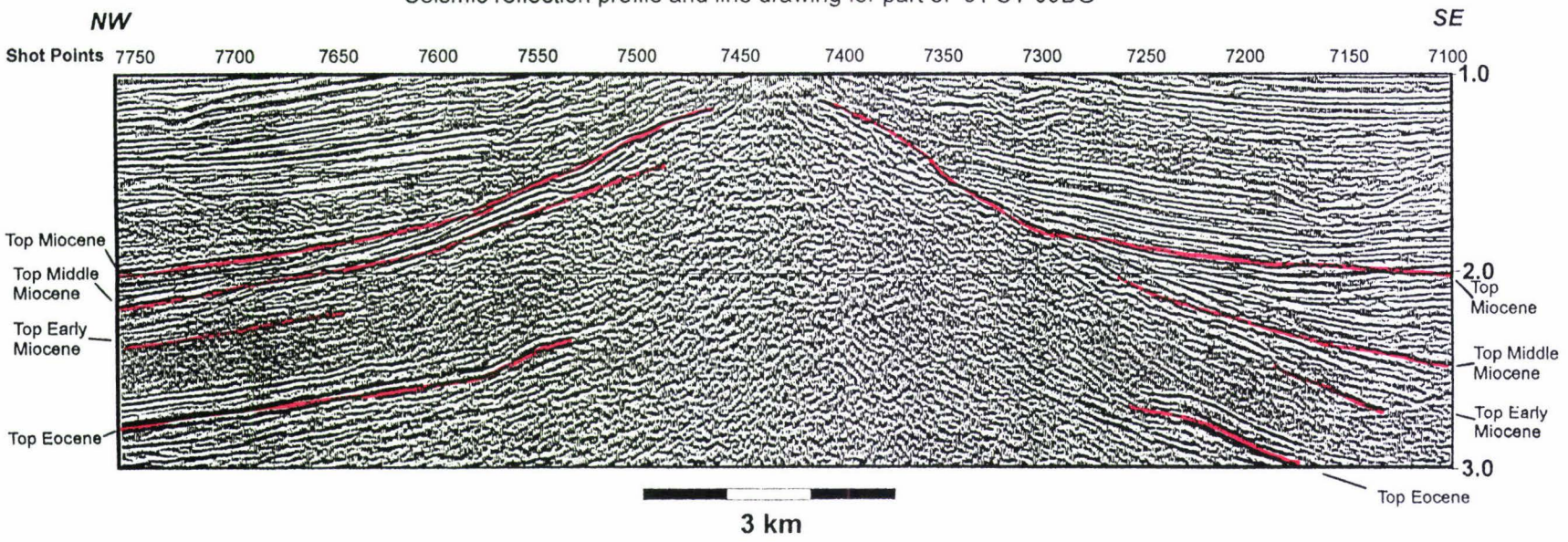

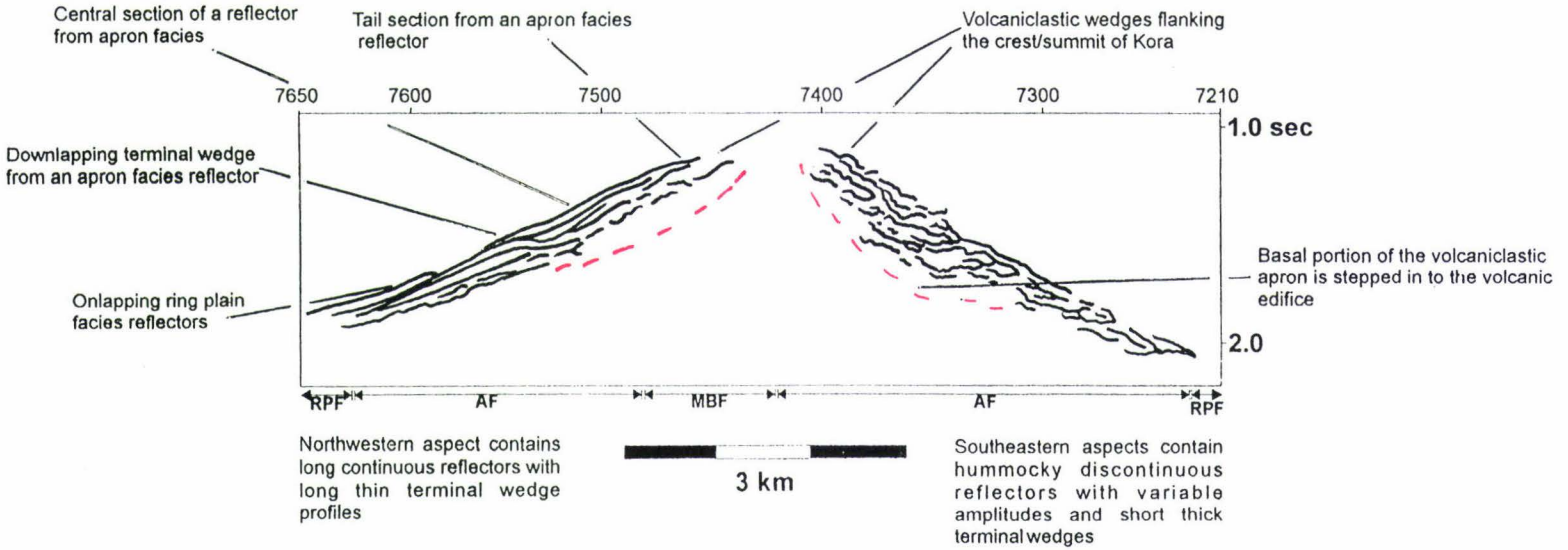

3.3.6 Seismic profile HF 540

Seismic line *HF 540* (Fig. 3.7) was acquired by Digicon in 1976 for Shell BP and Todd Oil Services Ltd. This 48 channel Dbas filtered stack, non-migrated section is orientated west - east through the summit of the Kora edifice (Fig. 3.1).

The overall morphology of apron facies reflectors in seismic line HF 540 is obscured by diffractions. However, the lateral extent of apron facies can be identified. It is approximately 3 km on eastern slopes and nearly 2 km on western slopes. The western aspect dominantly comprises continuous subparallel reflectors while the eastern aspect contains hummocky discontinuous reflectors (Fig. 3.7).

3.4 SEISMIC REFLECTION CHARACTERISTICS OF APRON FACIES AT KORA

Variations in the seismic reflection character of the volcaniclastic apron facies across the Kora edifice assist with the interpretation of the size, extent, and style of depositional processes involving volcaniclastic debris at Kora. The individual reflectors generally consist of three components. The first component is a downlapping terminal wedge, which marks the downslope limit of volcaniclastic debris or the surface along which they travelled. The second component is the tail, which delineates the spatial provenance of volcaniclastic debris and which sometimes merges with the chaotic main body facies reflectors. The third component of an individual seismic reflector is the central section between the tail and terminal wedge, which defines the lateral extent and continuity of the volcaniclastic debris. The character of each of these three components vary in terms of shape, size, continuity and length, depending on the aspect of slopes at Kora, and each variation in seismic reflection character, corresponds to a change in the style of depositional processes (see Fig. 3.8).

Variations in the continuity and length of individual reflectors are apparent across the entire volcanic edifice. For example, long continuous reflectors are typical of northern and western aspects in seismic reflection lines 81-SY-03, 81-SY-09BG and 81-SY-07BG (Figs. 3.4, 3.6 and 3.3). These seismic reflectors are subparallel with top bounding and internal reflectors that can be traced from near the crest of the edifice to the toe of the volcaniclastic apron near the base of the edifice slope. In contrast,

Figure 3.7
Seismic reflection profile and line drawing for part of HF 540

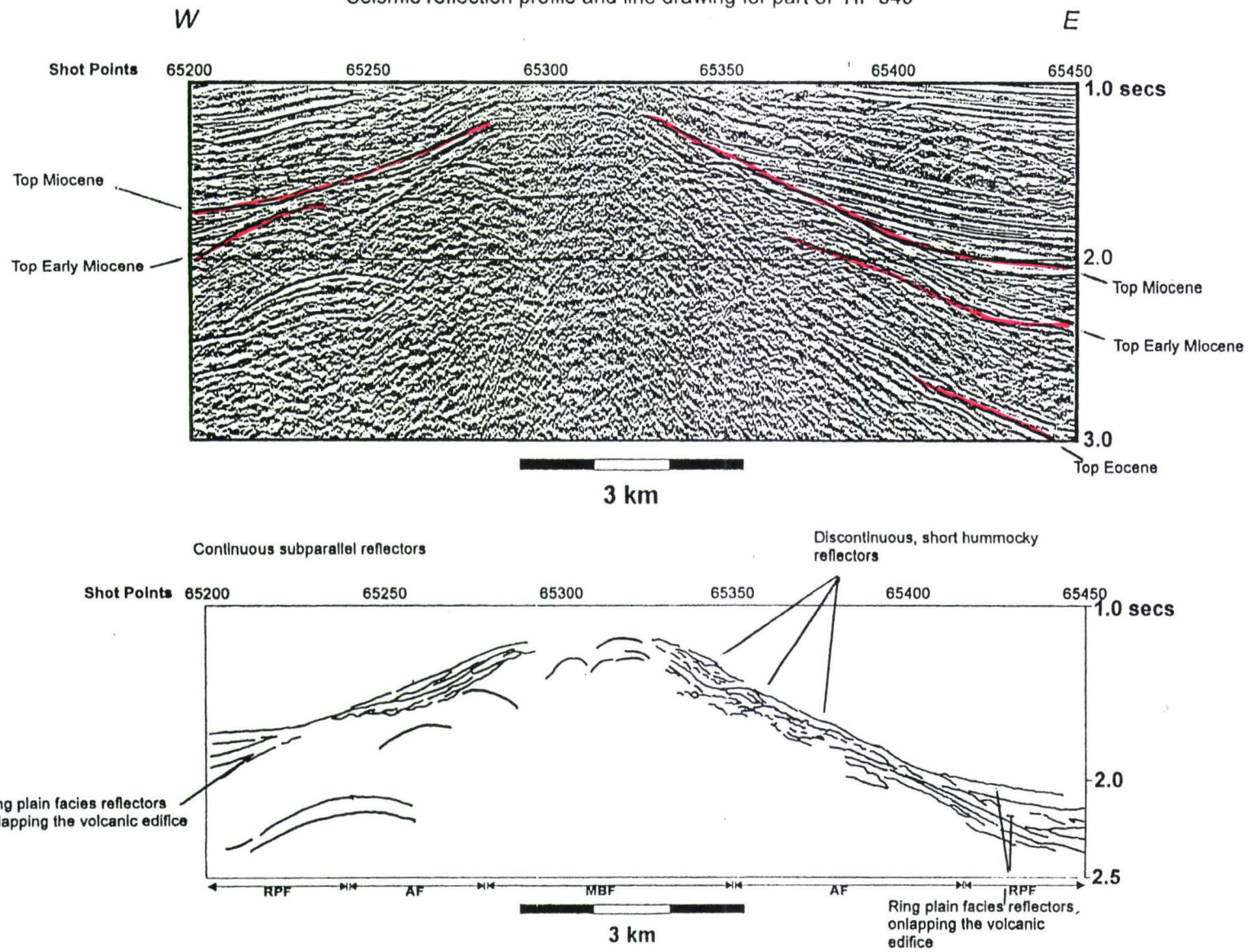

Figure 3.8

Surfer image of Kora and summary of observations made from seismic reflection profiles across the Kora edifice

Northern and western slopes are typically composed of long, continuous, parallel and sub-parallel reflectors with long, thin terminal wedges. These features are interpreted as infrequent but well developed medium to low energy flows of volcaniclastic debris

Apron facies vary in thickness between 0.2 and 0.4 secs (twt) and laterally the apron extends between 2 and 4 km down slope.

Reflectors on southern and eastern aspects at Kora are typically hummocky, continuous and discontinuous with variable amplitudes and short, thick terminal wedge profiles. These features are interpreted as high frequent small/low energy flows of volcaniclastic debris

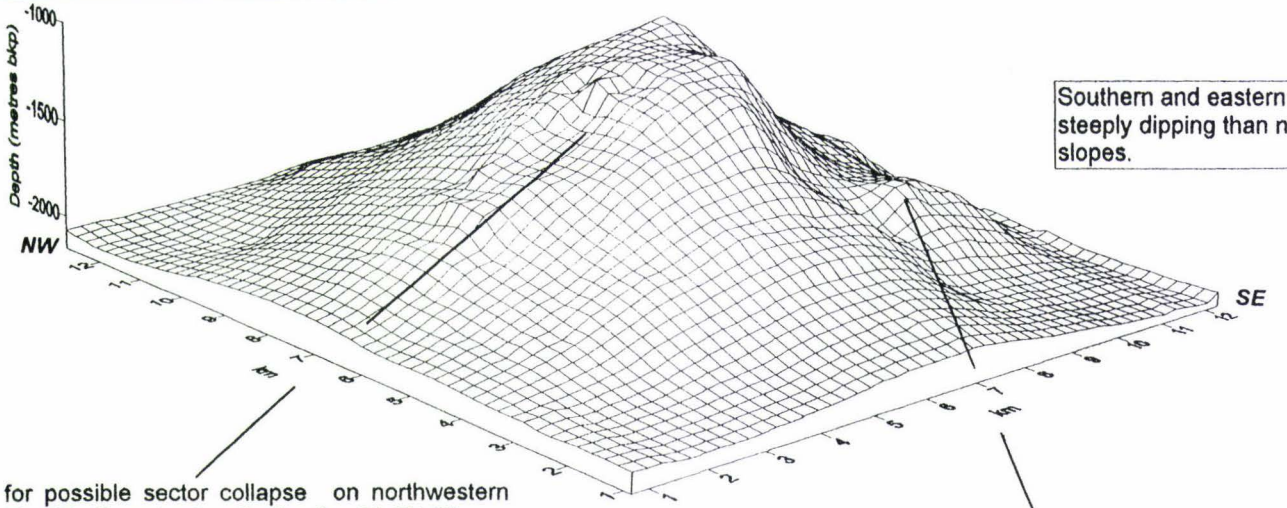

Southern and eastern slopes are more steeply dipping than north and western slopes.

Evidence for possible sector collapse on northwestern slopes i.e identified in seismic reflection line 81-SY-09

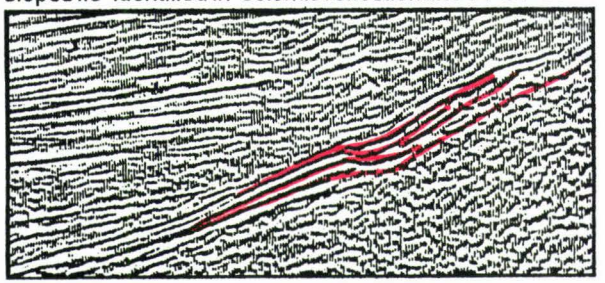

Possible satellite vent observed in seismic reflection profile 81 SY 03

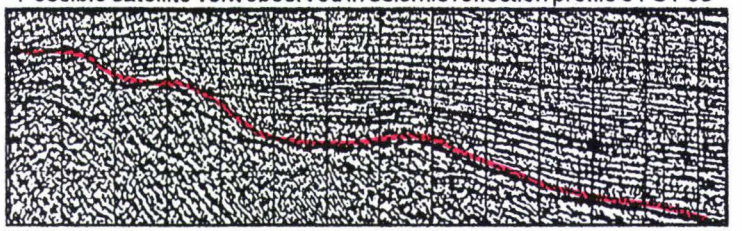

southern and eastern aspects contain short discontinuous reflectors that are generally subparallel and often intertwined (see Fig. 3.8).

Individual seismic reflectors vary in shape with respect to slope aspect. For example, in seismic reflection profile 81-SY-09BG (Fig. 3.6) individual reflectors are straight and parallel on northwestern slopes, while southeastern slopes contain mostly hummocky reflectors. The shape of the downlapping terminal wedge associated with individual reflectors also varies with respect to slope aspect. For example, seismic reflection lines 81-SY-03 (Fig. 3.4) and 81-SY-09BG (Fig. 3.6) contain long thin, eloquent terminal wedges associated with straight, parallel, continuous reflectors on northern aspects, while southern aspects typically display short thick, terminal wedges (see Fig. 3.8).

The amplitude of individual reflectors also varies with length along a given reflector. For example, seismic reflection lines 81-SY-07BG, 81-SY-09BG, and AR88-107A/AR88-M107 (Figs. 3.3, 3.6 and 3.2) show individual reflectors that vary in amplitude along their length. This variation is most pronounced in the internal and top bounding apron facies reflectors on the southeastern flanks of the Kora edifice in seismic reflection line 81-SY-09BG, and contrasts northern aspects of the edifice which are less prone to variations in amplitude along individual reflection planes.

In terms of thickness and extent of the volcaniclastic apron facies at Kora, the apron facies vary in thickness between approximately 210 m and 420 m and laterally the apron extends away from the edifice crest anywhere between 2 and 4 km down slope. The thickness of the volcaniclastic apron does not vary considerably across the edifice. However, there are two distinctive structural features that have probably acted as controls on the distribution of the volcaniclastic apron facies. The first is a slump scar on northwestern slopes in seismic reflection line 81-SY-09BG (Fig. 3.3), and the second is that eastern slopes appear to dip more steeply than western slopes. The latter may be a response to fault activity or the development of a satellite vent on eastern slopes (e.g. seismic line 81 – SY – 03 in Fig. 3.4 and Fig. 3.8).

3.5 WEST NORTHLAND SEISMIC FACIES

The Kora volcanic edifice is comparable to the relic subsurface volcanoes present along the offshore west Northland Peninsula. These have been studied in detail by Herzer (1995). In the Northland subsurface volcanoes, Herzer describes "high amplitude, hummocky and sub-parallel reflectors on the higher slopes". He interprets these as "proximal pyroclastic flows and base surge deposits". The "lenticular, discontinuous, sub-horizontal reflectors" are interpreted as debris flows within medial apron facies. Discontinuous, high amplitude reflectors near the surface in the 'main body', are interpreted as lava flows, breccias and intrusives, as well as shallow reflectors which he considers to be caused by pelagic deposits.

In terms of volcano morphology the west Northland volcanoes include large 15-40 km radius volcanoes and intermediate sized volcanoes which are 5 – 10 km in radius (Herzer, 1995). Most of the large volcanoes have flat tops and steep sides while the smaller intermediate sized volcanoes are cusp shaped, with summit depressions, these also have flat tops and terraces which suggests the volcanoes probably formed at sea level (Herzer, 1995).

Kora has a similar radius to the intermediate sized volcanoes of the West Northland Arc (i.e. 5 km – 6 km radius; after Bergman *et al.,* 1992), however Kora is more conical in shape and lacks the truncated summit observed by Herzer in the Northland volcanoes. Another significant difference between the west Northland volcanoes and Kora is that apron facies associated with Kora do not extend past the foot of the volcanic edifice whereas apron facies associated with the Northland volcanoes generally downlap out on to the flat region surrounding each volcanic edifice. Kora has existed under wholly submarine (i.e. see Chapter 1) conditions while the Northland volcanoes have existed at the submarine- subaerial interface. Schminke and von Rad (1979) consider that the transition between emergent and submergent volcanoes is reflected in contrasting submarine debris flows. Since Kora was situated well below the wave base prior to its burial by Plio-Pleistocene sediments (see Chapter 1. or Bergman *et al.,* 1992), the relatively large volume of volcaniclastic debris observed beyond the foot of the west Northland volcanoes is probably the response of steep unstable volcano slopes exposed to subaerial conditions prior to wave planation.

3.6 INTERPRETATION OF SEISMIC REFLECTION PATTERNS AT KORA

The seismic reflection patterns observed in apron facies at Kora elucidate to the possible forms and lateral extent of slope transport events involving volcaniclastic debris and are summarized in Figure 3.8. The hummocky, sub-parallel, continuous and discontinuous seismic reflection patterns and short thick terminal wedge profiles observed on southeastern aspects of the Kora edifice are interpreted as numerous, small, medium to low energy, intertwining flows, or slides of volcaniclastic debris. These were probably deposited as relatively frequent gravity driven low energy flows 1 - 2 km in lateral extent. The long continuous, straight parallel to sub-parallel reflectors and long thin terminal wedge profiles observed on northwestern aspects of the Kora edifice are interpreted as well-developed gravity driven flows of volcaniclastic debris that were initiated and terminated in one single mass-flow event. The long thin, terminal wedge profile indicates that the flow was well developed, did not end abruptly and probably involved medium to high energy. The strongest evidence for medium to large-scale flow of volcaniclastic debris is the structural feature observed in seismic reflection line 81-SY-09, which resembles the debris flow of Skinner and Porter (1987) or a coherent slide (Cas and Wright, 1987). This feature was probably emplaced during the early stages of eruptive volcanism at Kora when a portion of the middle northwestern slope collapsed and moved to the toe of the edifice in a single event. Succeeding volcaniclastic sedimentation in-filled the scar created by the initial slope failure, so that minimal surface expression remains in the top-bounding reflector of the volcaniclastic apron.

4.0 Discriminant Analysis of Major Element Geochemistry from Major North Island Volcanic Centres

4.1 INTRODUCTION

The North Island of New Zealand and surrounding offshore regions are littered with relict and currently active volcanic centres that range in age from Early Miocene to Recent. There has been considerable debate over the spatial and temporal relationships of these centres within the genesis and migration of arc volcanism in northern New Zealand. In particular, there has been divided opinion as to whether the northern Taranaki offshore volcanics belong to a Miocene Northland Arc or whether they form part of a northeasterly trending line of volcanoes which extends from North Taranaki to the Coromandel. Tectonic models in the past have mostly focused on younging trends and comparison of major and trace element chemistry amongst a limited number of volcanic centres (e.g. Brothers, 1984 and 1986; Kamp, 1984; Ballance *et al.,* 1985 and Ballance, 1988; Herzer, 1995), however, the exact relationship between the volcanics within these models remains unclear.

In this study, published major element geochemical analyses from ten volcanic centres distributed around the North Island are compared using Discriminant Function Analysis (DFA) in an attempt to place the Kora Volcanics in to an appropriate arc setting.

4.2 GEOLOGICAL SETTING - NORTH ISLAND VOLCANIC CENTRES

The distribution and ages of the North Island Volcanic Centres used in this study are illustrated in Fig. 4.1.

4.2.1 Coromandel Volcanics

Coromandel Peninsula was the location of a volcanic arc some 35 km in width and 200 km in length, from Great Barrier Island in the north to the base of the peninsula in the vicinity of Thames and Whangamata farther south. Volcanics were erupted between 18 Ma and 9 Ma (Black and Skinner, 1979; Skinner, 1986; Adams *et al.,* 1994) with andesites the dominant extrusive rock type. These andesites are associated with a continental margin arc (Adams *et al.,* 1994), and were erupted as a

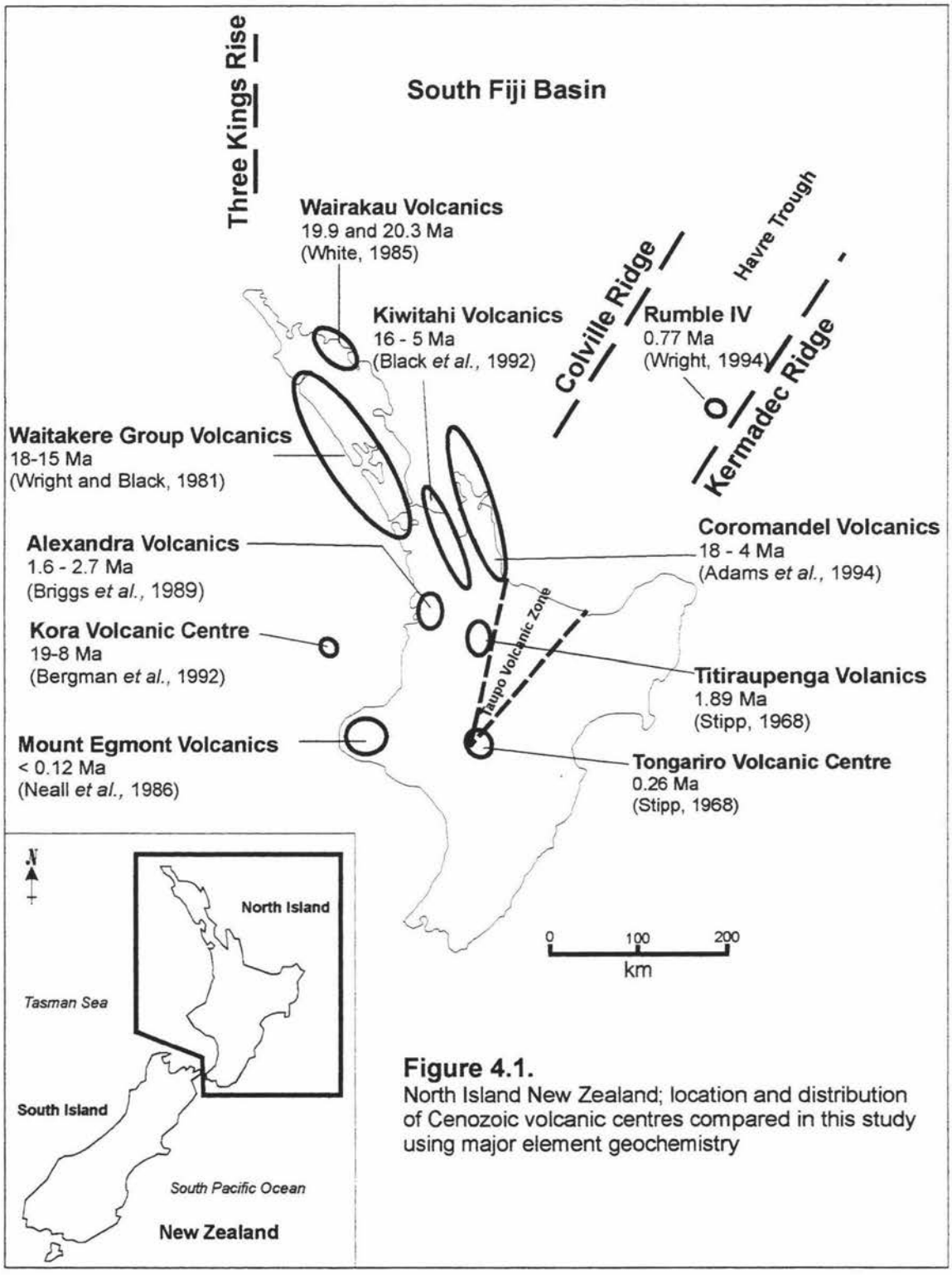

Figure 4.1.
North Island New Zealand; location and distribution of Cenozoic volcanic centres compared in this study using major element geochemistry

precursor to basaltic and rhyolitic eruptive activity. The eruptive activity finally ceased south of the Coromandel Peninsula in the Middle Pleistocene, as early volcanic activity in the Taupo Volcanic Zone (TVZ) began. The migration of volcanic activity is constrained by comprehensive age data which show that the focus of volcanism in the Coromandel region has migrated sporadically eastward at a rate of 3 mm/yr and southward by 8 mm/yr (Adams *et al.,* 1994). The major element data which have been used in this study include analyses published in Adams *et al.,* (1994). The samples are a combination of mafic to intermediate, mostly calc-alkaline and medium-K basalts and andesites from a number of stratigraphic units of different age (Adams *et al.,* 1994), for example Colville Formation, Port Charles Andesite, Beesons Island Volcanics, Matarangi Andesite (Appendix 5.1).

4.2.2 Waitakere Group Volcanics

The Waitakere Group Volcanics are located along the western coast of the Northland Peninsula from Auckland in the south to Hokianga Harbour in the north (Wright and Black, 1981) (Fig. 4.1). The Waitakere Group Volcanics consist of rocks from the Waitakere Group, which includes the Waipoua, Hukatere and Manakau Subgroups as well as a large number of volcanic structures located offshore immediately west of the Northland Peninsula (e.g. Herzer, 1995). The rocks of the Waitakere Group are mostly porphyritic, calc-alkaline basalts and andesites (Wright and Black, 1981). Ages are constrained by several K-Ar dates from the Tokatoka district (18.0 Ma and 17.4 Ma), and the Manakau Subgroup (16.8 Ma and 16.1 Ma) (Stipp and Thompson 1971; Bandy *et al.,* 1970; Wright and Black, 1981). The Waitakere Group volcanics collectively form the western belt of an Early Miocene to Middle Miocene Northland Arc which was active in conjunction with eruption of the Wairakau Andesites (Kear and Hay, 1961; Thompson, 1961; White, 1985) in the eastern belt of the Northland Arc (Fig. 4.1). Both the western and eastern belts are thought to be associated with obduction-related processes and emplacement of the Northland Allochthon (Isaac *et al.,* 1994). Consequently the major element data used in this study include 15 analyses of rock samples from the Manakau, Hukatere and Waipoua subgroups representative of the western belt which have been published in Wright and Black (1981) (Appendix 5.2).

4.2.3 Rumble IV

Rumble IV (Fig. 4.1) is a submarine volcano located at the southern end of the Kermadec island arc (Gamble *et al.,* 1993) approximately 200 km NNW of Whakatane. This volcanic edifice is one of seven large submarine volcanoes that comprise the frontal arc, which may be as old as 0.77 Ma (Wright, 1994). The major element data from Rumble IV used in this study (Appendix 5.3) include analyses for six porphyritic blocks of vesicular basalt with glassy surfaces (Smith and Brothers, 1988; Gamble *et al.,* 1993). These rocks were dredged from the flanks of the volcanic edifice in water depths of more than 440 m (Wright, 1996).

4.2.4 Wairakau Volcanics

The Wairakau Volcanics (Kear and Hay, 1961; Thompson, 1961) are an early Miocene suite of calc-alkaline rocks that occur at Whangaroa and Whangarei Heads (White, 1985). The major element data used in this study are 15 analyses of samples from subvolcanic intrusives published in White (1985) (Appendix 5.4). These are porphyritic, calc-alkaline rocks that formed coevally with Early Miocene rocks of the Waitakere Group in the western belt of the Northland Arc. This period of volcanic activity is attributed to either a NW dipping subduction system or from obduction related processes (White, 1985).

4.2.5 Mount Egmont Volcanics

Mount Egmont is predominantly an andesitic stratovolcano which has been active throughout the past 0.12 Myrs on the Taranaki Peninsula (Stewart *et al.,* 1996). Paritutu, Kaitake and Pouakai are three other Quaternary volcanoes that combine with Mount Egmont to delineate a southward migration of volcanic activity across the Taranaki Peninsula (Neall *et al.,* 1986; King and Thrasher, 1997). These volcanoes are thought to be subduction related and are associated with the Taupo Volcanic Zone located 140 km east in the central North Island (Stewart *et al.,* 1996). Major element data for analyses of samples from Mount Egmont used in this study were 12 basalt to andesite analyses published in Stewart *et al.,* (1996) and 10 analyses published in Price *et al.,* (1992) (Appendix 5.5).

4.2.6 Titiraupenga Volcano

Titiraupenga is a Quaternary volcano (1.87 +/- 0.02 Ma; Stipp, 1968) located approximately 20 km NW of Lake Taupo. This volcano is one of a line of andesite volcanoes that become younger from the Coromandel Peninsula to the Taupo Volcanic Centre (TVC) in the south (Froude and Cole, 1985). The major element data from Titiraupenga used in this study include 10 generally low-Si and medium K, porphyritic andesitic lavas (Froude and Cole, 1985). These lavas are thought to have been derived on the volcanic front from magma generated at a depth of ~110 km (Briggs, 1986) (Appendix 5.6).

4.2.7 Alexandra Volcanics

The Karioi, Pirongia, Kakepuku and Te Kawa volcanic centres collectively comprise the Alexandra Volcanics of Kear and Schofield (1978). They are located in the Waikato region between Raglan in the north and Kawhia Harbour in the south, and extend approximately 40 km inland from the coast. The Alexandra Volcanics are a NE-SW trending suite of Quaternary eruptives with ages that vary between 1.8 and 2.7 Ma (Briggs, *et al.,* 1989) and diverse compositions which include ankaramites, transitional olivine basalts, olivine tholeiites, high alumina basalts and high-K basic and acid andesites (Briggs, 1983). These rock compositions have been attributed to "back-arc mantle wedge convection above a subducting slab", and are not entirely related to subduction processes (Briggs, 1986, Appendix 5.7).

4.2.8 Kora Volcanic Centre

Kora is a relict submarine strato-volcano buried in the offshore North Taranaki Basin some 70 km NNW of New Plymouth (*see* Chapter 1). Magmatism at Kora began with an intrusive event at ~19 Ma, this was followed by extrusive volcanism and a pronounced phase of edifice construction between 16 Ma and 12 Ma. Volcanic activity ceased between 11 Ma and 8 Ma (Bergman *et al.,* 1992). The volcaniclastic rocks comprising the depositional units at Kora consist of depleted mantle source, high Al low-medium-K, calc-alkaline basaltic andesite and andesite clasts which have originated in an intra-arc setting (Bergman *et al.,* 1992; Appendix 5). The major element data used in this study come from four petroleum exploration wells (Appendix 5.8).

4.2.9 Kiwitahi Volcanics

The Kiwitahi Volcanics are a suite of Late Miocene extrusive rocks located on the western side of the Hauraki Rift, a post-Kiwitahi feature (< 5.5 Ma) that separates the Kiwitahi Volcanics from those of the Coromandel Peninsula (Black *et al.,* 1992). The Kiwitahi volcanics trend in what is almost a straight line towards the TVC, extending 120 km from Waiheke Island in the north to Te Tapui in the south (Black *et al.,* 1992). The age of the Kiwitahi Volcanics varies between 11.5 Ma and 5.58 Ma (Skinner, 1986; Black *et al.,* 1992) while rock compositions range from basaltic andesites to andesites and rare dacites considered typical of convergent margin magmas (Black *et al.,* 1992) (Appendix 1.9).

4.2.10 Tongariro Volcanic Centre

The Tongariro Volcanic Centre (TVC) is a Quaternary volcanic centre located in the central North Island, south of Lake Taupo and the Taupo Volcanic Zone. The TVC is dominated by four prominent composite volcanoes, Mount Ruapehu, Mount Tongariro, Pihanga and Kakaramea (Cole *et al.,* 1986). The oldest rocks from TVC are dated at 0.26 +/- 0.003 Ma (the Tongariro massif), and 0.22+/- 0.001 Ma (Kakaramea) (Stipp, 1968, in Cole *et al.,* 1986). The major element data from the TVC used in this study include 18 analyses of samples from representative lavas published in Cole *et al.,* (1986). These lavas are described as calc-alkaline with limited Fe enrichment, and interpreted as medium K – basic to acid orogenic andesites (Cole *et al.,* 1986; Appendix 5.10).

4.3 METHOD

4.3.1 Canonical Discriminant Function Analysis (DFA)

The concept of DFA is described in a number of texts, for example Srivastiva and Carter (1983), Emory and Cooper (1991), Johnson and Wichern (1992), and SAS Institute Inc. (1985). In a geological context, DFA has been used for a number of purposes such as the identification of unknown tephras (Cronin *et al.,* 1996), for environmental discrimination (Stokes *et al.,* 1988), determining the provenance of sandstones and mudstones on the basis of major element data (Roser *et al.,*1988) and for discriminating between rhyolites in the Taupo Volcanic Zone using major and trace element data (Hochstein *et al.,* 1993).

DFA has been used in this study to group together North Island Volcanic Centres with similar major element geochemical signatures. The volcanic centres investigated were Coromandel, Waitakere, Rumble IV, Wairakau, Mount Egmont, Mount Titiraupenga, Alexandra, Kora, Kiwitahi, and Tongariro, and data were obtained from geochemical analyses published in previous studies by a number of authors listed in Appendix 5.

4.3.2 Data Preparation

All the major element data from the Cenozoic North Island volcanic centres listed were entered in to an Excel spreadsheet with the format 'sample SiO_2 TiO_2 Al_2O_3 Fe_2O_3 MgO CaO FeO MnO K_2O P_2O_5 group'. The variable 'sample' is a universal observation identifier and 'group' is an integer representing each class to be discriminated (i.e. each group represents a separate volcanic centre). The data from Kora were entered as a separate sheet because they were to be compared as an 'unknown' against the composite data during DFA.

Prior to data entry, samples with SiO_2 values < 48.0 wt % and > 64.0 wt % were omitted, so that only basic intermediate to acid intermediate samples remained in the composite dataset. This gives all the data a degree of uniformity and makes the discrimination between variables from the different volcanic centres more distinctive by removing variability caused by fractionation. Following data entry and formatting as a single composite Excel file, the data were converted to a formatted text file and transferred to SAS (PC Windows version 6.11) (Appendix 7.1). The data for Kora were formatted and transferred to SAS as a separate file.

4.3.3 Statistical Procedures

Because there is a lack of certainty as to whether the North Taranaki Volcanics are a southward continuation of the western belt of the Northland arc or a western extension of the Kiwitahi-Coromandel-Colville arc, the data for Kora were tested against volcanic centres in the composite dataset. This was done to establish which of the volcanic centres is most similar to Kora. The CANDISC program (SAS Institute Inc., 1985) was used (Appendix 7.2) to illustrate the spatial relationship between canonical groupings representing the North Island volcanic centres in the composite data set. This was achieved by generating the canonical variables from the

composite data set and then plotting the first two canonical variates (Can1 and Can2). The class means for can1 and can2 were also plotted to illustrate the generalized spatial relationship between volcanic source regions. By doing this, the spread of individual samples from each volcanic centre is reduced and the overlap of samples is removed so that the position of each volcanic centre becomes clearer. A discriminant model was then constructed from the composite dataset (Appendix 7.3). The number of canonical variates generated in the discriminant model is the same as the number of volcanic centres used in the study i.e. ten. As part of this procedure the D^2 statistic between groups and the Posterior Probability establish how well the samples have been re-classified i.e. the better the classification efficiency the better the accuracy. The data for Kora were then tested against the discriminant model to identify which of the North Island volcanic centres from the composite data set is most similar to Kora in terms of major element chemistry (Appendix 7.4). As a final procedure, the most effective elements at discriminating between Kora and the data for the other North Island volcanic centres were identified using stepwise DFA (Appendix 7.5). The results list, in order, the most discriminating elements and illustrate the discriminating power of each individual variable.

4.4 DFA RESULTS

4.4.1 Canonical DFA and Plots of Canonical Variates

The results for canonical DFA of the composite dataset (excluding Kora data) and plot of the first two canonical variates (Fig. 4.2) reveal four distinct assemblages. Assemblage 1 is located in the lower left quadrant and contains samples from the Waitakere and Wairakau volcanic centres. Most of the Waitakere and Wairakau data overlap, although six samples from the Waitakere group are spatially distinct within this assemblage and plot lower down on the y axis. These outliers as a whole are not associated with any particular subgroup within the Waitakere Group analyses, however, they generally have relatively higher values (wt %) for Fe_2O_3 and relatively lower values (wt %) for SiO_2 compared with the other samples comprising assemblage 1. Assemblage 2 contains samples from the Mount Egmont dataset. These samples do not generally overlap with any of the other volcanic centres other than one slightly outlying sample that overlaps with the Rumble IV data. The bulk of assemblage 2 forms a relatively tight group near the upper central portion of the graph. The third assemblage contains all Rumble IV data and the single Egmont

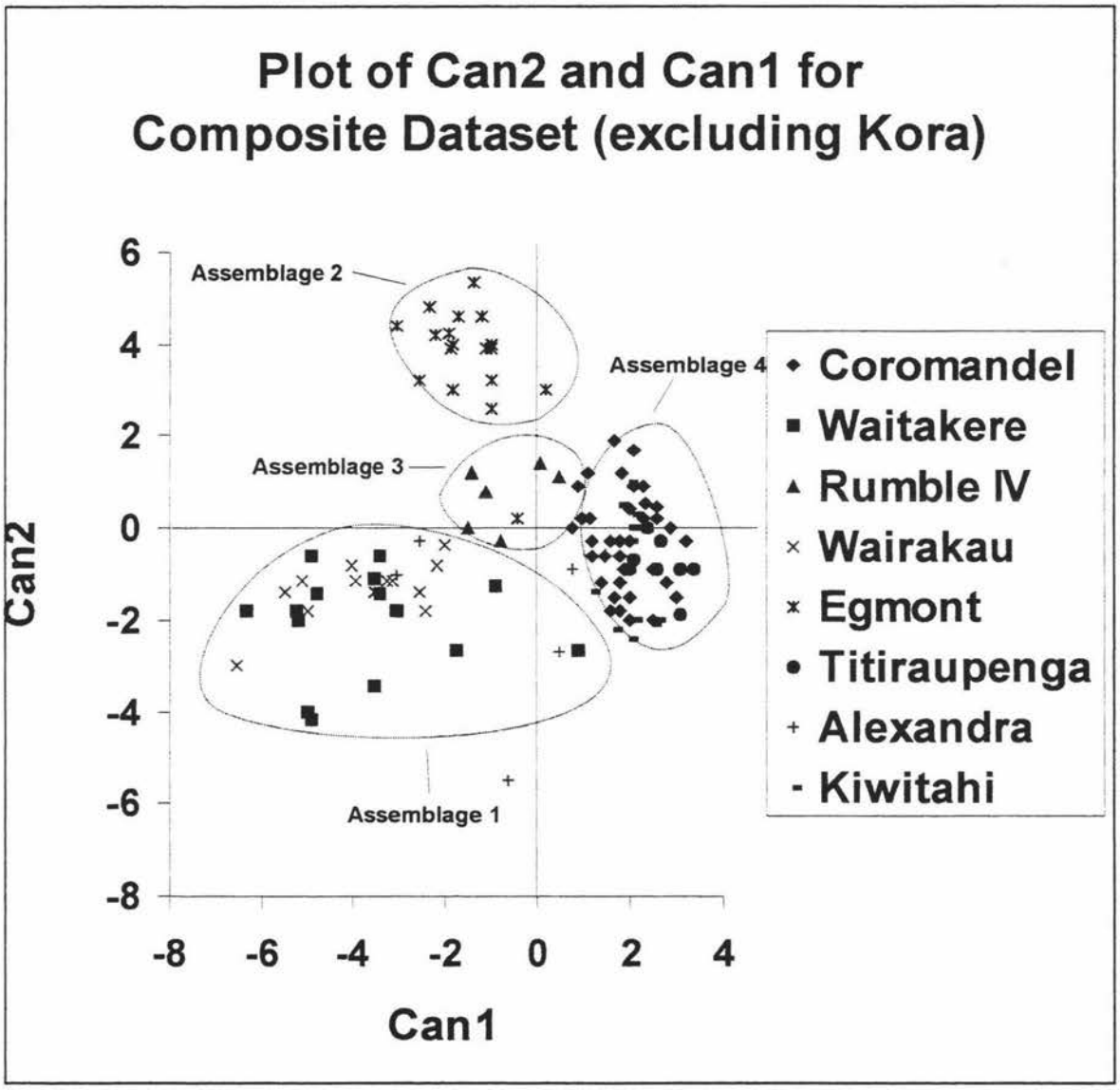
Plot of Can2 and Can1 for
Composite Dataset (excluding Kora)
Assemblage 2
Assemblage 3
Assemblage 4
Assemblage 1
Coromandel
Waitakere
Rumble IV
Wairakau
Egmont
Titiraupenga
Alexandra
Kiwitahi
Can2
Can1
6
4
2
0
-2
-4
-6
-8
-8
-6
-4
-2
0
2
4

Figure 4.2

outlier. The Rumble IV data have a centralized distribution pattern similar to assemblage 2 and lies in an intermediate position between assemblages 1, 2 and assemblage 4. Assemblage 4 contains data for the Coromandel, Kiwitahi, and Titiraupenga volcanic centres. All the samples represented in this assemblage overlap and form a concentrated cluster orientated roughly N-NW. Within the fourth assemblage, samples from the Titiraupenga dataset form a tight group in the SE portion of the assemblage.

Other distinctive features illustrated in this graph include a total absence of TVC data, which are listed as "hidden observations". This indicates that the observations from TVC overlap with other volcanic centres and are not graphically distinct. The wide spread of Alexandra data is another distinctive feature illustrated in the plot of can1 and can2. These data are mostly spread through assemblage 1.

Assemblages 1 and 4 are the dominant associations representing most of the North Island Volcanic Centres. The spatial relationship between these two assemblages is more clearly illustrated when the "class means" for can1 and can2 are plotted and the overlap of individual samples is removed. Fig. 4.3 is a plot of the class means for can 1 and can 2 which shows that the four assemblages identified in Fig. 4.2 are largely correct, except that the Alexandra samples now appear to be more closely related to assemblage 1 containing the Waitakere and Wairakau data. Also, samples from TVC are now illustrated and plot with assemblage 4, which contains the Coromandel, Kiwitahi and Titiraupenga data. The plot of class means also demonstrates the overall heterogeneity between assemblages, especially the Egmont and Rumble IV data (assemblages 2 and 3). That is to say, the data for Mount Egmont plot well away from all other assemblages and the Rumble IV data plot in an intermediary position between assemblage 1 and assemblage 4.

4.4.2 Test Preparation – Development of a Canonical Model

The canonical model generated for the composite dataset prior to comparison with the data for Kora produces the squared distance (D^2) between groups or North Island Volcanic Centres. This is an effective means of establishing how closely related the major element chemistry from each volcanic centre or group in the composite dataset is. In this study D^2 values <10 indicate a close relationship between volcanic centres,

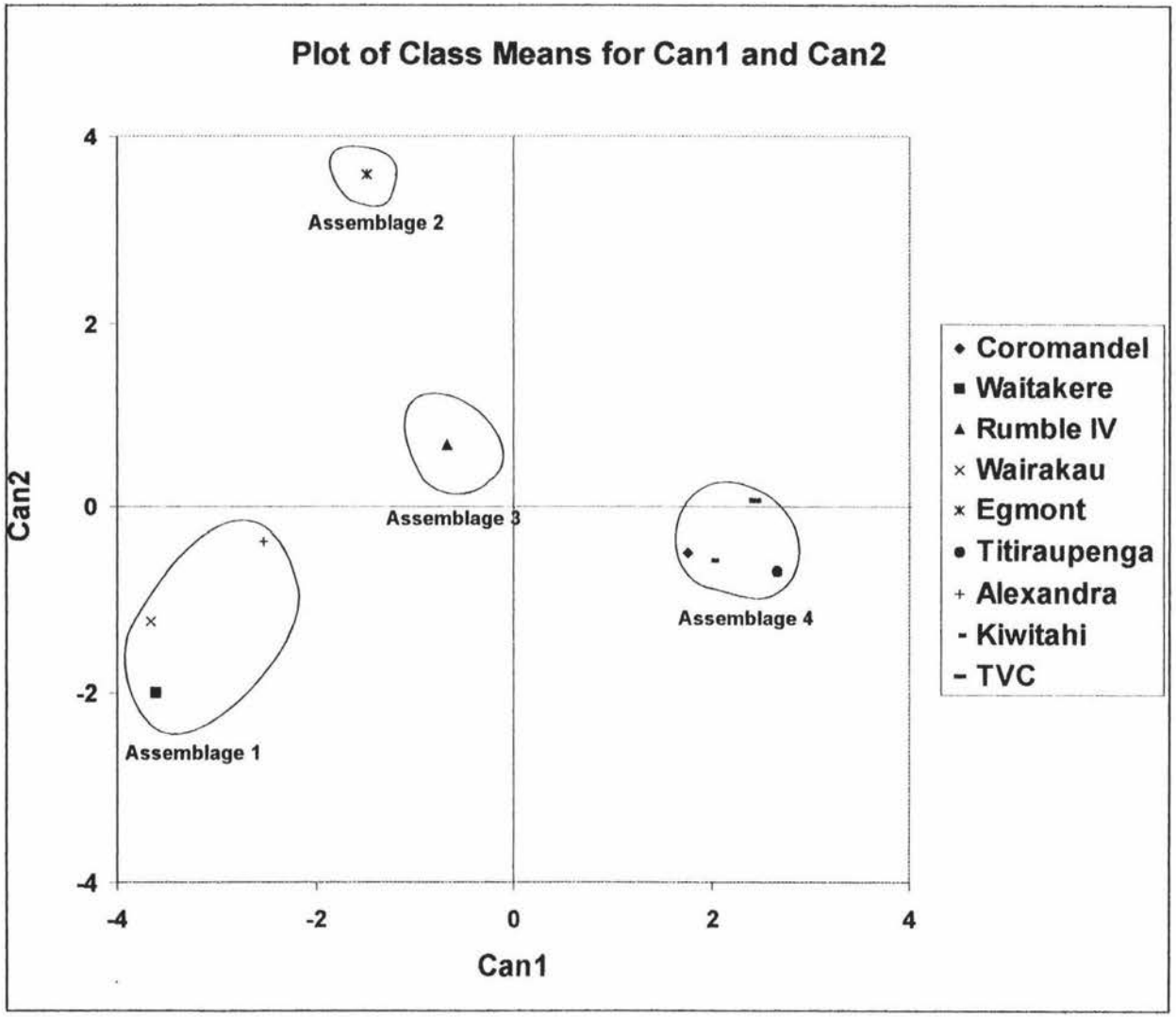
Plot of Class Means for Can1 and Can2
Assemblage 2
Assemblage 3
Assemblage 4
Assemblage 1
Coromandel
Waitakere
Rumble IV
Wairakau
Egmont
Titiraupenga
Alexandra
Kiwitahi
TVC
Can2
Can1
4
2
0
-2
-4
-4
-2
0
2
4

Figure 4.3

while increasing D^2 values (>10) indicate a progressively weaker relationship. The D^2 values for all of the data in the composite dataset are illustrated in Table 4.1. The D^2 values for each of the volcanic centres do not exceed 51 or fall below 1, and from these data the relationships between groups in the four assemblages of Fig. 4.2 in section 4.4.1 are verified.

Results show that the Waitakere Volcanics are most similar to the Wairakau and Alexandra Volcanics and that these three volcanic centres are uniformly distinct from all other volcanic centres, verifying the classification of groups in assemblage 1. The data for Mount Egmont and Rumble IV are distinct from each other and all other centres. Mount Egmont has D^2 values 20 – 41 and Rumble IV has no D^2 values < 28, essentially verifying the heterogeneous character of major element chemistry in assemblage 2 and assemblage 3. The four remaining volcanic centres of assemblage 4 in Fig. 4.2 section 4.4.1 including the Titiraupenga, Kiwitahi, TVC and Coromandel data, all have low D^2 values in relation to each other and relatively high values in relation to the other 3 assemblages.

4.4.3 Stepwise Analysis

Results for the Stepwise Discriminant Analysis show that the major elements used in DFA of the North Island Volcanic Centres (excluding Kora) are all relatively similar in terms of discriminating efficiency. The F statistics show that all elements range from 0.8 (MnO) to 21 (Fe_2O_3) (Table 4.2), with only MnO removed due to its relatively constant values in all of the datasets from the North Island Volcanic Centres. The results from Stepwise DFA suggest that the assemblages defined in Fig. 4.2 are discriminated by bulk major element differences as opposed to being influenced by just one or two dominant, highly variable elements, thus demonstrating the reality of the differences between the defined assemblages.

4.4.4 Kora Volcanics Compared with all Other North Island Volcanic Centres

Fig. 4.4 illustrates the percentage of samples from Kora that were re-classified with the assemblages defined in section 4.4.1, and Table 4.3 presents the Posterior Probability that those samples have been correctly re-classified. The results show that the major element chemistry of the Kora Volcanics is most similar to assemblage 1, while assemblages 2, 3 and 4 are least similar to Kora. The Posterior Probabilities

Squared Distance Between Groups

	Coromandel	Waitakere	Rumble IV	Wairakau	Egmont	Titiraupenga	Alexandra	Kiwitahi	TVC
Coromandel	0.00	36.41	28.01	33.71	29.18	14.72	26.52	2.02	3.85
Waitakere		0.00	40.62	11.17	37.91	49.55	9.99	36.15	44.35
Rumble IV			0.00	33.45	31.68	42.25	36.00	28.12	31.61
Wairakau				0.00	31.75	50.67	7.83	36.70	41.78
Egmont					0.00	41.77	19.82	30.17	28.47
Titiraupenga						0.00	31.28	8.55	6.56
Alexandra							0.00	25.03	27.04
Kiwitahi								0.00	1.80
TVC									0.00

Table 4.1

Results for Stepwise Discriminant Analysis of Major Element Geochemistry from North Island Volcanic Centres (excluding Kora)

Element	F Statistic	Wilk's Lambda
Fe2O3	21.6	0.420
CaO	18.6	0.090
MgO	16.4	0.010
K2O	15.6	0.210
TiO2	12.8	0.050
Na2O	11.4	0.005
FeO	6.4	0.020
Al2O3	6.3	0.038
SiO2	4.8	0.029
P2O5	2.1	0.004
MnO	0.8	Removed

Table 4.2

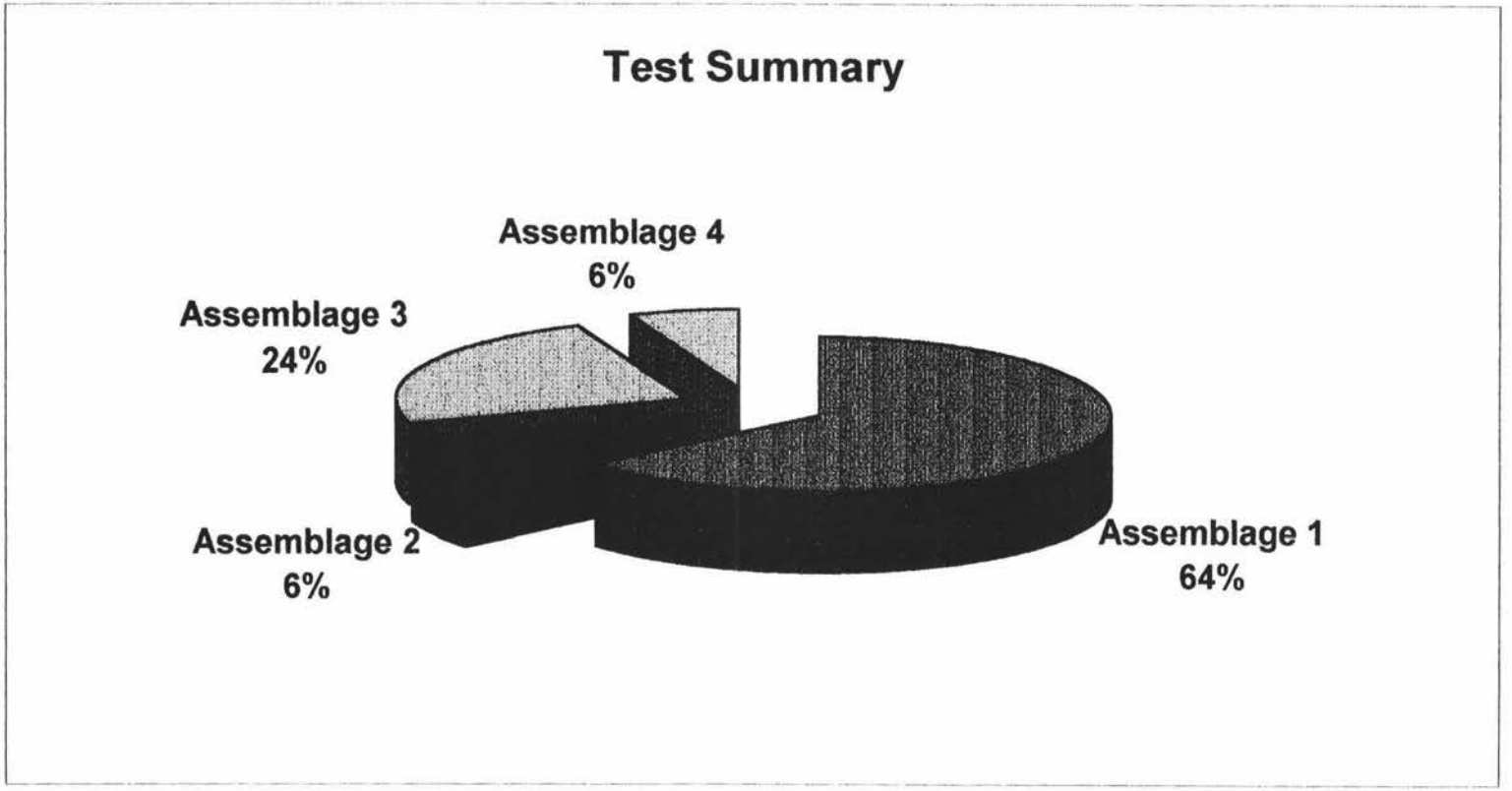

Figure 4.4
Chart illustrating the percentage of samples from Kora that reclassified in to the four assemblages defined in Section 4.4

Posterior Probabilities that samples from Kora were correctly re-classified

Sample	Lithology	Well	Well Depth (m)	Group Classified	Pr
kor1	WHT	Kora-1A	1785.7	WAITAKERE	0.99
kor2	WHT	Kora-1A	1787	WAITAKERE	0.88
kor3	RC	Kora-1A	1788.7	ALEXANDRA	0.60
kor4	GC	Kora-1A	1793.41	WAITAKERE	0.99
kor5	GC	Kora-1A	1794.6	ALEXANDRA	0.36
kor6	RC	Kora-1A	1795.42	WAITAKERE	0.98
kor7	GC	Kora-1A	1812.13	KIWITAHI	0.83
kor8	GC	Kora-1A	1824.68	ALEXANDRA	0.73
kor9	GC	Kora-1A	1825.55	RUMBLE IV	0.99
kor10	GC	Kora-1A	1826.59	ALEXANDRA	0.79
kor11	LT	Kora-1A	1827.73	WAITAKERE	0.99
kor12	GC	Kora-1A	1841.03	RUMBLE IV	0.98
kor13	GC	Kora-1A	1841.4	WAITAKERE	0.99
kor14	HTB	Kora-1A	1843.6	EGMONT	0.64
kor15	GC	Kora-1A	1895.72	RUMBLE IV	0.99
kor16	GC	Kora-1A	1899.42	ALEXANDRA	0.44
kor17	HTB	Kora-1A	1901.11	WAITAKERE	0.94
kor18	GC	Kora-1A	1904.2	KIWITAHI	0.54
kor19	GC	Kora-1A	1907.75	RUMBLE IV	0.82
kor20	GC	Kora-1A	1908.23	RUMBLE IV	0.90
kor21	HTB	Kora-1A	1910.06	ALEXANDRA	0.55
kor22	MS	Kora-2	1280	ALEXANDRA	0.69
kor23	MS	Kora-2	1285.2	WAIRAKAU	0.99
kor24	PC	Kora-2	1321.56	WAIRAKAU	0.93
kor25	PC	Kora-2	1321.96	WAITAKERE	0.58
kor26	PC	Kora-2	1323.4	WAITAKERE	0.96
kor27	PC	Kora-2	1323.8	WAIRAKAU	0.84
kor28	PC	Kora-2	1331.6	WAIRAKAU	0.94
kor29	TB	Kora-3	1809.5	WAITAKERE	0.66
kor30	T	Kora-3	1810.3	WAITAKERE	0.99
kor31	TB	Kora-3	1812.5	WAITAKERE	0.97
kor32	T	Kora-4	1718	EGMONT	0.98
kor33	T	Kora-4	1780.5	WAIRAKAU	0.99
kor34	T	Kora-4	1853	WAIRAKAU	0.97

Terminology defined in Bergman et al., (1992)

WHT = Welded Hyaloclastite Tuff
RC, GC, PC = Conglomerate Clasts
LT = Lapilli Tuff
MS = Mudstone
TB = Tuff Breccia
T = Tuff

Table 4.3

(Pr) listed in Table 4.3 demonstrate how realistic the reclassification results illustrated in the test summary (Fig. 4.4) are (I.e. where Pr=1 the classification between two volcanic centres is realistic, while a Pr value of 0 suggests the relationship between classified volcanic centres is doubtful). The results show that reclassification of samples from Kora to the volcanic centres comprising assemblage 1 and assemblage 3 is generally very good i.e. Pr values are between 0.80 and 0.99. In contrast Pr values for assemblage 2 and assemblage 4 are generally < 0.8 and as low as 0.4. These results suggest that the relationship between Kora and assemblage one illustrated in Fig. 4.4 is realistic, and that Kora most likely belongs to a volcanic arc that includes the Waitakere and Wairakau volcanic centres. In comparison the relatively low Pr values between assemblage 2, assemblage four and Kora suggests this relationship is doubtful.

4.4.5 Description of Final Assemblages

In a geological and geographical context, the comparison of major element chemistry from North Island Volcanic Centres using DFA and comparison with Kora show that Kora is most similar to the Waitakere, Alexandra and Wairakau Volcanic Centres of assemblage 1 illustrated in Fig. 4.5. Assemblage 1, which contains intermediate rocks from the Waitakere, Wairakau, and Alexandra Volcanic Centres as well as Kora, forms a NNW trending belt which extends from the top of the Northland Peninsula to Kora which is located farther south in the Northern Taranaki Basin. The southern portion of this belt is orientated more towards the NNE, as a slight "dog leg" in the centre of the belt.

Kora, the Waitakeres and Wairakau volcanics all overlap in age. Waitakere volcanism occurred between 18 Ma and 15 Ma (Wright and Black, 1981) and Wairakau volcanism occurred bewteen 19.9 and 20.3 Ma (White, 1985), while volcanism at Kora began with an intrusive event at ~19 Ma followed by an extended period of eruptive activity which finally ceased at approximately 8 Ma (Bergman *et al.,* 1992). In contrast the Alexandra Volcanics are dated at 1.6 – 2.7 Ma (Briggs *et al.,* 1989) somewhat anomalous in relation to the other volcanic centres in assemblage 1 but following the general trend of the migrating arc. Assemblage 2, despite being < 80 km SE from assemblage 1, are < 0.12 Myrs BP in age (Stewart *et al.,* 1996), and the major element chemistry is distinct from all other volcanic centres used in this

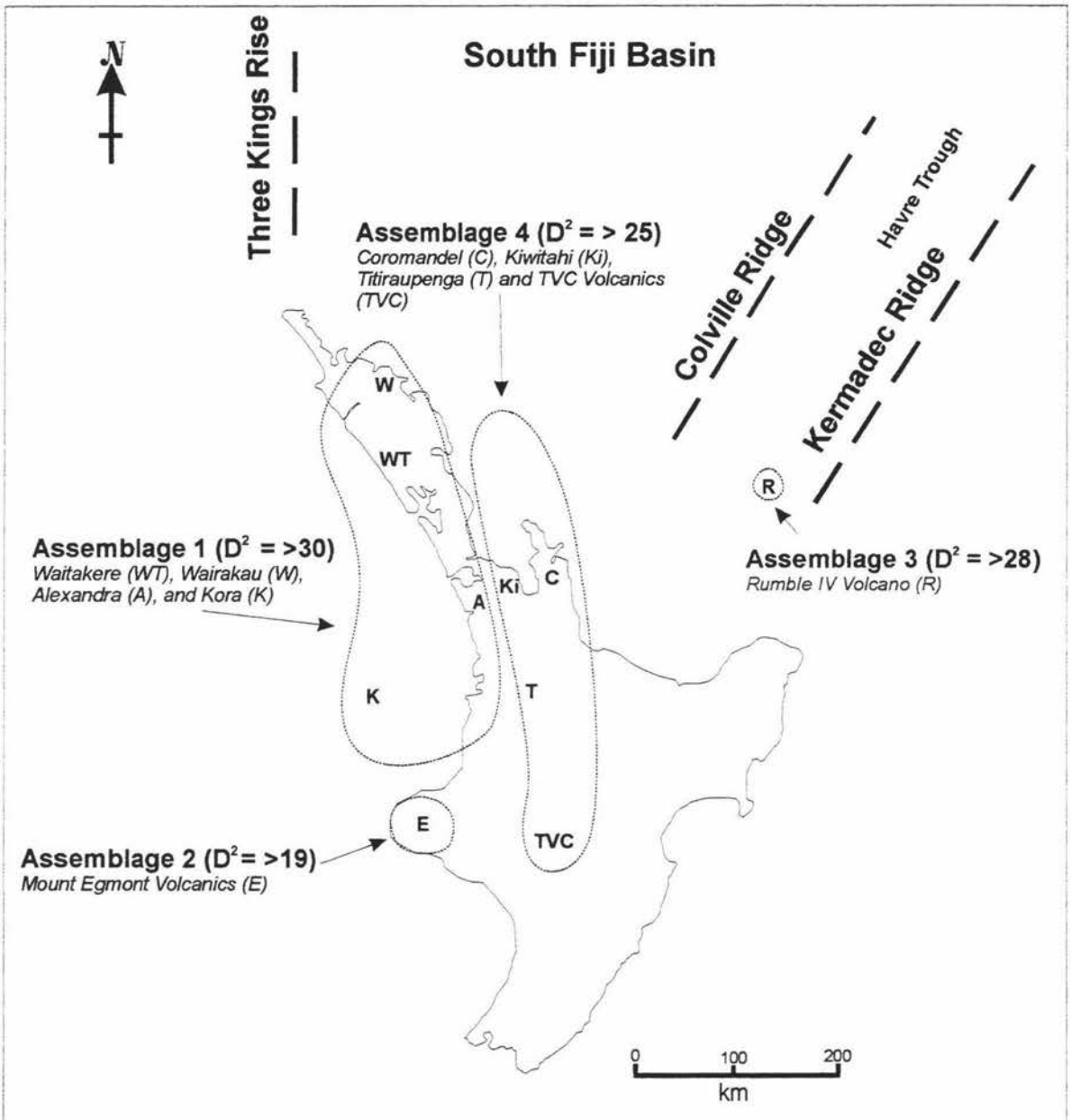

Figure 4.5
Illustration showing the statistical distance between assemblages defined from comparison of major element chemistry between North Island Volcanic Centres using DFA.

study. Assemblage 3 which contains Rumble IV, is very similar to Kora with regard to major element chemistry, however Rumble IV is ~600 km NE from Kora and might only be as old as 0.77 Ma (Wright, 1994). Rumble IV can therefore be regarded as a separate assemblage based on its geographic location and age. The Coromandel, Kiwitahi, Titiraupenga and TVC volcanics that comprise assemblage 4 are all closely associated in terms of major element chemistry and form a NNW trending arc that is subparallel with assemblage 1. The age of volcanic activity varies from 18 Ma in the Coromandel to between 0.26 Ma and 0.22 Ma at TVC (Stipp, 1968 in Cole *et al.*, 1986). Like assemblage 1, a slight "dog leg" occurs in the southern part of the assemblage where the orientation of the assemblage trends more towards the NNE.

4.5 INTERPRETATION OF RESULTS

4.5.1 The Geochemical Relationship between Assemblages

The two dominant assemblages, 1 and 4, consist of volcanic centres that are related primarily by major element chemistry and secondly by age and spatial location. Each individual assemblage displays two disparate orientations, for example, in assemblage 1 the Northland centres form a roughly north-south orientation before intersecting a generally younger northeast-southwest orientated Northern Taranaki Volcanic Centre. These orientations are emulated in assemblage 4 where the Kiwitahi and Coromandel Volcanic Centres form a roughly north-south lineament that intersects with the TVC, which is orientated more towards the NE-SW.

The subparallel orientations between assemblage 1 and assemblage 4 including the variable age data within these assemblages may correspond to a single volcanic arc that was jostled towards the east and southeast in intermittent steps from Miocene to Recent times. This pattern of arc migration would require asymmetric extension over a relatively short period of time to account for the present position of the modern arc. For example, King and Thrasher (1997) have suggested that the similar asymmetric, fan-like opening of the Northern Graben and Central Volcanic Region may mean that the Northern Graben was a pre-cursor to the Central Volcanic Region. Evidence for the localised extensional tectonic regimes required for this scenario include the fan-like opening of the Northern Graben which began in the late Miocene (King and Thrasher, 1997), the opening of the Hauraki Graben which occurred after 5.5 Ma (Adams *et al.*, 1994) and back-arc spreading associated with the Havre Trough,

which has occurred since 4 Ma in conjunction with extension in the Central Volcanic Region (Wright, 1993b). A further event is also evinced by the Gannet Island volcanics (c.0.5 Ma.), which are related to crustal relaxation and extension (Briggs *et al.* in press; King and Thrasher, 1997).

The variable orientations between the volcanic centres comprising assemblage 1 and assemblage 4 may suggest that the eastern North Island has rotated in a clockwise direction since the Early Miocene, while the Northland Peninsula has remained stationary. This relationship may be controlled in part by the presence of a deep-seated structural feature such as the Turi Fault Zone. Overall, the irregular pattern of Tertiary arc migration in the North Island is probably a response to differential dip angle along the length of the subducting slab (e.g. Knox, 1982), and the underlying convergent and transcurrent tectonic plate regime which is manifested in the Australian/Pacific plate boundary today (e.g. Brothers, 1984; Kamp 1984; Kear 1994; King and Thrasher, 1997).

4.5.2 Relationship between Kora and the Northland Arc

The results from this study help to clarify the relationship between Kora and the western and eastern belts of the Northland Arc. Most previous workers consider the Northern Taranaki volcanoes are a southern extension of the western belt of the Northland arc, which in this study is represented by the Waitakere Volcanic Centre (e.g. King and Thrasher, 1997; Bergman *et al.*,1992). However, Herzer (1995) suggested another possibility might be that the Northern Taranaki volcanoes are a southwestern extension of a volcanic arc extending from the North Taranaki volcanoes, through the Coromandel Volcanic Centre and towards Collville Ridge. If Kora is representative of the Northern Taranaki volcanics, however, then results from this study support the previously held view that the Northern Taranaki Volcanics are a southern extension of the Northland Arc. If the Northern Taranaki Volcanics do belong to a greater Northland Arc, then the results from this study also suggest that the rate of arc migration and subduction must vary considerably along the arc front, i.e. volcanism at Kora lasted more than 10 Myrs (Bergman *et al.,* 1992), and only 6 Myrs in the Northland Arc (Herzer, 1995).

4.5.3 The Geochemical Affinity between Kora and Rumble IV

The close similarity in major element chemistry between Rumble IV and Kora is somewhat anomalous to the overall results of this study. Kora is the only North Island Volcanic Centre with a similar geochemical signature to Rumble IV, despite both centres being spatially separate by nearly 600 km and temporally detached by approximately 8 Myrs. It is also interesting to note that Kora and Rumble IV were both active in a relatively deep-water environment, are similar in size, and have similar eruptive deposits (e.g. Bergman *et al.,* 1992; Wright, 1996). Bergman *et al.,* (1992) have also shown that sea water interaction and contamination by continental crust at both centres was minimal, i.e. Kora and the Kermadec Arc volcanoes are amongst the most depleted volcanic centres in New Zealand with respect to Nd and Sr isotope ratios (Bergman *et al.,* 1992). Because it is improbable that the two centres share the same magma batch, then the similar geochemical signatures must reflect the spatial proximity of both volcanic centres to the arc front, or position above the subducting slab (i.e. Kora and Rumble IV both evolved in a frontal arc setting).

4.5.4 The Geochemical Relationship Between Egmont and all North Island Volcanic Centres

Mount Egmont Volcanic Centre is distinct from all other centres in terms of major element chemistry despite being coeval to TVC with respect to eruptive activity and its proximity to the older northern Taranaki Volcanics. The volcanic activity associated with the Egmont Volcanics is considered a westerly extension of TVC volcanism (Neall *et al.,* 1986). If the Egmont Volcanics are an extension of TVC then the results from DFA in this study must reflect a cross-arc variation in major element chemistry. That is to say, major element compositions can change systematically with increasing distance away from a convergent margin and relatively less along the arc axis (Sillitoe, 1976). If this is correct then the results from DFA in this study may be detecting relict cross-arc variations in major element chemistry. This relationship may also provide an explanation for the similar geochemistry between Kora and Rumble IV whereby Kora was located in a frontal arc position similar to where Rumble IV is located today.

4.5.5 Geochemical Relationship between the Northland Arc and the Coromandel Volcanic Centres

Black *et al.,* (1981) stress that the relationship between the Coromandel Arc and the West Northland Volcanic Arc is unclear. Results from this study show that the western and eastern belts of the Northland Arc do not share similar major element chemistry despite overlapping age data. This observation suggests that volcanism extended a relatively long distance out from the arc front, possibly caused by a relatively shallow dipping subduction zone. For example, Black *et al.,* (1981) have suggested that the subducting slab beneath Northland may have dipped at an angle as shallow as 20 degrees. Furthermore, the two arcs are separated by a terrane boundary (Stokes Magnetic Anomally; e.g. Knox, 1982) and the subsequent variations in crustal thickness may also account for geochemical variations between the two arcs (Stewart, pers comm).

4.5.6 The Geochemical Relationships between Volcanic Centres in Assemblage 4

The inter-relationships between volcanic centres in assemblage 4 display the greatest amount of similarity in major element chemistry. It is interesting to note the major element signatures for TVC overlaps almost exactly with the Coromandel, adding weight to the point made by Adams *et al.,* (1994), that Coromandel volcanism was a precursor to volcanism in the Taupo Volcanic Zone, including the Tongariro Volcanic Centre. At the same time, results from this study also support the idea that the Coromandel and Kiwitahi Volcanic Centres were once part of the same arc before the Hauraki Rift developed after 5.5 Ma (Adams *et al.,* 1994).

4.6 SUMMARY

Discriminant analysis of major element chemistry from Early Miocene to Recent North Island Volcanic Centres define two distinctive, subparallel assemblages which may define independent palaeo-arc fronts or source magmas. These results suggest that:

1. if Kora is representative of the North Taranaki Volcanics then the North Taranaki Volcanics are an extension of the Northland Arc;
2. since the Early Miocene only one subduction zone has existed beneath the North Island;
3. this single North Island Arc has generally migrated east and south with time;

4. arc migration rates have varied widely along the arc front and these variations account for the disparate orientations of Miocene to Recent arc volcanism;
5. volcanic centres situated between the Coromandel Volcanic Centre and TVC belong to a volcanic arc which is the migrated equivalent of the Northland Arc.

5.0 Discussion

5.1 SYNTHESIS OF SEISMIC, GEOCHEMICAL, AND LITHOLOGICAL DATA

The depositional environment and depositional volcaniclastic processes that shaped Kora throughout the Miocene are summarized schematically in Fig. 5.1. Many of the volcaniclastic processes and environmental conditions illustrated in Fig. 5.1 are comparable to modern submarine arc volcanoes.

5.2 CONTEMPORARY SUBMARINE ARC-VOLCANOES

Process oriented studies that deal with submarine arc volcanoes are constrained by the practicalities of working in deep water. Consequently, most previous studies dealing with submarine arc-volcanoes are interpretations of ancient, uplifted sequences (for example Kano *et al.,* (1993), Kano (1989), Wright and Mutti (1981), Cas (1979), Cosineau (1994)). The interpretation of ancient submarine volcanic sequences has been hindered by the lack of documented modern analogues. Furthermore, ancient sequences are often restricted to a few metres of degraded and eroded outcrop. This makes the interpretation of volcaniclastic processes less conclusive than interpretations of volcaniclastic processes based on firsthand observations from modern submarine volcanoes. Recently oceanographic studies have observed volcaniclastic processes on modern submarine arc volcanoes using sea floor photography, remotely operated submarines and sidescan sonar technology. Such studies provide helpful analogues on which to base the interpretation of ancient submarine volcanic events. The interpretation of the volcaniclastic processes active at Kora during the Miocene has been greatly helped by the development of modern analogues.

5.3 THE PHYSICAL VOLCANOLOGY AND ERUPTIVE ENVIRONMENT OF MODERN SUBMARINE ARC VOLCANOES

The submarine conditions inferred at Kora in the Miocene are inferred to be similar to the submarine conditions that surround the volcanoes in the southern Kermadec frontal arc, located north of the Bay of Plenty in New Zealand. The Kermadec volcanoes Rumble II – V, Silent II, Clark and Whakatane have been studied by Wright (1994, 1996) (Fig. 5.2). These volcanoes are located in water depths that range

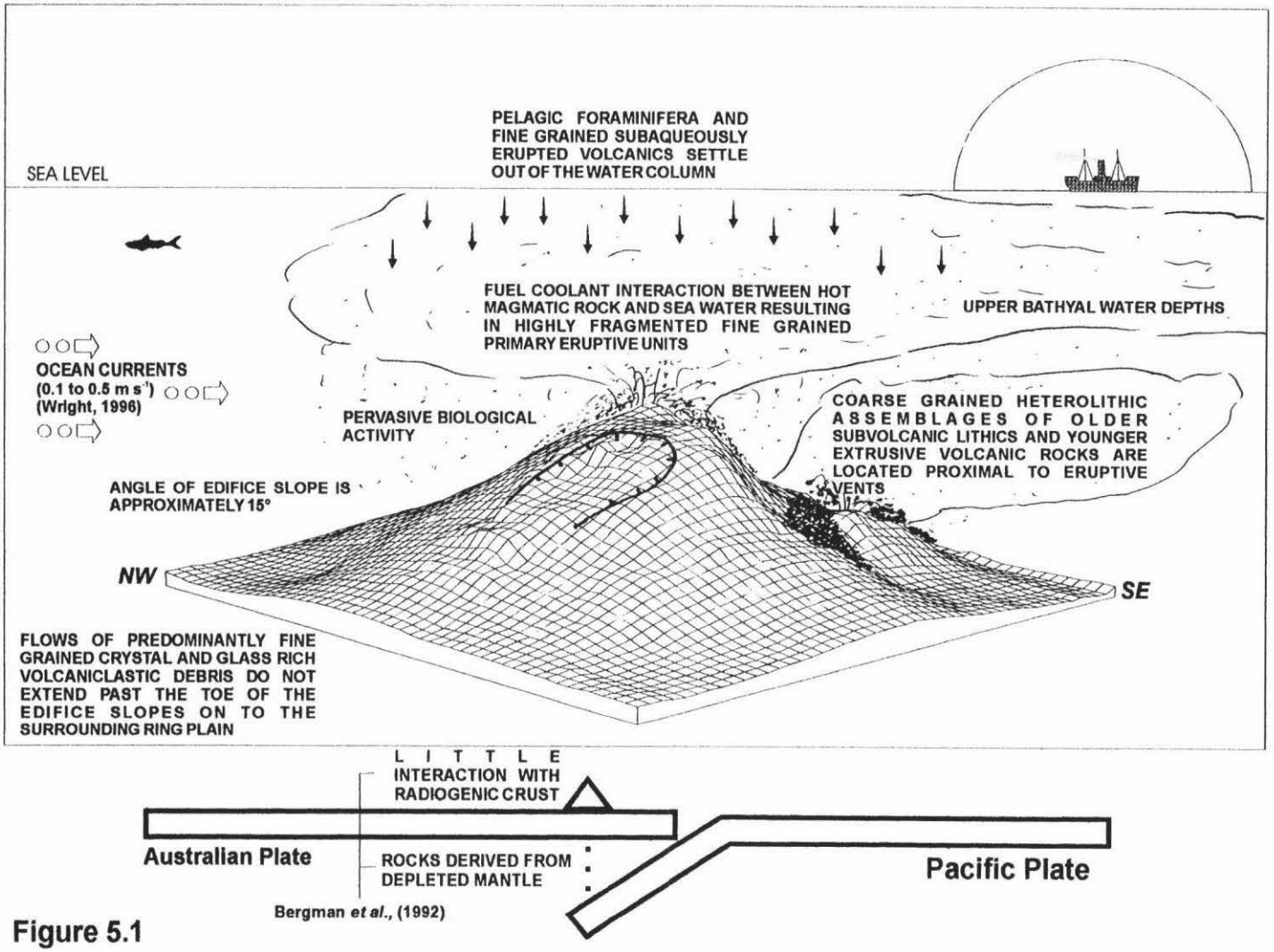
PELAGIC FORAMINIFERA AND FINE GRAINED SUBAQUEOUSLY ERUPTED VOLCANICS SETTLE OUT OF THE WATER COLUMN
SEA LEVEL
FUEL COOLANT INTERACTION BETWEEN HOT MAGMATIC ROCK AND SEA WATER RESULTING IN HIGHLY FRAGMENTED FINE GRAINED PRIMARY ERUPTIVE UNITS
UPPER BATHYAL WATER DEPTHS
OCEAN CURRENTS
(0.1 to 0.5 m s-1)
(Wright, 1996)
PERVASIVE BIOLOGICAL ACTIVITY
COARSE GRAINED HETEROLITHIC ASSEMBLAGES OF OLDER SUBVOLCANIC LITHICS AND YOUNGER EXTRUSIVE VOLCANIC ROCKS ARE LOCATED PROXIMAL TO ERUPTIVE VENTS
ANGLE OF EDIFICE SLOPE IS APPROXIMATELY 15°
NW
SE
FLOWS OF PREDOMINANTLY FINE GRAINED CRYSTAL AND GLASS RICH VOLCANICLASTIC DEBRIS DO NOT EXTEND PAST THE TOE OF THE EDIFICE SLOPES ON TO THE SURROUNDING RING PLAIN
L I T T L E
INTERACTION WITH RADIOGENIC CRUST
Australian Plate
ROCKS DERIVED FROM DEPLETED MANTLE
Pacific Plate
Bergman et al., (1992)

Figure 5.1

between 120 m and 1157 bsl and have maximum basal diameters that vary between 25 km

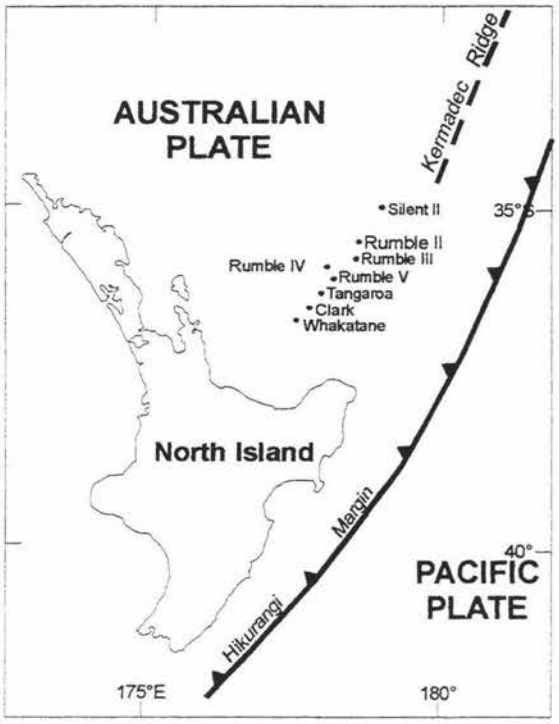

Fig. 5.2
Location of southern Kermadec arc volcanoes (*after* Wright, 1994).

and 13 km. The relief of each edifice also varies between 1040 m and 2280 m. In comparison, Kora has a basal diameter of approximately 12 km and a vertical relief of nearly 1000 m, while the inferred palaeo-water depth surrounding the Kora edifice is between 200 and 500 m bsl (i.e. mid-upper bathyal depths; Bergman *et al.,* 1992). Like Kora, some of the Recent volcanoes (Rumble IV and V) have no summit crater, and satellite cones are common.

It is interesting to note that while Kora is some 15 Ma older than the volcanoes of the southern Kermadec arc (*the arc front has an age of* 0.77 Ma (Wright, 1996)), Kora is only small to intermediate in size compared with the Kermadec volcanoes. The duration of volcanism at Kora was more than 10 Ma (Bergman *et al.,* 1992). This suggests that either the volume of erupted material at Kora was considerably less than the Kermadecs, or that ocean currents removed large volumes of volcaniclastic material from the Kora edifice while it was exposed on the sea floor. Volcaniclastics are well represented in the coastal stratigraphic sequences of northern Taranaki (e.g. Mohakatino Formation (Nodder *et al.,*1990; King *et al.,*1993)). The eruptive source for

these coastal volcaniclastics is offshore, west of the present day Taranaki coast (e.g. Hatherton, 1968). This suggests that the constructional volume of Kora and the other marine volcanoes located off the Taranaki coast during Mohakatino times were influenced by ocean currents and the ambient submarine conditions surrounding each subaqueous eruptive centre. This further suggests that the size of Kora inferred from seismic profiles is a minimum size.

Myojinsho is one of 19 submarine arc volcanoes identified along the northern portion of the Izu-Ogasawara arc, Japan. Located some 420 km south of Tokyo, this shallow silicic volcano (Yuasa *et al.,* 1991; Fiske *et al.,* 1998) is infamous for an eruptive episode between 1952 and 1953 which destroyed the Japanese survey ship No.5 Kaiyo-maru, killing its crew of 31. One of the explosive eruptions was photographed and reported by National Geographic (Dietz, 1954), and more recently Fiske *et al.,* (1998) have reconstructed some of the depositional events associated with Myojinsho during and since the 1952-1953 eruptions. During eruptions at Myojinsho, the ocean currents near the sea surface dispersed plumes of discoloured water. The plumes had such a high concentration of volcanic ejecta that the pilot of a ship that passed through one of the plumes could feel resistance on the screw of the ship. The plumes were 25 m thick (Tsuya et al., 1953), and enriched in volcanic dust and pyroxene crystals (Nakano et al., 1954; Fiske et al., 1998). Fiske *et al.,* (1998) have suggested that if these plumes were travelling upwards at 50 cm/s, then dense fragments up to 1 cm may have been redispersed by the ocean currents.

Given the fine grained character of the depositional units cored from near the crest of the Kora edifice in Kora-2 and Kora-3 wells, and with efficient current dispersal of the volcanic detritus, even the long duration of volcanism at Kora may have been insufficient for a large edifice to develop. Wright (1996), has attributed the presence of winnowed volcaniclastic sands observed near the crest of Rumble IV in the southern Kermadec arc to 0.1 – 0.5 m s^{-1} bottom currents. If similar magnitude ocean currents influenced the dispersal of post-eruptive and syneruptive detritus at Kora throughout its active phase, then the amount of material removed, while unknown, could be significant. Fiske *et al.*, (1998) have suggested that the tephra removed from Myojinsho during and after the 1952-1953 eruptions probably only totalled a small percentage of the total tephra erupted. However, if this small percentage is

extrapolated over a 10 Myr period, then the proportion of primary eruptives and secondary epiclastics removed from Myojin could be considerable.

5.4 VOLCANICLASTICS FROM MODERN SUBMARINE ARC VOLCANOES

Rumble IV and Rumble V are modern submarine volcanoes located in the southern Kermadec arc (Fig. 5.2). Wright (1996,1994), has described the physical volcanology of Rumble IV and Rumble V from sidescan sonar and sea floor photography. The lithologies from these volcanoes include matrix supported heterolithic breccias with varying degrees of sorting, lapilli tuffs, and winnowed volcaniclastic sands. Pelagic and hemipelagic sediments were also observed in the volcaniclastics on the flanks of Rumble IV and V (Wright 1996, 1994). Compared to the core lithologies from Kora, the matrix supported, heterolithic breccias described in Wright (1996, 1994) appear similar to the conglomerates and tuff breccias in Kora-1A. Likewise, the lapilli tuffs observed on the Rumble volcanoes appear similar to the lapilli tuffs in the upper cored interval of Kora-2 and Kora-3. The winnowed volcaniclastic sands of Rumble IV and V may also have a possible equivalent in the tuffs, which were observed in the upper depths of Kora-1A, Kora-2 and Kora-3.

Some of the lithologies associated with Rumble IV and V that were not observed at Kora include effusive and pillow lavas, monolithic clast supported talus breccias and fines-depleted units. Another significant difference is that none of the clasts in the cores from Kora showed any evidence for the multiple cooling and contraction, chilled carapace surfaces identified by Wright (1996). In general, the volcaniclastic sedimentation described by Wright (1996, 1994) seems to be controlled by the spatial location of pillow lava outcrop, small eruptive vents (5-10 m wide) and effusive lavas, which are mostly surrounded by clast fragments derived from these outcrops. The slope processes responsible for epiclastic redeposition of these units are described by Wright (1996) as avalanche slides, debris flows or local grain flow redeposition, with no evidence for large distributary channels within the flank deposits.

While some of the volcaniclastic deposits from Kora are similar to the fragmental deposits on Rumble IV and V, massive extrusive lavas and pillow lavas are absent at Kora. This suggests Kora has either experienced a higher degree of granulation and explosivity at the magma-water interface than the Rumble volcanoes, or that the

sparsely distributed exploration wells at Kora failed to intercept any lava. Seismic reflection profiles across Kora indicate that if lavas are present on the flanks of Kora, then they can be no more than ~10 m thick (see Chapter 3). This is because the flow has to be greater than 1/4 of a seismic wavelet thick to resolve the top and bottom of the flow and 1/30 of a wavelet for any reflection at all. Given that one seismic wavelet from the volcanics at Kora is generally about 180 m thick, if any lavas are present at Kora they are unlikely to be more than 10 m thick (Stagpoole pers comms., 2/1998). Bergman *et al.*, (1992) have suggested that explosive eruptions were more likely at Kora than non-explosive lava forming eruptions because abundant hornblende in the Kora eruptives implies high water content in the lavas. This study supports the model that Kora is almost entirely made up of fragmental deposits. This model is supported by the lack of pristine lavas, the abundance of clays derived from andesite glass, the abundance of eruptive rocks smaller than cobbles and the relatively small size of the volcanic edifice compared to modern submarine arc volcanoes. Lithic clasts in the volcaniclastics from near the summit of Kora were originally derived from subvolcanic intrusives. These also indicate that eruptions from Kora produced mostly fragmental deposits.

5.5 SCALE OF SLOPE TRANSPORT EVENTS ON MODERN SUBMARINE ARC-VOLCANOES

Large-scale epiclastic mass-flows of volcaniclastic debris are often associated with steeply inclined volcanoes in oceanic settings. For example, tephra associated with the eruption of Krakatau in 1883 AD were deposited within a 15 km radius of the caldera (Mandeville *et al.*, 1996), while two other more extreme examples are the collapse of the volcanic island of Hierro located in the Canary Islands (Masson, 1996), and the emplacement of Parnell Grits in Northern New Zealand (Ballance and Gregory, 1991). The latter two examples are of debris flows which extended laterally for more than 40 km.

The interpreted seismic reflection data from across the Kora edifice presented in this study show that the volcaniclastic units flanking the Kora edifice do not extend out on to the flat ring plain surrounding the volcano. Therefore it would appear that large-scale flows of volcaniclastic debris were not associated with Kora, despite the fine grained, fragmented nature of its flanking depositional units. Wright (1996) has also

noted the absence of volcaniclastic ring plains surrounding Rumble IV and Rumble V. The only real evidence for lateral mass movement of volcaniclastic debris on these two volcanoes is a lobe associated with possible sector collapse on the eastern flank of Rumble IV. A similar slump-like feature has been observed on the northwestern slopes of Kora (see Chapter 3, Figure 3.6). This may also be evidence for sector collapse. In both cases the lobes of these features do not extend past the toe of the edifice slopes, and Wright (1996) has attributed the general lack of large-scale deposits at Rumble IV and Rumble V to an absence of flow transformation (i.e. Fisher, 1983). An example of a volcaniclastic apron that has extended beyond edifice slopes on to the relatively flat surrounding ocean floor is the Hokianga volcano, which has been described by Herzer (1995). In seismic reflection profile, the Hokianga volcano displays a wave flattened top, and apron facies which extend some 4-5 km out on to a relatively flat ring plain (Herzer, 1995). The larger apron and relative lateral extent of the Hokianga volcano may suggest that submarine volcanoes which grow above sea level are more prone to large scale mass-flow of volcaniclastic debris than totally submarine, constructional volcanoes such as Kora and the southern Kermadec volcanoes.

5.6 SIGNIFICANCE OF A SINGLE WEST NORTHLAND-NORTH TARANAKI ARC

The Kora volcanics have similar major element chemistry to the western and eastern belts of the Northland arc. On this basis the northern Taranaki Volcanics are believed to represent a southward continuation of the Northland arc. There is a considerable range in the size of the volcanoes distributed along the arc. Herzer (1995) has observed that the west Northland volcanoes comprise 7 large massifs 15-40 km in radius together with many intermediate edifices 5-10 km radius, similar in size to Kora. This significant variation in volcano size along the arc front from Northland to Taranaki, and the broad southward migration of volcanic activity, must reflect changing eruptive environments. The constructional volcanoes in the Northland Peninsula probably erupted under variably subaerial and submarine conditions while the volcanoes in the Northern Taranaki Basin erupted under totally submarine conditions.

6.0 Conclusions

Kora is a well-preserved relict submarine arc-stratovolcano located offshore in the North Taranaki Basin. The volcano was active from late Early Miocene to Late Miocene times in water depths of 200 m bsl to 500 m bsl. The following conclusions have been drawn from this study:

1. Kora and the surrounding Early to Late Miocene offshore North Taranaki Volcanics are a southern extension of Early Miocene volcanism in the Northland arc based on a comparison of major element geochemical analyses from the Coromandel, Waitakere, Rumble IV, Wairakau, Egmont, Titiraupenga, Alexandra, Kora, Kiwitahi and Tongariro volcanic centres.
2. The style of volcaniclastic depositional processes has varied across the Kora edifice based on a study of seismic facies. The apron facies reflectors comprising northwestern slopes are 4-5 km in length, while the southeastern slopes contain apron facies reflectors that are 1-2 km in length. The thickness of apron facies across the entire Kora edifice varies between 200 m and 400 m, however, apron facies reflectors comprising the northwestern slopes are generally thicker than on the southeastern aspects of the volcanic edifice. The northwestern part of the edifice has also undergone a sector collapse. Unlike subaerial counterparts, the lateral extent of the volcaniclastic apron at Kora terminates at the toe of the edifice slopes, and the apron does not extend out on to the surrounding ring plain.
3. Large-scale mass flows of volcaniclastic debris failed to develop at Kora. Interpretation of core data from the Kora wells indicate suspension settling from subaqueous eruptions, particulate grain flows, and density modified grain flows as the prevalent depositional slope processes at Kora.
4. The volcanic deposits comprising the cores from Kora are entirely fragmental rocks generated from water-magma interaction. The rocks were not derived from collapsed pillow lava and massive lava outcrops as is typical of some volcaniclastic deposits on Rumble IV and Rumble V in the southern Kermadec arc. The Kora edifice is small in size and formed during a relatively long episode of volcanism. The high degree of fragmentation in the rocks from Kora increased the

potential for degradation of the volcanic edifice by ocean currents. Active ocean currents may explain the small to intermediate size of the Kora edifice, which was active for some 10 Myrs.

5. Early Miocene constructional volcanoes in the west Northland arc that were active in a marginal subaerial/submarine environment (e.g. the Hokianga Massif) tend to be larger than volcanoes in the same arc that were active under totally submarine conditions. These may also reflect the degrading influence that ocean currents have on completely submerged submarine arc-volcanoes.

REFERENCES

Adams, C.J., Graham, I.J., Seward, D., Skinner, D.N.B., 1994. Geochronological and geochemical evolution of late Cenozoic volcanism in the Coromandel Peninsula, New Zealand. New Zealand Journal of Geology and Geophysics, 37: 359-379.

Andrews, P.B., 1982. Revised Guide to Recording Field Observations in Sedimentary Sequences. Department of Scientific and Industrial Research New Zealand Report N.Z.G.S. 102.

Arco Petroleum New Zealand Inc., 1988a. Final Well Report, Kora-1, Kora-1A, PPL 38447. Ministry of Commerce, Wellington, New Zealand unpublished open-file petroleum report, PR 1374.

Arco Petroleum New Zealand Inc., 1988b. Final Well Report Kora-2, PPL 38447. Ministry of Commerce, Wellington, New Zealand, unpublished open-file petroleum report, PR 1439.

Arco Petroleum New Zealand Inc., 1988c. Final Well Report Kora-3, PPL 38447. Ministry of Commerce, Wellington, New Zealand, unpublished open-file petroleum report, PR 1441.

Ballance P.F., Hayward, B.W., Brook, F.J., 1985. Subduction regression of volcanism in New Zealand (matters arising). Nature, 313: 820.

Ballance, P.F., 1988. Late Cenozoic time-lines and calc-alkaline volcanic arcs in northern New Zealand-further discussion. Journal of the Royal Society of New Zealand, 18: 347-58.

Ballance, P.F., Gregory, M.R., Parnell Grits – large subaqueous volcaniclastic gravity flows with multiple particle support mechanisms. Sedimentation in Volcanic Settings, SEPM Special Publication, 45.

Bandy, O., Hornibrook, N. de B., Schofield, J.C., 1970. Age relationships of the *Globigerinoides trilobus* zone and the andesite at Muriwai Quarry, New Zealand. New Zealand Journal of Geology and Geophysics, 13: 980-995.

Beggs, J.M., 1990. Seismic stratigraphy of the Plio-Pleistocene Giant Foresets, Western Platform, Taranaki Basin. In: Proceedings of the 1989 New Zealand Oil Exploration Conference, 1: 201-207.

Bergman, S.C., Talbot, J.P., Thompson, P.R., 1992. The Kora Miocene submarine andesite stratovolcano hydrocarbon reservoir, northern Taranaki Basin, New Zealand. In: Proceedings of the 1991 New Zealand Oil Exploration Conference. Ministry of Commerce, Wellington, pp.178-206.

Black, P.M., Skinner, D.N.B., 1979. The major oxide geochemistry of upper Tertiary Coromandel Group (andesites and dacites), northern Hauraki Volcanic Region, New Zealand. Abstracts, Australia and New Zealand Association for the Advancement of Science Congress, 1: 182.

Black, P.M., Briggs, R.M., Itaya, T., Dewes, E.R., Dunbar, H.M., Kawasaki, K., Kuscel, E., Smith, I.E.M., 1992. K-Ar age data and geochemistry of the Kiwitahi Volcanics, western Hauraki Rift, North Island, New Zealand. New Zealand Journal of Geology and Geophysics, 35: 403-413.

Briggs, R.M., 1983. Distribution, form, and structural control of the Alexandra Volcanic Group, North Island, New Zealand. New Zealand Journal of Geology and Geophysics, 26: 47-55.

Briggs, R.M., 1986. Volcanic rocks of the Waikato region, western North Island, and some possible petrologic and tectonic constraints on their origin. In: Smith, I.E.M. (Editor), Late Cenozoic volcanism in New Zealand. Royal Society of New Zealand Bulletin, 23: 76-91.

Briggs, R.M., Itaya, T., Lowe, D.J., Keane, A.J., 1989. Ages of the Pliocene-Pleistocene Alexandra and Ngatutura Volcanics, western North Island, New Zealand, and some geological implications. New Zealand Journal of Geology and Geophysics, 32: 417-427.

Brothers, R.N., 1984. Subduction regression and oceanward migration of volcanism, North Island, New Zealand. Nature, 309: 698-700.

Brothers, R.N., 1986. Upper Tertiary and Quaternary volcanism and subduction zone regression, North Island, New Zealand. Journal of the Royal Society of New Zealand, 16(3): 275-298.

Cas, R., 1979. Mass-flow arenites from a Paleozoic interarc basin, New South Wales, Australia: Mode and environment of emplacement. Journal of Sedimentary Petrology, 49: 29-44.

Cas, R.A.F., and Wright, J.V., 1987. Volcanic successions, modern and ancient. Allen and Unwin, London, 528 pp.

Cole, J.W., Graham, I.J., Hackett, W.R., Houghton, B.F., 1986. Volcanology and petrology of the Quaternary composite volcanoes of Tongariro Volcanic Centre, Taupo Volcanic Zone. In: I.E.M. Smith (Editor), Late Cenozoic Volcanism in New Zealand. Royal Society of New Zealand Bulletin, 23: 225-250.

Cousineau, P.A., Subaqueous pyroclastic deposits in an Ordovician fore-arc basin: An example from the Saint-Victor Formation, Quebec Appalachians, Canada. Journal of Sedimentary Research, A64(4): 867-880.

Cronin, S.J., Neall, V.E., Stewart, R.B., Palmer, A.S., 1996. A multiple-parameter approach to andesitic tephra correlation, Ruapehu volcano, New Zealand. Journal of Volcanology and Geothermal Research, 72: 199-215.

Dietz, R.S., 1954. The explosive birth of Myojin Island. National Geographic, 150(1): 117-126.

Emory, W.C., Cooper, D.R., 1991. Business Research Methods. Irwin, Homewood, Boston., 4th ed., 760pp.

Fisher, R.V., 1983. Flow transformations in sediment gravity flows. Geology, 11: 273-274.

Fiske, R.S., Cashman, K.V., Shibata, A., Watanabe, K., 1998. Tephra dispersal from Myojinsho, Japan, during its shallow submarine eruption of 1952-1953. Bulletin of Volcanology, 59: 262-275.

Folk, R.L., Ward, W.C., 1957. Brazos river bar: a study in the significance of grain size parameters. Journal of Sedimentary Petrology, 27: 3-26.

Folk, R.L., Andrews, P.B., Lewis, D.W., 1970. Detrital sedimentary rock classification and nomenclature for use in New Zealand. New Zealand Journal of Geology and Geophysics, 13(4): 937-968.

Froude, D.O., Cole, J.W., 1985. Petrography, mineralogy and chemistry of Titiraupenga volcano, North Island, New Zealand. New Zealand Journal of Geology and Geophysics, 28: 487-496.

Gamble, J.A., Wright, I.C., Baker, J.A., 1993. Seafloor geology and petrology in the oceanic to continental transition zone of the Kermadec-Havre-Taupo Volcanic Zone arc system, New Zealand. New Zealand Journal of Geology and Geophysics, 36: 417-435.

Gill, J.B., 1981. Orogenic Andesites and Plate Tectonics, Springer-Verlag, Berlin.

Hampton, M.A., Locat, J., 1996, Submarine landslides: Reviews of Geophysics, 34: 33–59.

Hatherton, T., 1968. A source for volcanic material in the Mohakatino Beds. New Zealand Journal of Geology and Geophysics, 11: 1207-1210.

Hayward, B.W., and Strong, C.P., 1988. Biostratigraphy of Kora-1 offshore well. Unpubl. NZGS/DSIR Pal Report.

Hayward, B.W., 1986. A guide to paleoenvironmental assessment using New Zealand Cenozoic foraminiferal faunas. New Zealand Geological Survey Report Pal 109: 73pp.

Herzer, R.H., 1995. Seismic stratigraphy of a buried volcanic arc, Northland, New Zealand and implications for Neogene subduction. Marine and Petroleum Geology, 12(5): 511-531.

Hochstein, M.P., Smith, I. E.M., Regenauer-Lieb, K., Ehara, S., 1993. Geochemistry and heat transfer processes in Quaternary rhyolitic systems of the Taupo volcanic zone, New Zealand. Tectonophysics, 223: 213-237.

Hornibrook, N.de B., Brazier, R.C., Strong, C.P., 1989. Manual of New Zealand Permian to Pleistocene foraminiferal biostratigraphy. New Zealand Geological Survey, Paleontological Bulletin 56: 175pp.

Isaac, M.J., Herzer, R.H., Brook, F.J., Hayward, B.W., 1994. Cretaceous and Cenozoic sedimentary basins of Northland, New Zealand. Institute of Geological and Nuclear Sciences monograph 8. Institute of Geological and Nuclear Sciences Ltd. 203pp.

Johnson, R.A., Wichern, D.W., 1992. Applied Multivariate Statistical Analysis. Prentice-Hall, Englewood Cliffs, NJ., 3rd ed.

Kano, K., 1989. Interactions between andesitic magma and poorly consolidated sediments: Examples in the Neogene Shirahama Group, south Izu, Japan. Journal of Volcanology and Geothermal Research, 37: 59-75.

Kano, K., Yamaoto, T., Takeuchi, K., 1993. A Miocene island-arc volcanic seamount: the Takashibiyama Formation, Shimane Peninsula, SW Japan. Journal of Volcanology and Geothermal Research, 59: 101-119.

Kamp, P.J.J., 1984. Neogene and Quaternary extent and geometry of the subducted Pacific plate beneath North Island, New Zealand: implications for Kaikoura tectonics. Tectonophysics, 108: 241-266.

Kear, D., Hay, R.F., 1961. Sheet 1 North Cape. Geological Map of New Zealand 1:250 000, New Zealand Geological Survey. Department of Scientific and Industrial Research, Wellington.

Kear, D., Schofield, J.C., 1978. Geology of the Ngaruawhahia Subdivision. New Zealand Geological Survey bulletin 88.

Kear, D., 1994. The Cook tectonic boundary; showing relative mobility of the North and South Islands during the last few million years. Geological Society of New Zealand, Misc. Publ., 80A: p103.

King, C., 1992. Sedimentology book 1: Processes and analysis. Longman, Malaysia, PA., 86pp.

King, P.R., Thrasher, G.P., 1992. Post-Eocene development of the Taranaki Basin, New Zealand. In: J.S. Watkins, Feng Zhiqiang, K.J. McMillen (Editors) Geology and Geophysics of Continental Margins. American Association of Petroleum Geologists memoir 53: 93-118.

King, P.R., Scott, G.H., Robinson, P.H., 1993. Description, correlation and depositional history of Miocene sediments outcropping along north Taranaki coast. Institute of Geological and Nuclear Sciences, monograph 5. Institute of Geological and Nuclear Sciences Ltd. 199pp.

King, P.R., 1994. The habitat of oil and gas in Taranaki Basin. In: Proceedings of the 1991 New Zealand Petroleum Conference. Ministry of Commerce, Wellington, pp 180-203.

King, P.R., Thrasher, G.P., 1997. Cretaceous-Cenozoic geology and petroleum systems of the Taranaki Basin, monograph 13. Institute of Geological and Nuclear Sciences Ltd. 243pp., 6 enclosures.

Knox, G.J., 1982. Taranaki Basin, structural style and tectonic setting. New Zealand Journal of Geology and Geophysics, 25: 125-140.

Lapidus, D.F., 1987. Collins Dictionary of Geology. Collins, Glasgow, 2nd ed., 565pp.

Lash, G.G., 1984. Density-Modified Grain-Flow Deposits from an Early Paleozoic Passive Margin. Journal of sedimentary Petrology, 54(2): 557–562.

Lewis, D.W., 1981. Practical Sedimentology. Apteryx 150pp.

Lonsdale, P., Batiza, R., 1975. Hyaloclastite and lava flows on young seamounts examined with a submersible. Geological Society of America Bulletin, Part I, 91: 545-554.

Lowe, D.R., 1976. Grain flow and grain flow deposits. Journal of Sedimentary Petrology, 46: 188–199.

Lowe, D.R., 1982. Sediment Gravity Flows: II. Depositional models with special reference to the deposits of high-density turbidity currents. Journal of Sedimentary Petrology, 52(1): 279–297.

Masson, D.G., 1996. Catastrophic collapse of the volcanic island of Hierro 15 ka ago and the history of landslides in the Canary Islands. Geology, 24(3): 231-234.

Mandeville, C.W., Carey, S., Sigurdsson, H., 1996. Sedimentology of the Krakatau 1883 submarine pyroclastic deposits. Bulletin of Volcanology, 57: 512-529.

Mcmanamon, D., 1993. Kora Exploration and Drilling Results. Petroleum Exploration in New Zealand News, July 1993. pp 18-27.

McPhie, J., 1995. A Pliocene shoaling basaltic seamount : Ba Volcanic Group at Rakiraki Fiji, 64(3-4): 193-210.

Middleton, G.V., Hampton, M.A., 1976. Subaqueous sediment transport and deposition by sediment gravity flows. In: Stanley, D.J., and Swift, D.J.P. (editors).

Marine sediment transport and environmental management. New York, Wiley, pp 197–218.

Mohrig, D., Whipple, K.X., Midhat, H., Ellis, E., Parker, G., 1998. Hydroplaning of subaqueous debris flows. Geological Society of America Bulletin, 110(3): 387–394.

Nakano, M., Unoki, S., Hanzawa, M., Marumo, R., Fukuoka, J., 1954. Oceanographic features of a submarine eruption that destroyed the Kaiyo-Maru No. 5 Sears Foundation. Journal of Marine Research, 13: 48-66.

Neall, V.E., Stewart, R.B., Smith, I.E.M., 1986. History and Petrology of the Taranaki Volcanoes. In: Smith, I.E.M., (Editor). Late Cenozoic Volcanism in New Zealand. Royal Society of New Zealand bulletin, 23: 251-263.

Nodder, S.D., Nelson, C.S., Kamp, P.J., 1990. Mass-emplaced siliclastic-volcaniclastic-carbonate sediments in Middle Miocene shelf-to-slope environments at Waikawau, northern Taranaki, and some implications for Taranaki Basin development. New Zealand Journal of Geology and Geophysics, 33: 599-615.

Norem, H., Locat, J., Schieldrop, B., 1990. An approach to the physics and modeling of submarine flowslides: Marine Geotechnology, 9: 93 – 111.

Palmer, J.A., Andrews, P.B., 1993. Cretaceous-Tertiary sedimentation and implied tectonic controls on the structural evolution of Taranaki Basin, New Zealand. In: Balance, P.F. (Editor), South Pacific sedimentary basins. Elsevier Science Publishers. 413pp

Palmer, J.A., 1985. Pre-Miocene lithostratigraphy of Taranaki Basin, New Zealand. New Zealand Journal of Geology and Geophysics, 28: 197-219.

Powers, M.C., 1953. A new roundness scale for sedimentary particles. Journal of Sedimentary Petrology 23(2): 117-119.

Price, R.C., McCulloch, M.T., Smith, I.E.M., Stewart, R.B., 1992. Pb-Nd-Sr isotopic compositions and trace element characteristics of young volcanic rocks and comparisons with basalts and andesites from the Taupo Volcanic Zone. Geochim. Cosmochim. Acta., 56: 941-953.

Reed, J.D., 1992. Exploration geochemistry of the Taranaki Basin with emphasis on Kora. Proceedings of the 1991 New Zealand Oil Exploration Conference. Ministry of Commerce, Wellington, pp 364-372.

Roser, B.P., Korsch, R.J., 1988. Provenance signatures of sandstone-mudstone suites determined using discriminant function analysis of major element data. Chemical Geology, 67(1-2): 119-139.

SAS Institute Inc., 1985. SAS Users guide: Statistics. Version 5 Edition. SAS Institute., Cary, NC, 956 pp.

Schminke, H.U., von Rad, U., 1979. Neogene evolution of the Canary Island volcanism inferred from ash layers and volcaniclastic sandstones of DSDP site 397 (Leg 47A): Deep Sea Drilling Project Initial Report 46: 703-725.

Schneiderhöhn, P., 1954. Eine vergleichende Studie über Methoden zur quantitativen Bestimmung von Abrundung und Form an Sandkörnen (im Hinblick auf die Verwendbarkeit an Dünnschliffen) – Heidlb. Beitr. Mineralogy and Petrography, 4: 172-191.

Shepard, F.P., 1963. Submarine Geology. New York, Harper and Row. 557pp.

Sheridan, M.F., Wohletz, K.H., 1983. Hydrovolcanism: basic considerations and review: Journal of Volcanology and Geothermal Research, 17: 1–29.

Sillitoe, R.H., 1976. Andean mineralization; a model for the metallogeny of convergent plate margins. Special Paper – Geological Association of Canada, 14: 59-100.

Skinner, B.J, Porter, S.C., 1987. Physical Geology. Wiley and Sons, New York, 750pp.

Skinner, D.N.B., 1986. Neogene volcanism in the Hauraki Volcanic Region. In: Smith I.E.M. (Editor). Late Cenozoic Volcanism in New Zealand. Royal Society of New Zealand Bulletin 23: 21-47.

Smith, T.L., Batiza, R., 1989. New field and laboratory evidence for the origin of hyaloclastite flows on seamount summits. Bulletin of Volcanology, 51: 96–114.

Smith, I.E.M., Brothers, R.N., 1988. Petrology of Rumble seamounts, southern Kermadec Ridge, southwest Pacific. Bulletin of Volcanology, 50: 139-147.

Srivastiva, M.S., Carter, E.M., 1983. An Introduction to Applied Multivariate Statistics. Elsevier, New York, NY, 412 pp.

Stern, T.A., Holt, W.E., 1994. Platform subsidence and mantle flow behind subduction zones; evidence from Taranaki Basin well and seismic data. Geological Society of New Zealand Misc. Publ., 80A: p171.

Stewart, R.B., Price, R.C., Smith, I.E.M., 1996. Evolution of high-K arc magma, Egmont volcano, Taranaki, New Zealand: evidence from mineral chemistry. Journal of Volcanology and Geothermal Research, 74: 275-295.

Stipp, J.J., 1968. The geochronology and petrogenisis of the Cenozoic volcanics of North Island, New Zealand. Unpublished Ph.D. thesis, lodged in the library, Australian National University, Canberra.

Stipp, J.J., Thompson, B.N., 1971. K/Ar ages from the volcanics of Northland, New Zealand. New Zealand Journal of Geology and Geophysics 14: 403-413.

Stokes, S. and Lowe, D.J., 1988. Discriminant function analysis of late Quaternary tephras from five volcanoes in New Zealand using glass shard major element chemistry. Quaternary Research, 30: 270-283.

Thompson, B.N., 1961. Sheet 2A-Whangarei. Geological map of New Zealand 1:250 000. Department of Scientific and Industrial Research, Wellington, New Zealand.

Tsuya, H., Morimoto, R., Ossaka, G., 1953. A brief note on the petrography of the pumice ejected from Myojin-sho (reef), near the Beyonnaise rocks, September 23, 1952. J. Tokyo Univ. Fisheries, 40: 16-18.

Walcott, R.I., 1987. Geodetic strain and the deformational history of the North Island of New Zealand during the late Cenozoic. Trans. R. Soc. London A., 321: 163-181.

White, P.J., 1985. Age, petrology and geochemistry of Wairakau Andesites, Whangaroa, Northland. New Zealand Journal of Geology and Geophysics, 28: 635-647.

Wright, I.C., 1993a. Pre-spread rifting and heterogenous volcanism in the southern Havre Trough back-arc basin. Marine Geology, 113: 179-200.

Wright, I.C., 1993b. Southern Havre Trough-Bay of Plenty (New Zealand): structure and seismic stratigraphy of an active back-arc basin complex. In: P.F. Balance

(Editor), South Pacific Sedimentary Basins (Sedimentary Basins of the World 2). Elsevier, Amsterdam, pp. 195-211.

Wright, I.C., 1994. Nature and tectonic setting of the southern Kermadec submarine arc volcanoes: An overview. Marine Geology, 118: 217-236.

Wright, A.C., Black, P.M., 1981. Petrology and geochemistry of Waitakere Group, North Auckland, New Zealand. New Zealand Journal of Geology and Geophysics, 24: 155-165.

Wright, I.C., 1996. Volcaniclastic processes on modern submarine arc stratovolcanoes: sidescan and photographic evidence from Rumble IV and V volcanoes, southern Kermadec Arc (SW Pacific). Marine Geology, 136: 21-39.

Wright, J.V., Mutti, E., 1981. The Dali Ash, Island of Rhodes, Greece: a problem in interpreting submarine volcanogenic sediments. Bulletin of Volcanology, 44(2): 153-167.

Yuasa, M., Murakami, F., Saito, E., Watanabe, K., 1991. Submarine topography of seamounts on the volcanic front of the Izu-Ogasawara (Bonin) arc. Bull. Geol. Surv. Japan, 42 : 703-743.

APPENDIX 1 Visual Comparison Aids and Thin section Preparation Technique

Appendix 1.1 **Classes used for Determination of Roundness of Sand Sized Grains. Redrawn following Powers, (1953) and Shepard (1963) (*in* Andrews, 1982).**

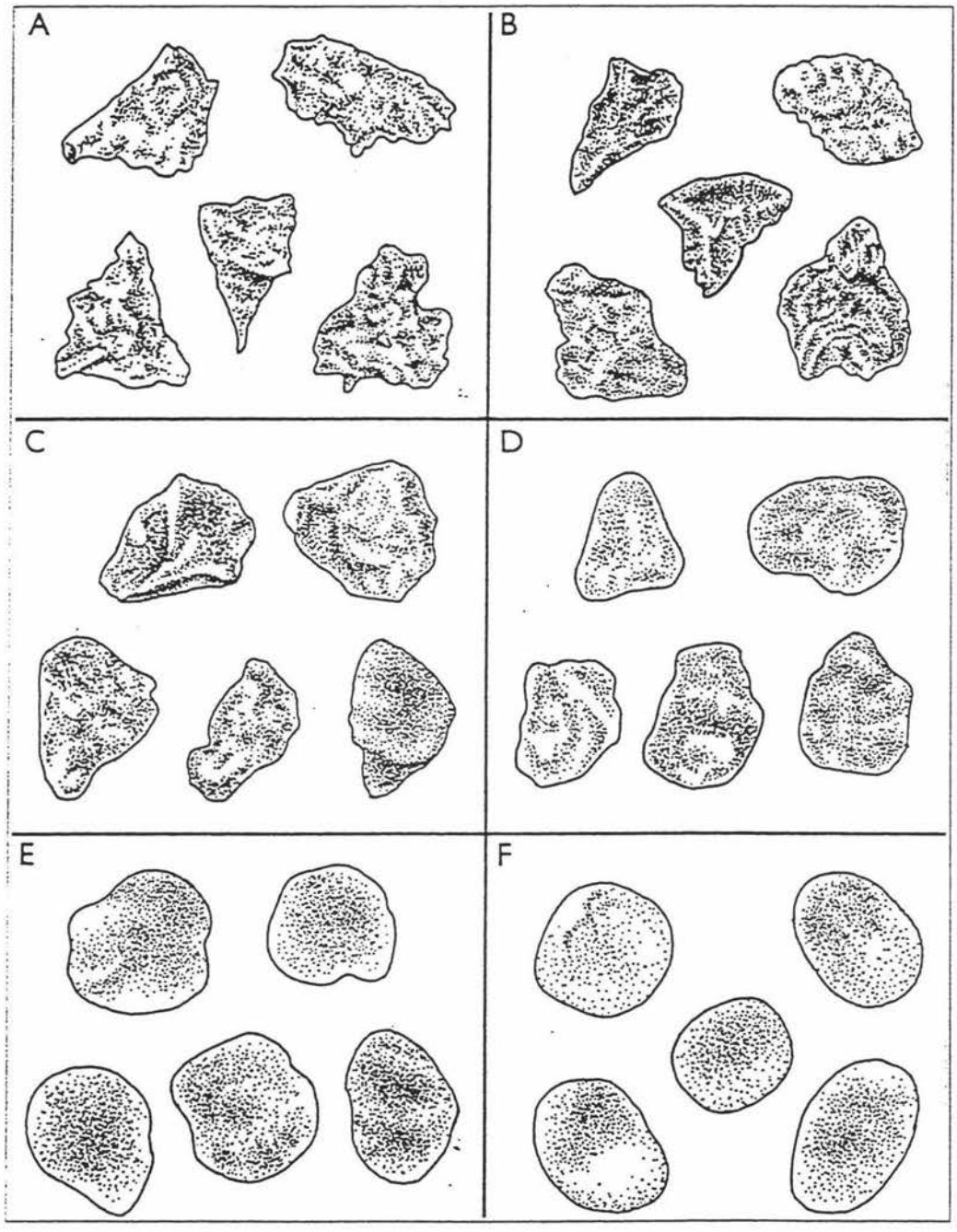

A = very angular..... 0.5
B = angular..... 1.5
C = subangular..... 2.0
D = subrounded..... 2.5
E = rounded..... 3.5
F = well-rounded..... 4.0

Numerical Values after Powers (1953) and Shepard (1963) in Andrews, (1982)

Appendix 1.2 Sediment Sorting Comparator (*after* Compton,1962; *in* Blatt, 1982)

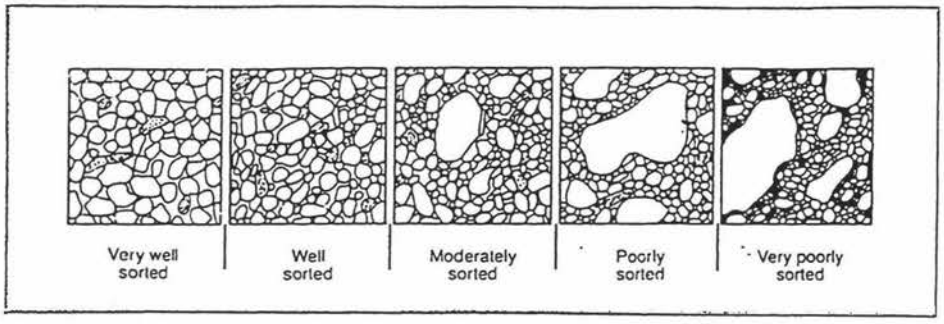

Appendix 1.3 Percentage Estimation Comparison Charts (Lewis, 1981)

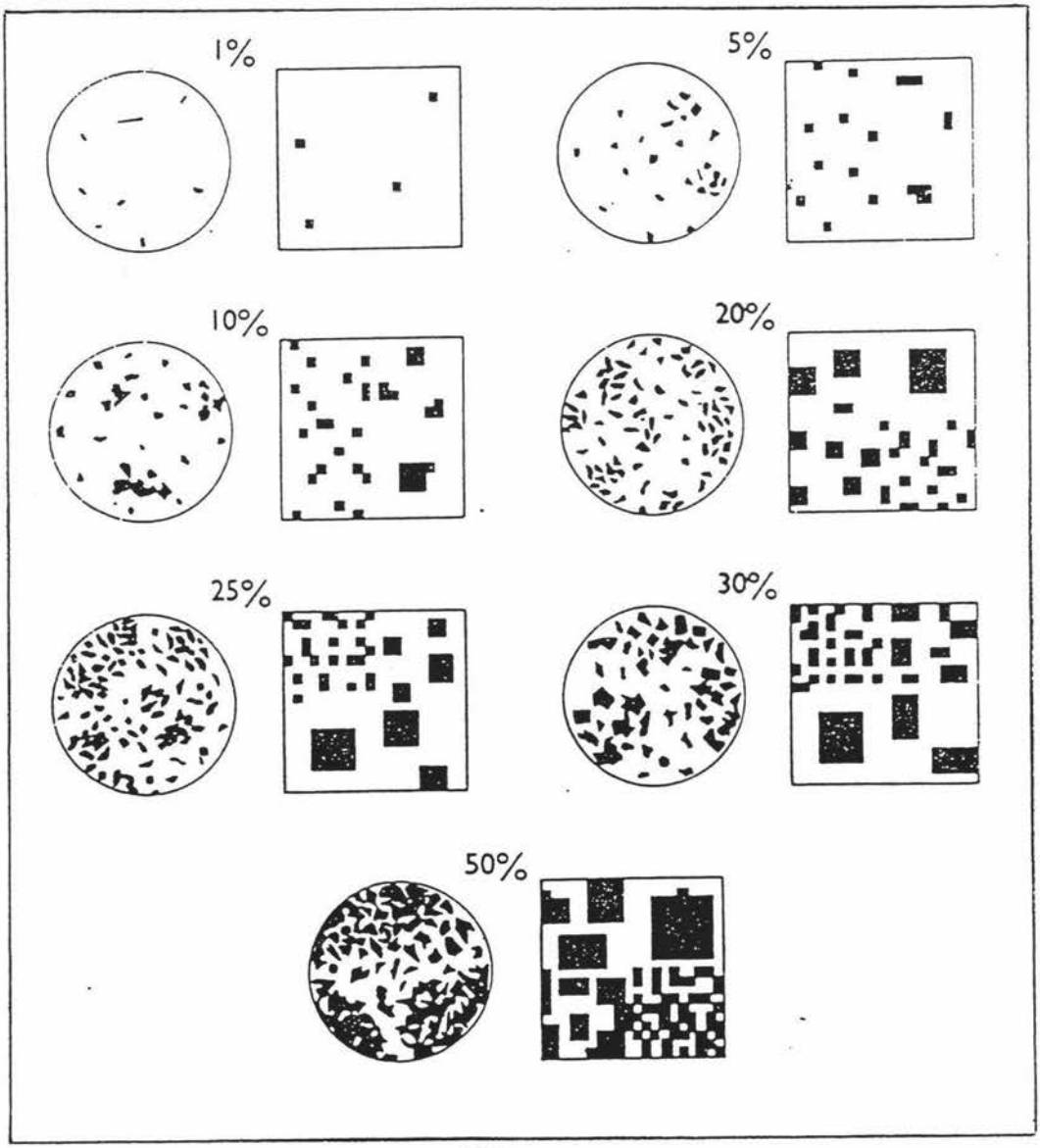

Appendix 1.4 Thin Section Preparation (Lewis, 1981)

PREPARING THIN SECTIONS

Thin Sectioning non-friable, insoluble rocks:

1. Cut rock to produce a 3 mm thick slice with parallel sides

2. Grind slice on one side, on a coarse grinding lap using 180 and then 320 grade carborundum with water as a lubricant (to remove diamond saw marks.) Rinse thoroughly after each grinding operation.

3. Continue grinding on a glass plate using 400 and after rinsing, 600 grade carborundum with water. Use a rotary action until a finely finished flat surface is produced.

4. Scrub with running water to remove waste carborundum and then dry on a hot plate.

5. Mount slice on a microscope slide with "Lakeside 70" thermoplastic cement, using a hotplate at 100°C. The cement is applied to the hot rock slice and the slide pressed down until excess cement and any bubbles are squeezed out.

6. Grind upper surface of rock slice on a coarse grinding lap using 180 and then 320 carborundum with water. Continue until light can be seen through it.

7. Grind surface on glass plate using 400 and then 600 carborundum with water. Use a rotary action and make sure that the surface is kept parallel to the surface of the microscope slide. Check the thickness regularly, using a polarising microscope, until a final thickness of 0.03 mm is obtained. Judge the correct thickness by the birefringence of a common mineral - e.g., quartz will show a very pale first order yellow colour when it is 0.03 mm thick.

8. Wash thoroughly, then dry the thin slice on a hot plate. Coat with cellulose acetate to prevent breaking-up and trim to a convenient size with a razor blade.

9. Heat thin rock slice on hotplate at 85°C then transfer from the old slide to a new microscope slide with Canada Balsam on it. The Balsam should be cooked for about three minutes. The Balsam is cooked when a bead, picked-up on the points of tweezers, forms a brittle thread which snaps on cooling when the tweezers are opened. Place more Canada Balsam on the upper surface, then cover with coverslip. The completed thin section is then cleaned with alchohol or acetone and labelled.

APPENDIX 2 Formulae and Verbal Scale for Sedimentary Grain Size Parameters

(Folk and Ward, 1957; *in* Lewis, 1981)

Mode: Most frequently occurring particle size.
Inflection point(s) on the cumulative curve.

Graphic Mean:

$$M_z = \frac{\phi 16 + \phi 50 + \phi 84}{3}$$

Inclusive Graphic Standard Deviation:

$$\sigma_1 = \frac{\phi 84 - \phi 16}{4} + \frac{\phi 95 - \phi 5}{6.6}$$

< 0.35Ø	very well sorted
0.35 to 0.50Ø	well sorted
0.50 to 0.71Ø	moderately well sorted
0.71 to 1.0Ø	moderately sorted
1.0 to 2.0Ø	poorly sorted
2.0 to 4.0Ø	very poorly sorted
>4.0Ø	extremely poorly sorted

Inclusive Graphic Skewness:

$$Sk_1 = \frac{\phi 16 + \phi 84 - 2\phi 50}{2(\phi 84 - \phi 16)} + \frac{\phi 5 + \phi 95 - 2\phi 50}{2(\phi 95 - \phi 5)}$$

$$= \frac{\phi 84 - \phi 50}{\phi 84 - \phi 16} - \frac{\phi 50 - \phi 5}{\phi 95 - \phi 5}$$

(see Warren, G. 1974, J. Sed. Petr 44: 259).

+1.0 to +0.3	very fine skewed
+0.3 to +0.1	fine skewed
+0.1 to -0.1	near symmetrical
-0.1 to -0.3	coarse skewed
-0.3 to -1.0	very coarse skewed

Graphic Kurtosis:

$$K_G = \frac{\phi 95 - \phi 5}{2.44(\phi 75 - \phi 25)}$$

<0.67	very platykurtic
0.67 to 0.90	platykurtic
0.90 to 1.11	mesokurtic
1.11 to 1.50	leptokurtic
1.50 to 3.00	very leptokurtic
>3.00	extremely leptokurtic

APPENDIX 3 Core Observations

Appendix 3.1 Kora-1A: Personal Observations and Lithological Description adapted from Arco Petroleum NZ Inc., (1988a)

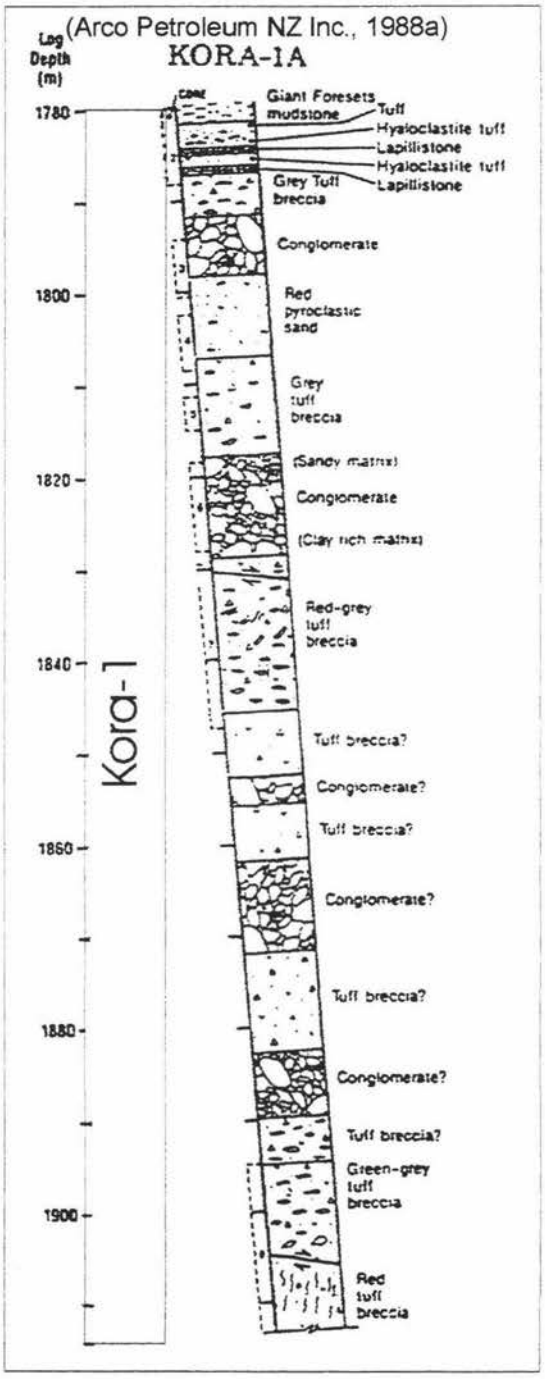

1783.0 m to 1783.98 m
Coarse sands grading down into gritty, equigranular, rounded and sub-rounded pebbles. The base of the core unit contains dark grey/black, glassy hornblende crystals (~2 mm) in a fine sandy, bioturbated matrix. At the extreme base of this core unit, framework clasts are supported in a fine silty/sandy matrix.

1784.2 m to 1784.3 m
Densely packed, well-sorted, fine and medium sand sized crystals. Shiny black hornblende crystals up to 8 mm are supported in a sandy matrix, which forms 10 % of the core. The base of the core unit is poorly sorted, and mottled with numerous bioturbation structures.

1784.3 m to 1784.4 m
Subhedral hornblende crystals 1 mm-4 mm contribute up to 20 % of the core. The core has a slightly mottled appearance and also contains rare quartz crystals and plagioclase crystals.

1784.42 m to 1784.51 m
The base of the core unit is graded, and contains large weathered plagioclase and hornblende crystals. The crystals are supported in a silt to clay matrix.

1784.51 m to 1784.63 m
Silt and clay matrix comprises 90 % of the core.

1784.63 m to 1784.8 m
Distinct colour change - very sharp and distinct from the sections above.

1784.8 m to 1784.94 m
Randomly dispersed pebble trains. The pebbles are subangular clasts of andesite.

1785.06 m to 1785.16 m
Fine clay and sand matrix forms 60 % of the core. The framework clasts are fine, angular pebbles of andesite. Other framework components include smaller 0.5 mm to 3 mm hornblende crystals.

1785.16 m to 1785.23 m
Same as above

1785.3 m to 1785.36 m
100 mm thick andesite pebble lenses. The clasts are densely packed, and the matrix forms 10 % of the core. The matrix contains densely packed hornblende crystal fragments, and clay.

1785.36 m to 1785.46 m
Same as above

1785.46 m to 1785.58 m
Blue-grey, andesite grit. The matrix supporting these clasts varies from fine sand and silt, to coarse volcanic sands.

1785.68 m to 1785.82 m
Dark coloured ash rich unit containing sparse angular andesite pebbles. The matrix comprises up to 90 % of the core. The base of the core contains calcite lined vugs.

1785.82 m to 1785.93 m
Calcite lined vugs 2 mm to 3 mm in size.

1785.93 m to 1786.04 m
Andesite grit in a sand and clay matrix.

1786.37 m to 1786.52 m
Same as above

1786.52 m to 1786.75 m
Medium to coarse volcanic sands mixed with medium sized andesite pebbles.

1786.75 m to 1787.0 m
The upper part of the core contains dark, grey coloured subangular grit and pebble sized clasts of andesite. The matrix is clay rich, and contains crystal fragments smaller than 0.5 mm. The lower part of the core unit grades down into grit sized, subangular, andesite clasts. The base of the core contains subrounded andesite pebbles, and a clay matrix.

1787.2 m to 1787.55 m
A single cobble of very hard, porphyritic andesite. The dominant phenocrysts are hornblende and plagioclase (2-4 mm long). A conglomerate occurs beneath the andesite cobble. The conglomerate contains numerous, well-rounded andesite cobbles and coarse pebbles, and some of these have been fractured in interclast collisions. The conglomerate matrix contains fine clay and andesite fragments derived from the conglomerate framework clasts.

1793.3 m to 1794 m
Unconsolidated conglomerate same as above.

1794.16 m to 1794.83 m
Same as above.

1795.0 m to 1795.8 m
Same as above.

1796.3 m to 1797.2 m
Same as above.

1797.2 m to 1798.0 m
Same as above.

1802 m to 1802.94 m
Unconsolidated volcanic conglomerate. The clay matrix in the conglomerate contains angular pebbles of andesite, and medium sand sized clasts of andesite.

1802.94 m to 1803.83 m
Unconsolidated volcanic conglomerate.

1804.63 m to 1805.43 m
Andesitic grit.

1811.5 m to 1812.35 m
Tuff breccia matrix is 75 % of the core. The framework clasts in the tuff breccia are the same hard, porphyritic clasts that comprise the conglomerates in Kora-1A. The clasts are more densely packed deeper in the core, for example, the matrix at 1812.39 m comprises 60 % of the core. A number of the framework clasts are fractured.

1818.0 m to 1818.9 m
Framework clasts are well-rounded, cobbles and large pebbles of porphyritic andesite. The framework clasts in the top of the core are fractured, apparently from inter-clast collisions. The conglomerate matrix is sandy and comprises 50 % of the core.

1818.35 m to 1818.45 m
Same as above.

1818.9 m to 1819.88 m
Same as above.

1819.88 m to 1820 m
Volcanic conglomerate matrix is fine silt and clay. The framework clasts are porphyritc, coarse pebbles, and cobbles.

1821 m to 1821.93 m
Same as above.

1821.93 m to 1822.79 m
Fine sandy matrix containing hornblende crystals. The framework clasts at the top of the unit are a mixture of angular and rounded, hard porphyritic clasts. The larger clasts, which are 100 mm x 100 mm in size are generally more rounded than the smaller 50 mm - 30 mm clasts. Some of the clasts near the base of the unit are 200 mm x 200 mm (cobbles). The matrix forms 40 % to 30 % of the core unit, and is mostly comprised of clay and crystal fragments. Larger 5 mm x 5 mm angular andesite lithic clasts appear to be derived from the larger framework clasts.

1826.24 m to 1827 m
Same as above.

1827.5 m to 1828.25 m
Crystal rich matrix. The crystals are generally smaller than 1 mm. The larger framework clasts are typically 10 mm x 10 mm in size and these clasts are matrix supported.

1828.25 m to 1831.1 m
Poorly sorted matrix containing clay, crystal fragments, and lithic clasts of andesite up to 2 mm.

1831.1 m to 1832 m
Same as above.

1832.76 m to 1833.56 m
Angular 20 mm x 40 mm clasts of andesite supported in a fine sand and silt matrix.

1834.45 m to 1835.41 m
The upper part of the core unit contains large angular 40 mm x 30 mm clasts of andesite, and a coarse sandy, gritty matrix. The base of the core is well lithified, and the matrix contains angular 1 mm to 3 mm clasts. The matrix contributes up to 70% of the core.

1836 m to 1838 m
Equigranular, sandy textured breccia. The core shows a distinct lack of clasts larger than 1 mm.

1838 m to 1838.9 m
Moderately to well sorted core. The framework clasts are andesite, and the largest clasts are 10.5 mm x 20 mm. The framework clasts are supported in a clay to grit matrix. The matrix is up to 60 % of the core. The base of the core unit contains a coarse sandy breccia, and many angular 10 mm clasts of andesite.

1838.9 m to 1839.74 m
Rounded, hard, and varicoloured framework clasts comprise 25 % of the core.

1839.74 m to 1840.66 m
Well-rounded, coarse pebbles of porphyritic andesite. The clasts form up to 30 % of the core and are surrounded by coarse gritty angular clasts of andesite. The matrix is fine clay.

1840.66 m to 1841.56 m
Same as above.

1841.5 m to 1845.2 m
Poorly sorted core components, the size of the framework clasts vary between 1 mm and 100 mm. The proportion of angular framework clasts is approximately the same as the proportion of rounded clasts. The matrix consists of medium sand sized crystal fragments, and clay.

1845.21 m to 1845.8 m
Poorly sorted breccia. The matrix comprises 70 % of the core. The framework clasts are between 20 mm and 30 mm.

1895 m to 1897.75 m
Clay and calcite rich matrix containing gritty and gravely andesite fragments. The framework clasts are a combination of subrounded and angular andesite clasts. These clasts vary in size from 2 mm - 3 mm to 50 mm - 100 mm.

1897.75 m to 1901.64 m
A lithological contact occurs where the base of the conglomerate overlays the tuff breccia. Both lithologies contain green and grey, porphyritic, framework clasts. The contact between the two lithologies is ripped up. Above the contact the largest clasts are 20mm - 30 mm. The matrix forms up to 80 % of the core and is well sorted. Below the contact the tuff breccia is poorly sorted and consists of subangular to angular clasts. These clasts are typically 20 mm to 30 mm in size and are matrix supported. The matrix comprises 60-70 % of the core.

1901.64 m to 1901.57 m
Well lithified, chaotic mixture of subrounded and angular andesite clasts. The clasts are 10 mm to 100 mm and form 20 % of the core. The matrix contains very coarse, volcanic sand and pebbles (i.e. lapilli tuff matrix).

1901.57 m to 1902.57 m
Same as above.

1902.57 m to 1903.57 m
Same as above.

1903.57 m to 1904.57 m
Well sorted core components. The largest clast is 15 mm x 5 mm and matrix comprises up to 90 % of the core.

1905.25 m to 1908.9 m
The upper 1 metre of core consists of subrounded red and blue-grey porphyritic andesite clasts. The average clast size varies between 2 mm and 20 mm, and these clasts form 30 % of the core. Overall the core is matrix supported, matrix contributing to 70 % of the core. The matrix contains coarse sand size fragments of andesite.

1908.9 m to 1909.88 m
10 mm to 100 mm, subangular and subrounded, red and grey porphyritic clasts. These clasts are supported in a coarse sandy matrix.

Appendix 3.2 Kora-2: Personal Observations and Lithological Description adapted from Arco Petroleum NZ Inc., (1988b)

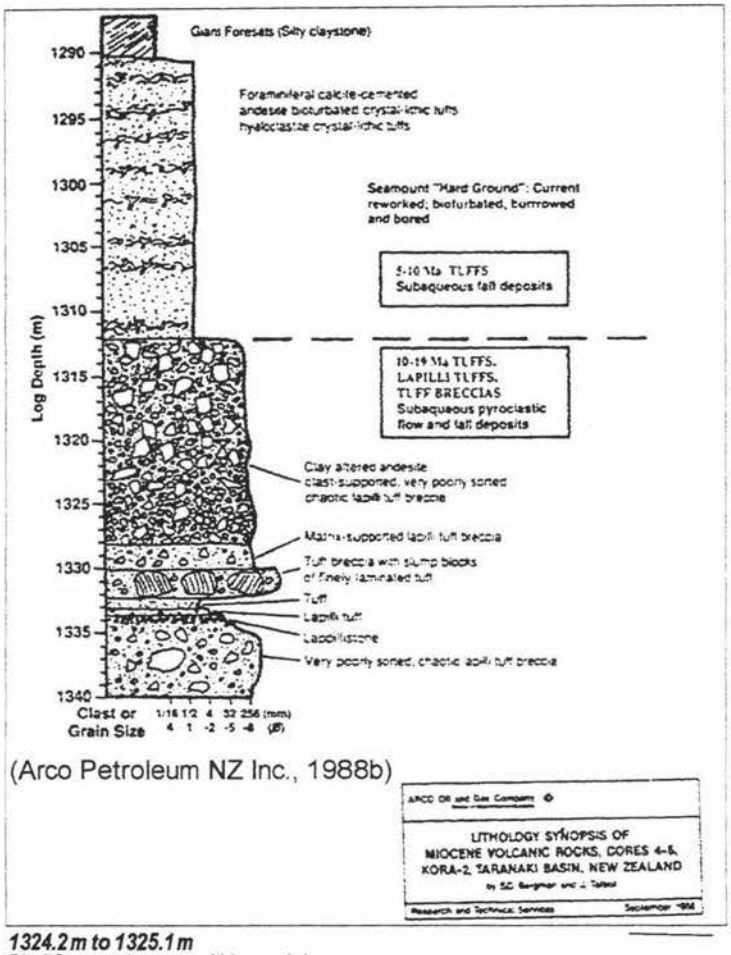

(Arco Petroleum NZ Inc., 1988b)

1289.8 m to 1290.7 m
Massive, bioturbated, andesitic sandstone. The base of the core has altered to a green colour.

1290.7 m to 1291.6 m
Mottled, massive andesitic sandstone. The unit contains abundant 2 mm subhedral hornblende and plagioclase crystals.

1292.5 m to 1293.4 m
Mottled, andesitic sandstone. The core is more bioturbated than the units above.

1293.4 m to 1294.3 m
3 mm to 5 mm shell fragments.

1294.3 m to 1295.0 m
Massive andesitic sandstone containing borings, and crystals of hornblende and plagioclase.

1318.82 m to 1319.7 m
Two lithological units. The upper unit is a massive, bioturbated, andesitic sandstone. The lower unit is slightly mottled, and contains densely packed, coarse pebble sized crystals of hornblende and plagioclase.

1322.4 m to 1323.3 m
Hard calcite cemented volcaniclastic sediments comprise the top 200 mm 300 mm of core. Beneath, the core contains angular, medium to coarse pebbles of andesite in a silty matrix.

1323.3 m to 1324.2 m
Tuff breccia. The framework clasts are porphyritic, cobble sized, and highly spherical. The smaller framework clasts are moderately spherical, angular, coarse pebble sized clasts of andesite. The matrix in the core contains fine, silt sized volcaniclastics.

1324.2 m to 1325.1 m
Shell fragments occur within sandy lenses.

1325.1 m to 1326.0 m
Alternating fine and coarse tuff lenses containing shell fragments.

1326.0 m to 1326.9 m
Alternating tuff and lapilli tuff.

1326.9 m to 1327.8 m
Breccia changes down into a light grey coloured, equigranular tuff/lapilli tuff. The contact between the two lithologies is not preserved in the core.

1327.8 m to 1328.7 m
Massive andesitic tuff. The tuff is finer at the base of the core.

1328.7 m to 1329.6 m
Breccia consisting of subangular, fine to pebble sized andesite clasts. The unit as a whole is weathered and the fine clay to sand matrix is very crumbly. The framework clasts are densely packed and comprise up to 60-70% of the core.

1329.6 m to 1330.5 m
Weathered breccia containing evenly spaced, subangular, fine to medium sized andesite pebbles. The matrix is up to 10 % of the core and contains fine to medium sand sized volcaniclastic material.

1330.5 m to 1331.4 m
The same breccia as above. The framework clasts are equant, medium to very coarse pebbles of andesite.

1331.4 m to 1332.3 m
Weathered andesitic tuff.

1332.3 m to 1333.2 m
Weathered breccia, with a very crumbly clay matrix. The framework clasts are subangular, lowly spherical, very coarse pebbles and cobbles.

Appendix 3.3 Kora-3: Personal Observations and Lithological Description adapted from Arco Petroleum NZ Inc., (1988c)

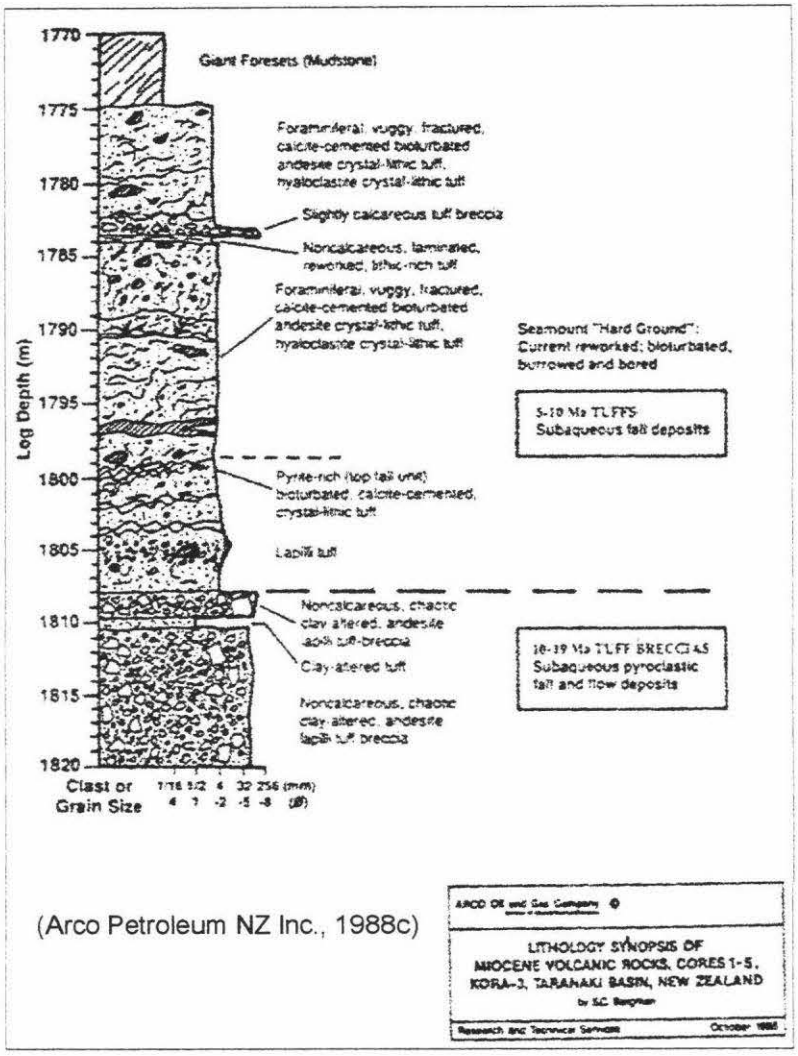

(Arco Petroleum NZ Inc., 1988c)

1782 m to 1783 m
Hard, grey-blue coloured crystal and lithic rich, tuff. The unit is fractured and vuggy.

1783.6 m to 1785.5 m
Same as above slightly coarser texture. The core unit also contains abundant shell fragments.

1785.5 m to 1788.5 m
Same as above.

1788.5 m to 1791.5 m
Same as above.

1791.5 m to 1794.0 m
Same as above.

1794 m to 1796.5 m
Same as above.

1796.5 m to 1799.5 m
Same as above.

1799.5 m to 1802.5 m
Same as above.

1802.5 m to 1805.5 m
Very hard, blue-grey, crystal and andesite lithic rich, tuff. The lithic clasts and crystals vary in grainsize with depth, from 5 to 15 mm near the top of the unit to between 4 mm and 32 mm near the base.

APPENDIX 4 Summary Profile of Thin-Sections

Kora-1A

TS1: Kora-1A 1784.3-1784.4m

Moderately sorted, andesite lithics and crystals in a calcitic cement. Hornblende (10 %), plagioclase (30 %), and augite (5 %) are the dominant crystal types. Glauconite (5-15 %) and opaque minerals (5-10 %) also occur as infilling minerals around the larger crystals. The plagioclase crystals are anhedral and subhedral forms, up to 1 mm in size, and fragmented. The augite and hornblende crystals are subhedral forms, and many of the crystal cores are dissolving. The calcitic matrix constitutes up to 50 % of the total thin section.

TS2: Kora-1A 1786.96

Moderately sorted, andesite lithics and crystals of Hornblende (15-20 %), plagioclase (20 %) and augite (15-20 %). Opaque minerals and glauconite (25-30 %) occur as mineral growths around the larger crystals and andesite lithic clasts.

TS3: Kora-1A 1797.5m

Poorly sorted, crystals of plagioclase (30 %) and hornblende (20 %), and andesite lithics. The hornblende crystals are dissolving. Opaques (5 %) occur as mineral growths around the crystals and lithic clasts. The lithics and crystals occur in a fine clay matrix.

TS4: Kora-1A 1803m (grain mount)

Angular lithic clasts containing euhedral crystals, broken and disarranged crystal fragments and a matrix of fine clay. Hornblende (20 %), plagioclase (20 %), augite (20 %), and opaque minerals (1-5 %) are the predominant crystal types.

TS5: Kora-1A 1812.8

Poorly sorted hornblende (5 %) and plagioclase (20 %) crystals; opaque minerals (5 %) also occur as mineral growths. The matrix is calcitic, and contains numerous, <.02 mm individual crystal fragments, and andesite lithics.

TS6: Kora-1A 1820m

Poorly sorted, severely fractured and dissolving hornblende (20-30 %) and plagioclase (25-30 %) crystals. Opaque minerals (5 %) occur as secondary mineral growths around the larger hornblende and plagioclase crystals. The matrix contains subhedral crystals, and crystal fragments.

TS7: Kora-1A 1829.9

Poorly sorted, euhedral and subhedral hornblende (5 %) and plagioclase (30 %) crystals. Opaque mineral growths (2-5 %) occur around the rims of the hornblendes and plagioclase crystals. The rims of the plagioclase and hornblende crystals are dissolving. The matrix is very fine (< 0.002mm), and contains 0.01mm x 0.06mm plagioclase crystals.

TS* (not illustrated in Figure 4.2): Kora-1A 1837

Hornblende (10-15 %), augite (5-10 %) and plagioclase (>30 %) are the dominant crystal types. Opaque minerals comprise 5 % of the grain mount. The hornblende crystals are a combination of subhedral and broken subhedral crystals. The plagioclase crystals are typically fragmented, and often pitted due to dissolution. The matrix contains 0.02 mm and smaller angular crystal fragments.

Kora-2

TS1: Kora-2 1290m

Moderately sorted plagioclase (5-10 %) and hornblende (2 %) cystals. Glauconite and opaque minerals (5 %) also occur as secondary mineral growths. The plagioclase crystals are disintegrating. The matrix forms up to 50 % of the thin section, and contains pelagic foraminifera, and clays.

TS2: Kora-2 1324m

Poorly sorted hornblende (30 %), plagioclase (35-40 %), and augite (<1 %) crystals. Opaque minerals comprise up to 5 % of the thin section. The framework crystal components are matrix supported (40 %), and the matrix consists of angular crystal fragments mixed with clays.

TS3: Kora-2 1327m

Poorly sorted framework crystals of plagioclase (20 %) and hornblende (5 %). The framework crystal components are angular, and the hornblendes have almost dissolved completely. Opaque minerals are 5 % of the thin section. A clay matrix forms 50 % of the thin section.

TS4: Kora-2 1332.5m (a)

Moderately sorted, very angular lithic clasts. The lithic clasts contain subhedral, plagioclase, hornblende, and augite crystals, and these are supported in a clay matrix.

TS5: Kora-2 1332.5m (b)

Poorly sorted, euhedral plagioclase (30 %) and hornblende (25 %) crystals. Opaque minerals are 10-15 % of the thin section. The thin section as a whole is matrix supported (matrix is 40 %) and the matrix consists of clay.

TS6: Kora-2 1328-1329m

Poorly sorted plagioclase (30 %) and hornblende (30 %) crystals. The matrix contains clay and fine crystal fragments.

Kora-3

TS1: Kora-3 1803m

Poorly sorted, angular andesite lithic clasts. The lithics make up to 15 % of the thin section. The matrix contains up to 60 % pelagic foraminifera, and the remaining matrix consists of hornblende and quartz fragments.

APPENDIX 5

Appendix 5.1 Major element data from the Coromandel Volcanic Centre used in this study (Source: Adams *et al.*, 1994)

Published Analysis #	SiO2	TiO2	Al2O3	Fe2O3	MgO	CaO	FeO	MnO	Na2O	K2O	P2O5
1	48.58	1.18	20.68	1.42	4.66	10.5	7.23	0.44	4.11	0.49	0.71
2	56.6	1.05	17.81	1.19	4.61	8.18	6.08	0.15	3.36	0.86	0.1
3	59.46	0.7	17.77	0.98	4.32	7.39	4.99	0.13	3.2	0.92	0.13
4	59.53	0.89	18	0.92	3.95	7.13	4.68	0.11	3.3	1.35	0.13
5	57.9	0.97	17.63	1.17	4.02	7.3	5.98	0.17	3.23	1.47	0.14
6	60.91	0.73	18.33	0.94	2.73	5.99	4.8	0.1	3.65	1.59	0.22
7	63.79	0.69	19.02	0.67	1.04	5.7	3.43	0.07	3.65	1.79	0.14
9	55.83	0.69	15.43	1.15	7.79	9.41	5.86	0.16	2.71	0.91	0.06
10	59.73	0.73	17.67	1.05	3.98	6.67	5.38	0.12	3.04	1.54	0.09
11	60.89	0.65	16.8	0.95	4.31	6.6	4.84	0.12	3.1	1.66	0.07
13	61.46	0.72	17.54	0.94	3.04	6.22	4.8	0.12	2.95	2.11	0.1
14	57.46	0.72	16.38	1.1	6.38	8.18	5.63	0.18	2.59	1.28	0.09
15	60.41	0.7	17.59	0.98	3.54	7.03	5.01	0.12	2.69	1.78	0.15
17	56.54	1.03	18.22	1.26	3.85	7.66	6.44	0.17	3.27	1.38	0.17
18	60.53	0.7	17.06	1.01	4.08	6.67	5.15	0.15	3.07	1.5	0.07
19	62.39	0.74	16.88	0.95	3.35	5.82	4.84	0.13	3.04	1.76	0.1
20	60.17	0.61	16.21	0.98	4.93	7.61	4.98	0.12	2.85	1.46	0.08
21	63.33	0.62	16.12	0.86	3.35	6.31	4.39	0.12	3.17	1.66	0.08
26	50.46	1.06	17.09	1.33	9.01	9.68	6.76	0.16	3.39	0.78	0.28
27	51.85	1.17	15.99	1.47	8.66	9.86	7.51	0.17	2.65	0.52	0.16
28	53.71	1.13	17.25	1.67	4.97	9.09	8.51	0.19	2.9	0.48	0.1
29	51.79	0.72	14.24	1.38	12.26	9.82	7.03	0.16	2.01	0.49	0.1
30	49.67	1.25	17.89	1.38	7.13	11.64	7.04	0.15	3.19	0.48	0.18
31	52.18	1.05	18.31	1.43	6.18	10.2	7.31	0.17	2.57	0.43	0.16
32	58.83	1.05	16.74	1.11	4.1	7.29	5.64	0.11	3.47	1.47	0.21
33	54.67	0.88	17.8	1.22	5.58	8.65	6.2	0.13	3.78	0.83	0.25
34	47.2	1.13	19.92	1.87	5.2	11.1	9.35	0.2	2.97	0.5	0.56

1, Colville Fm; 2&3, Port Charles Andesite; 4, Tuateawa Andesite; 5-8, Beesons Island Volcanics; 9&10, Whangapoua Andesite; 11&12, Matarangi Andesite; 13, Maumaupaki Fm; 14, Te Tutu Andesite; 15&16, Mahinapua Andesite; 17, Taurahuehue Andesite; 18&19, Tapuaetahi Andesite; 20&21, Taurauikau Andesite; 26-28 MBS (Kuaotunu); 29, MBS (Alderman Is.); 30-32, MBS (Mercury Is.);33, MBS (Woody Hill); 34, Colville Ridge Basalt.

Appendix 5.2 MAJOR ELEMENT DATA FROM THE WAITAKERE VOLCANICS USED IN THIS STUDY (Source: Wright and Black, 1981)

	Published Sample #	SiO2	TiO2	Al2O3	Fe2O3	MgO	CaO	FeO	MnO	Na2O	K2O	P2O5
M	24071	50.54	0.85	15.16	1.99	7.38	10.93	6.80	0.12	2.70	0.70	0.20
M	10346	50.62	0.92	17.19	2.73	6.56	10.38	7.30	0.20	2.45	0.40	0.12
M	24222	53.24	1.36	17.04	5.40	3.21	8.09	4.60	0.14	3.60	0.69	0.22
M	24172	53.70	0.91	19.49	2.89	2.97	8.11	4.80	0.11	3.75	0.78	0.17
M	24037	55.78	1.16	15.46	3.23	2.91	6.29	6.00	0.14	4.75	1.09	0.35
M	10357	55.79	0.95	17.20	2.44	3.46	7.74	6.30	0.16	3.15	0.99	0.16
M	31998	59.61	1.03	15.88	1.20	1.71	5.15	6.20	0.17	3.30	2.13	0.33
M	24073	63.80	0.70	19.03	2.64	1.11	4.51	2.10	0.10	4.00	1.49	0.19
H	890	51.62	1.13	16.30	5.71	5.28	8.61	4.00	0.26	3.50	1.08	0.28
H	960	55.26	1.22	17.93	2.67	3.52	8.06	4.80	0.23	3.15	1.57	0.27
H	941	57.21	1.02	18.03	0.20	2.14	6.14	6.60	0.17	3.35	2.04	0.28
W	26412	48.95	1.00	18.03	6.19	5.76	11.42	3.19	0.22	2.60	0.56	0.25
W	26407	49.90	1.21	18.09	6.77	4.66	10.21	3.50	0.20	2.75	0.80	0.26
W	26410	50.13	1.31	16.26	7.27	4.79	10.28	4.70	0.25	2.75	0.97	0.30
W	26411	48.89	1.46	16.84	7.37	4.86	9.53	4.10	0.26	3.10	1.20	0.36

M = Manakau Subgroup
H = Hukatere Subgroup
W = Waipoua Subgroup

Appendix 5.3 Major element chemistry from Rumble IV (Source: Gamble *et al.*, 1993)

Published sample #	SiO2	TiO2	Al2O3	Fe2O3	MgO	CaO	FeO	MnO	Na2O	K2O	P2O5
168/1A	52.03	0.82	16.56	0.97	7.27	10.55	6.46	0.16	2.96	0.59	0.2
168/1B	50.25	0.65	15.4	1.11	8.31	12.52	7.37	0.14	2.11	0.45	0.06
162/2	50.38	0.84	18.4	1.14	5.16	11.22	8.71	0.17	2.64	0.47	0.11
162/1	50.88	0.87	18.3	1.15	5.08	11.12	7.68	0.17	2.62	0.45	0.11
161	48.6	0.82	15.54	1.04	10.01	12.96	6.95	0.16	2.27	0.27	0.08
169/1	49.64	0.82	16.96	0.95	9.1	12.22	6.34	0.14	2.78	0.25	0.09

Appendix 5.4 Major element data from the Wairakau Andesites used in this study (Source: White, 1985)

Published Sample #s	SIO2	TIO2	AL2O3	FE2O3	MGO	CAO	FEO	MNO	NA2O	K2O	P2O5
34917	56.02	0.8	13.93	1.23	7.88	8.03	6.02	0.14	2.45	1.82	0.1
34924	56.68	1.25	16.98	1.55	4.38	7.8	5.09	0.15	2.93	1.83	0.21
34923	57.02	0.97	15.63	2.46	4.62	7.9	4.6	0.17	3.11	1.69	0.12
34930	57.16	0.82	14.48	1.37	6.22	7.63	5.23	0.17	2.36	2.15	0.17
34925	57.47	1.15	16.59	1.86	4.9	7.67	4	0.13	3.06	1.98	0.19
34928	57.5	1.07	17.11	2.71	3.44	6.4	2.89	0.1	3.43	1.91	0.23
34929	57.55	0.96	16.74	1.66	3.16	6.83	4.8	0.18	3.24	2.05	0.22
34919	57.81	0.85	17.19	3.88	3.4	6.33	3.12	0.1	3.42	1.7	0.2
34926	58.08	1.02	17.21	2.08	4.23	7.19	4.21	0.13	2.56	1.87	0.18
34918	58.09	0.89	18.15	3.06	2.57	6.09	2.93	0.12	3.96	1.77	0.23
34927	58.65	0.82	16.42	1.77	4.41	6.37	3.99	0.13	3.36	1.89	0.19
34921	60.07	0.71	15.86	3.06	3.07	5.7	2.36	0.07	3.89	2.05	0.17
34442	60.22	0.72	18.02	1.01	1.82	5.65	3.73	0.1	3.13	2.27	0.25
34443	60.33	0.7	15.86	1.63	3.4	6.15	3.46	0.07	3.07	2.2	0.08
34922	62.33	0.72	16.43	1.37	2.65	5.65	3.63	0.14	3.64	2.37	0.17

Appendix 5.5 Major element data from Mount Egmont used in this study (Source: Stewart *et al.*, 1996; and Price *et al.*, 1992)

Published Sample #	SiO2	TiO2	Al2O3	Fe2O3	MgO	CaO	FeO	MnO	Na2O	K2O	P2O5	
T90/39	56.67	0.85	18.24	3.05	2.96	7.78	4.05	0.17	3.42	2.15	0.29	Stewart *et al.*, 1996
BR1	56.50	0.71	18.41	3.17	2.57	7.95	3.50	0.17	3.70	2.12	0.32	
T90/2B	57.60	0.76	17.91	3.26	2.75	7.03	2.84	0.14	3.69	3.01	0.32	
T89/14	49.93	1.14	17.68	6.18	5.07	10.71	4.07	0.19	3.20	1.56	0.28	
T89/13	53.04	0.93	19.15	4.33	3.12	9.19	3.79	0.18	3.69	1.99	0.35	
T89/.15	54.57	0.98	17.78	4.13	3.55	8.19	3.65	0.17	3.69	2.50	0.39	
T90/16	55.00	0.93	17.66	3.48	3.76	8.39	4.32	0.17	3.46	2.25	0.31	
T89/12A	56.02	0.87	17.95	3.56	2.93	7.99	3.49	0.16	3.83	2.36	0.31	
T90/13	54.59	0.94	17.46	4.68	3.87	8.39	3.17	0.16	3.41	2.51	0.38	
T89/16	56.89	0.78	17.78	3.58	3.07	7.30	3.10	0.15	3.96	2.83	0.29	
T90/3	57.53	0.77	17.89	3.42	2.85	7.19	2.99	0.14	3.66	2.79	0.31	
89/74	52.14	1.01	18.37	4.38	3.67	9.46	4.40	0.19	3.40	1.84	0.31	Price *et al.*, 1992
89/75	51.49	1.05	18.31	4.56	4.14	10.11	4.63	0.19	3.46	1.70	0.31	
89/76	53.92	0.98	17.44	4.66	3.75	8.36	3.22	0.17	3.90	2.42	0.34	
89/77	49.54	1.17	16.39	4.82	6.40	11.09	5.51	0.17	2.99	1.53	0.26	
89/81	54.57	0.98	17.78	4.13	3.55	8.19	3.65	0.17	3.69	2.50	0.39	
89/82	56.89	0.78	17.78	3.58	3.07	7.30	3.10	0.15	3.96	2.83	0.29	
89/85	55.51	0.78	18.37	3.52	3.01	8.28	3.87	0.18	3.65	1.99	0.35	
90/4A	54.22	0.96	17.63	3.08	4.81	8.91	4.87	0.15	3.35	1.77	0.29	
T10	51.94	0.72	15.14	1.18	7.60	10.19	7.87	0.17	2.39	0.66	0.08	
T15	48.52	0.89	18.09	1.05	9.12	11.16	6.99	0.13	2.49	0.27	0.14	

Appendix 5.6 Major element chemstry from Titiraupenga (Source: Froude and Cole, 1985)

Published Sample #	SiO2	TiO2	Al2O3	Fe2O3	MgO	CaO	FeO	MnO	Na2O	K2O	P2O5
29575	56.71	0.55	15.06	1.61	7.92	8.46	6.3	0.13	2.34	0.85	0.07
29567	56.9	0.55	15.13	1.77	7.38	8.56	5.89	0.12	2.73	0.9	0.07
24147	56.33	0.52	15.02	2.45	8.05	9.15	5.13	0.14	2.23	0.86	0.12
24146	56.7	0.52	14.68	2.3	7.89	9.2	5.3	0.14	2.28	0.87	0.12
24148	56.76	0.53	15.04	2.55	7.74	9.05	4.98	0.14	2.23	0.86	0.12
29570	56.23	0.44	12.15	1.58	10.65	9.04	6.74	0.16	2.25	0.72	0.04
24145	56.07	0.42	11.88	1.66	11.52	9.5	6.4	0.16	1.7	0.59	0.1
29578	56.69	0.47	13.13	1.48	9.49	9.19	6.37	0.13	2.3	0.69	0.06
29579	56.93	0.49	13.91	2.2	8.53	8.92	5.59	0.14	2.48	0.75	0.06
29571	57.23	0.58	16.26	1.61	5.78	8.37	5.94	0.14	3.2	0.79	0.1

Appendix 5.7 Major element chemistry from the Alexandra Volcanics (Source: Briggs, 1986)

Published Sample #	SiO2	TiO2	Al2O3	Fe2O3	MgO	CaO	FeO	MnO	Na2O	K2O	P2O5
5	56.5	1.01	17.55	1.37	3.15	6.6	5.5	0.14	3.73	2.21	0.41
9	55.94	0.83	17.17	3.99	3.42	6.57	3.61	0.13	3.57	1.8	0.21
14	59.29	0.74	17.38	3.84	2.81	6.12	2.73	0.11	3.2	1.99	0.19
15	63.67	0.53	16.3	2.52	2.01	4.48	2.22	0.08	3.68	2.55	0.16
16	56.2	0.64	14.89	2.68	6.8	9.21	5.5	0.17	2.41	0.97	0.12

Appendix 5.8 Major element chemistry from Kora

(Unpublished oil company data courtesy of S. Bergman, Arco Exploration and Production Technology)

Well	Depth (m)	SiO2	TiO2	Al2O3	Fe2O3	MgO	CaO	FeO	MnO	Na2O	K2O	P2O5
Kora-1A	1785.7	48.9	0.77	18.1	7.79	4.87	8.83	2.9	0.13	2.54	0.43	0.12
Kora-1A	1787	51.3	0.48	15.2	9.7	6.23	6.44	3	0.14	2.63	0.68	0.1
Kora-1A	1788.7	58.2	0.6	18.9	6.12	1.63	8.43	0.1	0.09	3.68	1.09	0.13
Kora-1A	1793.41	57	0.51	17.8	2.67	3.64	8.15	3.2	0.19	2.93	0.31	0.15
Kora-1A	1794.6	58.4	0.58	18.7	3.66	3	8.2	1	0.08	3.76	0.84	0.14
Kora-1A	1795.42	57	0.56	17.9	5.1	4.13	7.97	1.3	0.15	3.27	0.45	0.13
Kora-1A	1812.13	61	0.53	19	3	1.94	7.5	1.6	0.07	3.86	1.01	0.14
Kora-1A	1824.68	57.5	0.61	18.5	5.48	2.95	8.4	0.8	0.1	3.62	0.96	0.1
Kora-1A	1825.55	56.9	0.64	19.5	4.04	2.46	9.32	1.5	0.13	3.67	0.99	0.14
Kora-1A	1826.59	57.8	0.54	18.2	4.32	3.94	7.7	2	0.16	3.19	0.91	0.13
Kora-1A	1827.73	54.7	0.7	17.7	5.38	4.67	8.28	1.9	0.14	3.27	0.59	0.12
Kora-1A	1841.03	54.8	0.67	19.4	4.55	3.37	10	1.8	0.09	3.54	0.8	0.13
Kora-1A	1841.4	48	0.74	18.8	5.77	7.02	9.76	3.4	0.23	2.39	0.18	0.06
Kora-1A	1843.6	55.9	0.68	19.3	4.72	2.73	9.53	1.8	0.11	3.53	1.1	0.15
Kora-1A	1895.72	58.7	0.58	18.7	3.51	2.57	9.27	1.5	0.08	3.38	0.7	0.15
Kora-1A	1899.42	57.3	0.56	18.8	4.08	3.3	8.99	1.6	0.1	3.44	0.56	0.15
Kora-1A	1901.11	55.7	0.54	17.9	4.21	4.35	8.69	2.2	0.14	3.14	0.5	0.15
Kora-1A	1904.2	60.4	0.45	18.4	3	2.91	7.45	2.2	0.12	3.6	0.78	0.14
Kora-1A	1907.75	58.6	0.52	19.4	3.23	2.37	8.39	1.2	0.08	3.64	0.88	0.16
Kora-1A	1908.23	58.9	0.5	19.3	3.36	2.54	8.51	1.3	0.09	3.57	0.78	0.15
Kora-1A	1910.06	57.2	0.57	18.9	4.98	2.87	8.04	0.9	0.1	3.51	0.96	0.13
Kora-2	1280	63.9	0.72	15.9	2.03	2.02	1.59	3.3	0.04	3.28	3.1	0.18
Kora-2	1285.2	63	0.76	16	2.32	2.08	1.25	2.8	0.04	2.86	2.94	0.15
Kora-2	1321.56	51.5	0.63	18.7	4.79	4.88	8.6	1.6	0.08	3.26	0.33	0.13
Kora-2	1321.96	55.8	0.59	19.1	4.56	2.01	7.47	0.5	0.06	3.63	1.01	0.13
Kora-2	1323.4	50.7	0.59	17.4	5.44	4.85	9.11	1.1	0.09	3.16	0.26	0.12
Kora-2	1323.8	55.6	0.55	18.7	3.92	3.15	9.35	0.6	0.1	3.58	0.67	0.13
Kora-2	1331.6	53	0.56	19.7	4.02	3.56	8.88	0.5	0.1	3.55	0.62	0.13
Kora-3	1809.5	50.1	0.66	21.1	4.74	1.92	5.25	0.1	0.05	2.97	0.56	0.15
Kora-3	1810.3	65	0.28	13.7	2.45	2.17	1.97	0.1	0.04	1.89	0.4	0.08
Kora-3	1812.5	61.8	0.43	15.5	3.92	0.98	3.38	0.1	0.05	2.75	1.41	0.12
Kora-4	1718	49.5	0.61	18.8	4.22	3.38	10.1	1.8	0.12	3.69	2.89	0.25
Kora-4	1780.5	56.1	0.37	18	2.42	2.92	6.06	2.2	0.13	3.24	2.4	0.15
Kora-4	1853	56.3	0.4	19	2.5	3.37	6.06	2.1	0.12	3.13	2.38	0.13

Appendix 5.9 Major element data from the Kiwitahi Volcanics used in this study (Source: Black *et al.*, 1992)

Published Sample #	SiO2	TiO2	Al2O3	Fe2O3	MgO	CaO	FeO	MnO	Na2O	K2O	P2O5
43905	61.51	0.74	17.92	1.27	2.89	6.41	4.59	0.12	3.06	1.32	0.17
43908	58.16	0.93	18.34	1.6	3.66	7.34	5.76	0.16	2.91	1.01	0.13
42563	53.11	1.06	15.96	1.36	8.46	9.48	6.8	0.12	2.72	0.75	0.17
42564	54.28	1.22	17.52	1.3	5.44	9.19	6.51	0.14	3.31	0.86	0.21
42551	59.89	0.69	17.9	1.01	4.04	7.14	5.04	0.09	3.28	0.79	0.12
42552	58.91	0.84	16.76	1.23	4.04	7.34	6.19	0.19	3.34	1.01	0.15
28364	57.45	0.79	18.01	1.5	3.99	7.73	5.98	0.14	3.05	1.24	0.12
28371	64.01	0.59	17.85	0.92	2.59	5.12	3.64	0.1	3.3	1.76	0.12
27303	60.01	0.59	18.71	1.3	2.76	6.91	4.66	0.12	3.46	1.32	0.15
27305	60.16	0.56	19.13	1.3	2.11	7.24	4.65	0.13	3.37	1.18	0.16
27291	56.46	0.81	17.75	1.59	5.2	8.51	5.7	0.13	2.72	1.03	0.1
27299	59.15	0.77	17.83	1.43	3.67	7.22	5.13	0.12	3.08	1.46	0.13
27289	55.13	0.72	16.46	1.81	6.35	9.33	6.5	0.15	2.65	0.8	0.1
27286	54.68	0.75	16.93	1.92	6.16	9.08	6.9	0.16	2.59	0.74	0.1
27250	53.72	0.76	15.58	2.06	6.87	10.08	7.41	0.14	2.43	0.88	0.08
27235	54.08	0.79	17.21	1.89	5.99	9.4	6.81	0.15	2.68	0.89	0.1
27264	56.17	0.62	14.59	1.78	7.19	9.52	6.43	0.15	2.46	1.02	0.07
27255	56.45	0.65	14.83	1.7	7.2	9.59	6.11	0.14	2.35	0.91	0.08
27284	56.01	0.56	13.47	1.81	8.76	9.48	6.54	0.15	2.2	0.94	0.08
27273	57.95	0.59	14.49	1.69	6.63	8.57	6.08	0.13	2.45	1.34	0.09

Appendix 5.10 Major element data from Tongariro Volcanic Centre used in this study (Source: Cole *et al.*, 1986)

Published Sample #	SiO2	TiO2	Al2O3	Fe2O3	MgO	CaO	FeO	MnO	Na2O	K2O	P2O5
14855	52.7	0.7	15.7	1.5	8.8	9.7	7.5	0.2	2.6	0.6	0.1
11965	53.1	0.7	15.5	1.5	7.8	10.4	7.7	0.2	2.4	0.7	0.1
24497	56	0.5	12.7	1.2	11.4	9	6.2	0.2	2	0.8	0.1
29250	56.2	0.8	16.6	1.4	5.2	8.3	7	0.1	3.1	1.2	0.2
24266	56.4	0.7	15.9	1.3	6.9	8.1	6.3	0.1	2.9	1.3	0.1
14737	56.5	0.7	18.2	1.4	4.7	7.6	6.8	0.1	3.2	0.8	0.1
24471	57.3	0.6	14.8	1.2	6.9	9.3	6.2	0.1	2.5	0.9	0.1
14848	57.3	0.7	14.4	1.2	8.7	7.3	6	0.2	2.8	1.5	0.1
14817	57.4	0.6	15.7	1.3	6.3	8.8	6.6	0.2	2.3	0.7	0.1
14795	57.4	0.5	15	1.3	6.6	9.1	6.6	0.2	2.5	0.7	0.1
14782	58.1	0.7	17.3	1.2	4.7	7.6	5.9	0.1	3.1	1.2	0.1
24487	58.1	0.5	17.1	1.2	5.2	8	6	0.1	2.7	1	0.1
14913	58.2	0.7	20.5	0.9	2.2	8.2	4.3	0.1	3.6	1.3	0.1
24256	60	0.7	16.4	1.1	3.9	7.1	5.7	0.1	3.2	1.7	0.1
24262	60.7	0.6	16.8	1.1	3.6	6.8	5.4	0.1	3.4	1.4	0.1
16721	60.9	0.8	15.3	1	5.4	6.2	5	0.1	3.2	2	0.2
16722	61.6	0.6	15.8	0.9	4.7	6.5	4.7	0.1	3.4	1.7	0.1
14813	64.3	0.8	16.1	0.9	2.5	4.7	4.3	0.1	3.4	2.9	0.1

Appendix 6 Composite Major Element Dataset (including data from Kora)

Sample	SiO2	TiO2	Al2O3	Fe2O3	MgO	CaO	FeO	MnO	Na2O	K2O	P2O5	Group
c1	48.58	1.18	20.68	1.42	4.66	10.5	7.23	0.44	4.11	0.49	0.71	1
c2	56.6	1.05	17.81	1.19	4.61	8.18	6.08	0.15	3.36	0.86	0.1	1
c3	59.46	0.7	17.77	0.98	4.32	7.39	4.99	0.13	3.2	0.92	0.13	1
c4	59.53	0.89	18	0.92	3.95	7.13	4.68	0.11	3.3	1.35	0.13	1
c5	57.9	0.97	17.63	1.17	4.02	7.3	5.98	0.17	3.23	1.47	0.14	1
c6	60.91	0.73	18.33	0.94	2.73	5.99	4.8	0.1	3.65	1.59	0.22	1
c7	63.79	0.69	19.02	0.67	1.04	5.7	3.43	0.07	3.65	1.79	0.14	1
c8	55.83	0.69	15.43	1.15	7.79	9.41	5.86	0.16	2.71	0.91	0.06	1
c9	59.73	0.73	17.67	1.05	3.98	6.67	5.38	0.12	3.04	1.54	0.09	1
c10	60.89	0.65	16.8	0.95	4.31	6.6	4.84	0.12	3.1	1.66	0.07	1
c11	61.46	0.72	17.54	0.94	3.04	6.22	4.8	0.12	2.95	2.11	0.1	1
c12	57.46	0.72	16.38	1.1	6.38	8.18	5.63	0.18	2.59	1.28	0.09	1
c13	60.41	0.7	17.59	0.98	3.54	7.03	5.01	0.12	2.69	1.78	0.15	1
c14	56.54	1.03	18.22	1.26	3.85	7.66	6.44	0.17	3.27	1.38	0.17	1
c15	60.53	0.7	17.06	1.01	4.08	6.67	5.15	0.15	3.07	1.5	0.07	1
c16	62.39	0.74	16.88	0.95	3.35	5.82	4.84	0.13	3.04	1.76	0.1	1
c17	60.17	0.61	16.21	0.98	4.93	7.61	4.98	0.12	2.85	1.46	0.08	1
c18	63.33	0.62	16.12	0.86	3.35	6.31	4.39	0.12	3.17	1.66	0.08	1
c19	50.46	1.06	17.09	1.33	9.01	9.68	6.76	0.16	3.39	0.78	0.28	1
c20	51.85	1.17	15.99	1.47	8.66	9.86	7.51	0.17	2.65	0.52	0.16	1
c21	53.71	1.13	17.25	1.67	4.97	9.09	8.51	0.19	2.9	0.48	0.1	1
c22	51.79	0.72	14.24	1.38	12.26	9.82	7.03	0.16	2.01	0.49	0.1	1
c23	49.67	1.25	17.89	1.38	7.13	11.64	7.04	0.15	3.19	0.48	0.18	1
c24	52.18	1.05	18.31	1.43	6.18	10.2	7.31	0.17	2.57	0.43	0.16	1
c25	58.83	1.05	16.74	1.11	4.1	7.29	5.64	0.11	3.47	1.47	0.21	1
c26	54.67	0.88	17.8	1.22	5.58	8.65	6.2	0.13	3.78	0.83	0.25	1
c27	47.2	1.13	19.92	1.87	5.2	11.1	9.35	0.2	2.97	0.5	0.56	1

m1	50.54	0.85	15.16	1.99	7.38	10.93	6.8	0.12	2.7	0.7	0.2	2
m2	50.62	0.92	17.19	2.73	6.56	10.38	7.3	0.2	2.45	0.4	0.12	2
m3	53.24	1.36	17.04	5.4	3.21	8.09	4.6	0.14	3.6	0.69	0.22	2
m4	53.7	0.91	19.49	2.89	2.97	8.11	4.8	0.11	3.75	0.78	0.17	2
m5	55.78	1.16	15.46	3.23	2.91	6.29	6	0.14	4.75	1.09	0.35	2
m6	55.79	0.95	17.2	2.44	3.46	7.74	6.3	0.16	3.15	0.99	0.16	2
m7	59.61	1.03	15.88	1.2	1.71	5.15	6.2	0.17	3.3	2.13	0.33	2
m8	63.8	0.7	19.03	2.64	1.11	4.51	2.1	0.1	4	1.49	0.19	2
m9	51.62	1.13	16.3	5.71	5.28	8.61	4	0.26	3.5	1.08	0.28	2
m10	55.26	1.22	17.93	2.67	3.52	8.06	4.8	0.23	3.15	1.57	0.27	2
m11	57.21	1.02	18.03	0.2	2.14	6.14	6.6	0.17	3.35	2.04	0.28	2
m12	48.95	1	18.03	6.19	5.76	11.42	3.19	0.22	2.6	0.56	0.25	2
m13	49.9	1.21	18.09	6.77	4.66	10.21	3.5	0.2	2.75	0.8	0.26	2
m14	50.13	1.31	16.26	7.27	4.79	10.28	4.7	0.25	2.75	0.97	0.3	2
m15	48.89	1.46	16.84	7.37	4.86	9.53	4.1	0.26	3.1	1.2	0.36	2
kerm1	52.03	0.82	16.56	0.97	7.27	10.55	6.46	0.16	2.96	0.59	0.2	3
kerm2	50.25	0.65	15.4	1.11	8.31	12.52	7.37	0.14	2.11	0.45	0.06	3
kerm3	50.38	0.84	18.4	1.14	5.16	11.22	8.71	0.17	2.64	0.47	0.11	3
kerm4	50.88	0.87	18.3	1.15	5.08	11.12	7.68	0.17	2.62	0.45	0.11	3
kerm5	48.6	0.82	15.54	1.04	10.01	12.96	6.95	0.16	2.27	0.27	0.08	3
kerm6	49.64	0.82	16.96	0.95	9.1	12.22	6.34	0.14	2.78	0.25	0.09	3
w1	56.02	0.8	13.93	1.23	7.88	8.03	6.02	0.14	2.45	1.82	0.1	4
w2	56.68	1.25	16.98	1.55	4.38	7.8	5.09	0.15	2.93	1.83	0.21	4
w3	57.02	0.97	15.63	2.46	4.62	7.9	4.6	0.17	3.11	1.69	0.12	4
w4	57.16	0.82	14.48	1.37	6.22	7.63	5.23	0.17	2.36	2.15	0.17	4
w5	57.47	1.15	16.59	1.86	4.9	7.67	4	0.13	3.06	1.98	0.19	4
w6	57.5	1.07	17.11	2.71	3.44	6.4	2.89	0.1	3.43	1.91	0.23	4
w7	57.55	0.96	16.74	1.66	3.16	6.83	4.8	0.18	3.24	2.05	0.22	4
w8	57.81	0.85	17.19	3.88	3.4	6.33	3.12	0.1	3.42	1.7	0.2	4
w9	58.08	1.02	17.21	2.08	4.23	7.19	4.21	0.13	2.56	1.87	0.18	4
w10	58.09	0.89	18.15	3.06	2.57	6.09	2.93	0.12	3.96	1.77	0.23	4
w11	58.65	0.82	16.42	1.77	4.41	6.37	3.99	0.13	3.36	1.89	0.19	4
w12	60.07	0.71	15.86	3.06	3.07	5.7	2.36	0.07	3.89	2.05	0.17	4

w13	60.22	0.72	18.02	1.01	1.82	5.65	3.73	0.1	3.13	2.27	0.25	4
w14	60.33	0.7	15.86	1.63	3.4	6.15	3.46	0.07	3.07	2.2	0.08	4
w15	62.33	0.72	16.43	1.37	2.65	5.65	3.63	0.14	3.64	2.37	0.17	4
e1	56.67	0.85	18.24	3.05	2.96	7.78	4.05	0.17	3.42	2.15	0.29	5
e2	56.5	0.71	18.41	3.17	2.57	7.95	3.5	0.17	3.7	2.12	0.32	5
e3	57.6	0.76	17.91	3.26	2.75	7.03	2.84	0.14	3.69	3.01	0.32	5
e4	49.54	1.17	16.39	4.82	6.4	11.09	5.51	0.17	2.99	1.53	0.26	5
e5	49.93	1.14	17.68	6.18	5.07	10.71	4.07	0.19	3.2	1.56	0.28	5
e6	53.04	0.93	19.15	4.33	3.12	9.19	3.79	0.18	3.69	1.99	0.35	5
e7	54.57	0.98	17.78	4.13	3.55	8.19	3.65	0.17	3.69	2.5	0.39	5
e8	55	0.93	17.66	3.48	3.76	8.39	4.32	0.17	3.46	2.25	0.31	5
e9	56.02	0.87	17.95	3.56	2.93	7.99	3.49	0.16	3.83	2.36	0.31	5
e10	54.59	0.94	17.46	4.68	3.87	8.39	3.17	0.16	3.41	2.51	0.38	5
e11	56.89	0.78	17.78	3.58	3.07	7.3	3.1	0.15	3.96	2.83	0.29	5
e12	57.53	0.77	17.89	3.42	2.85	7.19	2.99	0.14	3.66	2.79	0.31	5
e13	52.14	1.01	18.37	4.38	3.67	9.46	4.4	0.19	3.4	1.84	0.31	5
e14	51.49	1.05	18.31	4.56	4.14	10.11	4.63	0.19	3.46	1.7	0.31	5
e15	53.92	0.98	17.44	4.66	3.75	8.36	3.22	0.17	3.9	2.42	0.34	5
e16	49.54	1.17	16.39	4.82	6.4	11.09	5.51	0.17	2.99	1.53	0.26	5
e17	54.57	0.98	17.78	4.13	3.55	8.19	3.65	0.17	3.69	2.5	0.39	5
e18	56.89	0.78	17.78	3.58	3.07	7.3	3.1	0.15	3.96	2.83	0.29	5
e19	55.51	0.78	18.37	3.52	3.01	8.28	3.87	0.18	3.65	1.99	0.35	5
e20	54.22	0.96	17.63	3.08	4.81	8.91	4.87	0.15	3.35	1.77	0.29	5
e21	51.94	0.72	15.14	1.18	7.6	10.19	7.87	0.17	2.39	0.66	0.08	5
e22	48.52	0.89	18.09	1.05	9.12	11.16	6.99	0.13	2.49	0.27	0.14	5
tit1	56.71	0.55	15.06	1.61	7.92	8.46	6.3	0.13	2.34	0.85	0.07	6
tit2	56.9	0.55	15.13	1.77	7.38	8.56	5.89	0.12	2.73	0.9	0.07	6
tit3	56.33	0.52	15.02	2.45	8.05	9.15	5.13	0.14	2.23	0.86	0.12	6
tit4	56.7	0.52	14.68	2.3	7.89	9.2	5.3	0.14	2.28	0.87	0.12	6
tit5	56.76	0.53	15.04	2.55	7.74	9.05	4.98	0.14	2.23	0.86	0.12	6
tit6	56.23	0.44	12.15	1.58	10.65	9.04	6.74	0.16	2.25	0.72	0.04	6
tit7	56.07	0.42	11.88	1.66	11.52	9.5	6.4	0.16	1.7	0.59	0.1	6
tit8	56.69	0.47	13.13	1.48	9.49	9.19	6.37	0.13	2.3	0.69	0.06	6

tit9	56.93	0.49	13.91	2.2	8.53	8.92	5.59	0.14	2.48	0.75	0.06	6
tit10	57.23	0.58	16.26	1.61	5.78	8.37	5.94	0.14	3.2	0.79	0.1	6
a1	56.5	1.01	17.55	1.37	3.15	6.6	5.5	0.14	3.73	2.21	0.41	7
a2	55.94	0.83	17.17	3.99	3.42	6.57	3.61	0.13	3.57	1.8	0.21	7
a3	59.29	0.74	17.38	3.84	2.81	6.12	2.73	0.11	3.2	1.99	0.19	7
a4	63.67	0.53	16.3	2.52	2.01	4.48	2.22	0.08	3.68	2.55	0.16	7
a5	56.2	0.64	14.89	2.68	6.8	9.21	5.5	0.17	2.41	0.97	0.12	7
kor1	48.9	0.77	18.1	7.79	4.87	8.83	2.9	0.13	2.54	0.43	0.12	8
kor2	51.3	0.48	15.2	9.7	6.23	6.44	3	0.14	2.63	0.68	0.1	8
kor3	58.2	0.6	18.9	6.12	1.63	8.43	0.1	0.09	3.68	1.09	0.13	8
kor4	57	0.51	17.8	2.67	3.64	8.15	3.2	0.19	2.93	0.31	0.15	8
kor5	58.4	0.58	18.7	3.66	3	8.2	1	0.08	3.76	0.84	0.14	8
kor6	57	0.56	17.9	5.1	4.13	7.97	1.3	0.15	3.27	0.45	0.13	8
kor7	61	0.53	19	3	1.94	7.5	1.6	0.07	3.86	1.01	0.14	8
kor8	57.5	0.61	18.5	5.48	2.95	8.4	0.8	0.1	3.62	0.96	0.1	8
kor9	56.9	0.64	19.5	4.04	2.46	9.32	1.5	0.13	3.67	0.99	0.14	8
kor10	57.8	0.54	18.2	4.32	3.94	7.7	2	0.16	3.19	0.91	0.13	8
kor11	54.7	0.7	17.7	5.38	4.67	8.28	1.9	0.14	3.27	0.59	0.12	8
kor12	54.8	0.67	19.4	4.55	3.37	10	1.8	0.09	3.54	0.8	0.13	8
kor13	48	0.74	18.8	5.77	7.02	9.76	3.4	0.23	2.39	0.18	0.06	8
kor14	55.9	0.68	19.3	4.72	2.73	9.53	1.8	0.11	3.53	1.1	0.15	8
kor15	58.7	0.58	18.7	3.51	2.57	9.27	1.5	0.08	3.38	0.7	0.15	8
kor16	57.3	0.56	18.8	4.08	3.3	8.99	1.6	0.1	3.44	0.56	0.15	8
kor17	55.7	0.54	17.9	4.21	4.35	8.69	2.2	0.14	3.14	0.5	0.15	8
kor18	60.4	0.45	18.4	3	2.91	7.45	2.2	0.12	3.6	0.78	0.14	8
kor19	58.6	0.52	19.4	3.23	2.37	8.39	1.2	0.08	3.64	0.88	0.16	8
kor20	58.9	0.5	19.3	3.36	2.54	8.51	1.3	0.09	3.57	0.78	0.15	8
kor21	57.2	0.57	18.9	4.98	2.87	8.04	0.9	0.1	3.51	0.96	0.13	8
kor22	63.9	0.72	15.9	2.03	2.02	1.59	3.3	0.04	3.28	3.1	0.18	8
kor23	63	0.76	16	2.32	2.08	1.25	2.8	0.04	2.86	2.94	0.15	8
kor24	51.5	0.63	18.7	4.79	4.88	8.6	1.6	0.08	3.26	0.33	0.13	8
kor25	55.8	0.59	19.1	4.56	2.01	7.47	0.5	0.06	3.63	1.01	0.13	8
kor26	50.7	0.59	17.4	5.44	4.85	9.11	1.1	0.09	3.16	0.26	0.12	8

kor27	55.6	0.55	18.7	3.92	3.15	9.35	0.6	0.1	3.58	0.67	0.13	8
kor28	53	0.56	19.7	4.02	3.56	8.88	0.5	0.1	3.55	0.62	0.13	8
kor29	50.1	0.66	21.1	4.74	1.92	5.25	0.1	0.05	2.97	0.56	0.15	8
kor30	65	0.28	13.7	2.45	2.17	1.97	0.1	0.04	1.89	0.4	0.08	8
kor31	61.8	0.43	15.5	3.92	0.98	3.38	0.1	0.05	2.75	1.41	0.12	8
kor32	49.5	0.61	18.8	4.22	3.38	10.1	1.8	0.12	3.69	2.89	0.25	8
kor33	56.1	0.37	18	2.42	2.92	6.06	2.2	0.13	3.24	2.4	0.15	8
kor34	56.3	0.4	19	2.5	3.37	6.06	2.1	0.12	3.13	2.38	0.13	8
kiw1	61.51	0.74	17.92	1.27	2.89	6.41	4.59	0.12	3.06	1.32	0.17	9
kiw2	58.16	0.93	18.34	1.6	3.66	7.34	5.76	0.16	2.91	1.01	0.13	9
kiw3	53.11	1.06	15.96	1.36	8.46	9.48	6.8	0.12	2.72	0.75	0.17	9
kiw4	54.28	1.22	17.52	1.3	5.44	9.19	6.51	0.14	3.31	0.86	0.21	9
kiw5	59.89	0.69	17.9	1.01	4.04	7.14	5.04	0.09	3.28	0.79	0.12	9
kiw6	58.91	0.84	16.76	1.23	4.04	7.34	6.19	0.19	3.34	1.01	0.15	9
kiw7	57.45	0.79	18.01	1.5	3.99	7.73	5.98	0.14	3.05	1.24	0.12	9
kiw8	64.01	0.59	17.85	0.92	2.59	5.12	3.64	0.1	3.3	1.76	0.12	9
kiw9	60.01	0.59	18.71	1.3	2.76	6.91	4.66	0.12	3.46	1.32	0.15	9
kiw10	60.16	0.56	19.13	1.3	2.11	7.24	4.65	0.13	3.37	1.18	0.16	9
kiw11	56.46	0.81	17.75	1.59	5.2	8.51	5.7	0.13	2.72	1.03	0.1	9
kiw12	59.15	0.77	17.83	1.43	3.67	7.22	5.13	0.12	3.08	1.46	0.13	9
kiw13	55.13	0.72	16.46	1.81	6.35	9.33	6.5	0.15	2.65	0.8	0.1	9
kiw14	54.68	0.75	16.93	1.92	6.16	9.08	6.9	0.16	2.59	0.74	0.1	9
kiw15	53.72	0.76	15.58	2.06	6.87	10.08	7.41	0.14	2.43	0.88	0.08	9
kiw16	54.08	0.79	17.21	1.89	5.99	9.4	6.81	0.15	2.68	0.89	0.1	9
kiw17	56.17	0.62	14.59	1.78	7.19	9.52	6.43	0.15	2.46	1.02	0.07	9
kiw18	56.45	0.65	14.83	1.7	7.2	9.59	6.11	0.14	2.35	0.91	0.08	9
kiw19	56.01	0.56	13.47	1.81	8.76	9.48	6.54	0.15	2.2	0.94	0.08	9
kiw20	57.95	0.59	14.49	1.69	6.63	8.57	6.08	0.13	2.45	1.34	0.09	9
TVC1	52.7	0.7	15.7	1.5	8.8	9.7	7.5	0.2	2.6	0.6	0.1	10
TVC2	53.1	0.7	15.5	1.5	7.8	10.4	7.7	0.2	2.4	0.7	0.1	10
TVC3	56	0.5	12.7	1.2	11.4	9	6.2	0.2	2	0.8	0.1	10
TVC4	56.2	0.8	16.6	1.4	5.2	8.3	7	0.1	3.1	1.2	0.2	10
TVC5	56.4	0.7	15.9	1.3	6.9	8.1	6.3	0.1	2.9	1.3	0.1	10

TVC6	56.5	0.7	18.2	1.4	4.7	7.6	6.8	0.1	3.2	0.8	0.1	10
TVC7	57.3	0.6	14.8	1.2	6.9	9.3	6.2	0.1	2.5	0.9	0.1	10
TVC8	57.3	0.7	14.4	1.2	8.7	7.3	6	0.2	2.8	1.5	0.1	10
TVC9	57.4	0.6	15.7	1.3	6.3	8.8	6.6	0.2	2.3	0.7	0.1	10
TVC10	57.4	0.5	15	1.3	6.6	9.1	6.6	0.2	2.5	0.7	0.1	10
TVC11	58.1	0.7	17.3	1.2	4.7	7.6	5.9	0.1	3.1	1.2	0.1	10
TVC12	58.1	0.5	17.1	1.2	5.2	8	6	0.1	2.7	1	0.1	10
TVC13	58.2	0.7	20.5	0.9	2.2	8.2	4.3	0.1	3.6	1.3	0.1	10
TVC14	60	0.7	16.4	1.1	3.9	7.1	5.7	0.1	3.2	1.7	0.1	10
TVC15	60.7	0.6	16.8	1.1	3.6	6.8	5.4	0.1	3.4	1.4	0.1	10
TVC16	60.9	0.8	15.3	1	5.4	6.2	5	0.1	3.2	2	0.2	10
TVC17	61.6	0.6	15.8	0.9	4.7	6.5	4.7	0.1	3.4	1.7	0.1	10
TVC18	64.3	0.8	16.1	0.9	2.5	4.7	4.3	0.1	3.4	2.9	0.1	10

Appendix 7 — *SAS Programs used in this study*

(All of the following programs have been adapted from Cronin, 1996)

Appendix 7.1 **Excel spreadsheet data were transferred to SAS using the following program:**

```
data libname.datasetname;
        infile 'drive:\file name.filetype';
        input sample $ SiO2 TiO2 Al2O3 Fe2O3 MgO CaO FeO MnO Na2O K2O P2O5
group;
proc print;
        title 'Composite Dataset (all volcanics)';
run;
```

Appendix 7.2 **The plot of can1 and can2 was generated using the following program:**

```
Proc candisc data=libname.compositedataset-name out=libname.outcan-
        dataset-name;
        class group;
        var SiO2 TiO2 Al2O3 Fe2O3 MgO CaO FeO MnO Na2O K2O P2O5;
run;
proc plot data=libname.outcan-dataset-name;
        plot can2*can1=group/href=0 vref=0;
run;
```

Appendix 7.3 **The discriminant model was created using the following program:**

```
proc discrim data=libname.compositedataset-name outstat=libname.output-name
ncan=7 listerr distance simple;
        class group;
        var SiO2 TiO2 Al2O3 Fe2O3 MgO CaO FeO MnO Na2O K2O P2O5;
        id sample;
run;
```

Appendix 7.4 **The major element data from Kora were tested against all other North Island Volcanic Centres in the composite dataset using the following program:**

Proc discrim data=libname.outstatdataset-nametestdata=libname.Koradataset testout=libname.outputdataset-name testlist;
class group;
var SiO_2 TiO_2 Al_2O_3 Fe_2O_3 MgO CaO FeO MnO Na_2O K_2O P_2O_5;
testclass group;
testid sample;
run;

Appendix 7.5 **The most discriminating elements were identified using the following program:**

proc stepdisc data=libname.sas-dataset-name stepwise;
class group;
var SiO_2 TiO_2 Al_2O_3 Fe_2O_3 MgO CaO FeO MnO Na_2O K_2O P_2O_5;
run;